TORSIONAL ANALYSIS OF A COMPOSITE I-BEAM

by

VISHAL MUKESH SMITA SANGHAVI

Presented to the Faculty of the Graduate School of

The University of Texas at Arlington in Partial Fulfillment

of the Requirements

for the Degree of

MASTER OF SCIENCE IN MECHANICAL ENGINEERING

THE UNIVERSITY OF TEXAS AT ARLINGTON

December 2012

Acknowledgements

I would like to first acknowledge the below mentioned organizations / charitable trusts:

- R. D. Sethna Scholarship Fund
- Jain Jagruti Central Board & Charitable Trust
- New York Gold Co. (Mr. V. M. Gandhi)

It is because of their financial help that I was able to purse my Master's in USA. They were more interested in my academic history rather than the credit history to provide me with scholarship loan to pursue my dream.

Next, I would like to express my deepest gratitude to Dr. Wen Chan, my research advisor for all his help and guidance. In him I found a mentor, a guide, a role model and I will always consider him as my "Academic Father".

I would also like to thank Dr. Kent Lawrence for all his help and advice which helped me reinforce my fundamentals of FEM and ANSYS™. I would like to thank Dr. Erian Armanios for serving as my committee member.

I am immensely grateful to Jinal Vora as she was the one who has always supported and encouraged me towards my goals. I have discussed all my research work with her, and I am sure she never understood a word of it but she made sure to always patiently listen to it and appreciate the work.

Finally, I would like to thank and dedicate this work to three most important individuals of my life, my Mom - Smita Sanghvi, my Dad - Mukesh Sanghvi and my Grandfather - Rajnikant Sanghvi.

November 19, 2012

Abstract

TORSIONAL ANALYSIS OF A COMPOSITE I-BEAM

Vishal Sanghavi, M.S.

The University of Texas at Arlington, 2012

Supervising Professor: Wen S. Chan

A simple methodology for analysis of thin walled composite I-Beam subjected to free torsion and restrained torsion is developed. Classical Lamination Theory is extended from the laminate level to the structural level for analysis purpose.

The developed expressions for shear center, equivalent torsional rigidity and equivalent warping rigidity for a composite mono-symmetric I-Beam depends on the material properties, ply stacking sequence, fiber orientation and geometry

The results from the proposed theory gives better agreement with the ANSYS™ results than the traditional smeared property approach.

Table of Contents

List of Illustrations

List of Tables

List of Symbols

q :	Shear Flow
τ :	Shear force
t :	Thickness
σ_x :	Axial stress
M_y :	Moment about y axis
M_z :	Moment about z axis
I_z :	Moment of Inertia about z –z Axis
I_y :	Moment of Inertia about y –y Axis
I_{yz} :	Product Moment of Inertia
V_y :	Shear Force in y – direction
V_z :	Shear Force in z - direction
b_{f1}, b_{f2} :	Width of I-Beam top flange and bottom flange respectively
t_{f1}, t_{f2} :	Thickness of I-Beam top flange and bottom flange respectively
h_w, t_w :	I-Beam web height and thickness respectively
G :	Shear Modulus
θ_{sv} :	Total angle of twist in free torsion case
K :	Polar moment of inertia / torsional constant
T_{sv}:	St. Venant's Torsion
μ :	Width correction factor
T_w:	Warping torsion
E:	Axial Stiffness
Γ:	Warping Constant
GK :	Torsional stiffness / Torsional Rigidity
$E\Gamma$:	Warping rigidity / Warping stiffness
T :	Total Torsional Load
A_R :	Area swept out by a generator
σ_Γ :	Direct stresses developed
$\theta_{warp}/\ \theta_{total}$:	Total angle of twist when I-Beam is subjected to restrained torsion
ε_1 and ε_2 :	Strain in 1 and 2 directions respectively
γ_{12}:	Shear strain in 1-2 plane

$[S]_{1-2}$: Compliance matrix of the order 3 x 3 in 1-2 co-ordinate system

$[Q]_{1-2}$: Reduced stiffness matrix of the order 3 x 3 in 1-2 co-ordinate system

$E_1, E_2, \upsilon_{12}, G_{12}$: Independent material constants in respective directions

$[\bar{S}]_{x-y}$: Compliance matrix in x-y co-ordinate system

$[\bar{Q}]_{x-y}$: Reduced stiffness matrix in x-y co-ordinate system

$\varepsilon_x^0, \varepsilon_y^0, \gamma_{xy}^0$: Midplane strains in x-y directions

$\kappa_x, \kappa_y, \kappa_{xy}$: Curvatures in the laminate

N_x, N_y : Normal forces per unit lenght

N_{xy} : Shear forces per unit lenght

M_x, M_y : Bending moments per unit lenght

M_{xy} : Twisting moment per unit lenght

$[A]$: Extensional stiffness matrix

$[B]$: Extensional-bending coupling stiffness matrix

$[D]$: Bending stiffness matix

$\bar{M}_z$: sum of the total moments components of each sub-laminate

$D_y^c = \bar{E}\bar{I}_{zz}$: equivalent bending stiffness of I-Beam with respect to z-z Axis

$\frac{1}{\rho_z^c}$: Curvature at the centroid of I-Beam

$\overline{EA} =$ Equivalent axial stiffness of the composite I-Beam

$\bar{T}$ = Total torsional load applied

Φ = Rate of twist of composite I-Beam = $d\theta/dx$

v_{f1} = Displacement of top flange due to rotation about x-axis

$v_{f2} =$ Displacement of bottom flange due to rotation about x-axis

$\bar{T}$ = Total torque applied to composite I-Beam

$\bar{T}_{sv}$ = Total Saint –Venant torque in composite

$\bar{T}_w$ = Total Restrained warping induced torque in composite

Chapter 1

Introduction

1.1 General Introduction

A composite material is the one in which two or more materials are combined on a macroscopic scale to get the useful third material whose mechanical performance and properties are superior to those of the constituent materials acting independently. The basic difference in a composite material and an alloy is the macroscopic examination of the material wherein the components can be identified by the naked eye in the former. A composite material has two phases: one is called as reinforcement which is stiffer & stronger and the less stiff, continuous phase is called the matrix. Composites have the following advantages over monolithic materials

- High Specific stiffness
- High Specific strength
- Low density
- Corrosion resistance
- Design flexibility
- Low thermal expansion
- Parts count reduction
- Easy fabrication

The basis of the superior structural performance of composite material lies in high specific strength, high specific stiffness and in the anisotropic & heterogeneous character of the material.

The technology of composite materials has experienced a rapid development in last two decades. Because of the aforementioned reasons composites are now replacing isotropic materials and one of the major revamp is taking place in the aerospace industries where weight saving and cost competitiveness are of major importance. Composites are now used as primary load carrying structural members in aircrafts.

Thin-walled beams with open and closed cross-sections made of isotropic and composite materials are used extensively in the aerospace industry, both as direct load

carrying member and as stiffeners in panel construction. Most composite structures are designed as assemblies of beams, column, plates and shell. Beams are structural members that carry bending loads and have one dimension much larger than the other two dimensions (width and height). From geometric point of view,

- Beams and columns are one dimensional elements
- Plates and shells are two dimensional elements

Most of the beams are thin-walled and composed of assembly of flat panels. In addition to weight savings generated by certain composite materials, a thin walled composite beam has the extra advantage of allowing the designers to tailor the material properties of different parts of the beam cross section. This enables the shape of the cross section to be exploited to the fullest by arrangement of the unidirectional plies within the laminated composite panels. But due to lack of well established analytical solutions we are yet not able to explore the maximum use of composite materials.

Design Validation

Presently, design can be validated by the following methods:

- Closed form Analytical solutions
- Finite Element Method
- Testing

Composite structures are normally certified by test and not by analysis. But testing in nature is very tedious, expensive in terms of cost and time and cannot be performed for bulk specimens. In such cases, Finite Element Methods (FEM) and software are handy as they can analyze large complex structures with high accuracy. However, the accuracy of FEM is mostly dependent upon the quality of modeling and boundary conditions applied. An incorrect model will result in meaningless solutions. Hence, it is

recommended to perform an initial analysis on a simplified structure using the classical or analytical solutions. Added advantage of analytical solutions are, that once they are programmed into a mathematical software like MATLAB, the parameters can be easily modified to study the changes and effect of each variables. The FEM and analytical solutions should be checked for the validation of FEM model as well as analytical solution. Thus at initial stages of development we should rely on analytical closed form solutions. Once the parameters are finalized we should go for FEM as here we can add more complexities in modeling the structure and once the design passes the FEM we should go for real time testing of article. This will ensure saving of time, cost and more insightful design experience.

1.2 Why Torsion of Composite I-Beam structure?

As a guide line for designers, if a section has to carry torsional load then a closed beam should be preferred. Although the open sections are not designed to carry torsional loads they have to resist some magnitude of torsion for e.g. when an I-beam is used as stiffeners for airplane wings. Torsional loading causes warping displacements. Warping, in broader terms can be defined as the axial displacements taking place in a thin-walled beam due to a non axial loading. The torsional analysis of thin walled beams forms a basis in determining the longitudinal behavior of beams which are either restrained against warping or that induce warping. If a thin walled beam is restrained against warping in any way leads to warping stresses, which are axial and direct.

Warping stresses are quite significant compared with the bending stresses predicted by the classical theories and they are usually not considered in preliminary designs.

1.3 Literature Review

As torsional loads are normally applied to closed sections, there are number of direct analytical methods for the torsional analysis of thin walled composite box beams. But not many literatures were found which discusses the torsional analysis of an open section.

Springer and Kollar [1] in their book have described the warping and torsional stiffness and the location of shear center of open cross-section beams which possess an orthotropic layup of each wall segment. The formulation can be applied for the beams with unsymmetrical laminate layup and stresses and strains for the individual plies can also be evaluated.

Kollar and Pluzsik [2] formulated the stiffness and compliance matrices of a beam with arbitrary layup with plain strain consideration and further extend the theory to formulate expressions for torsional, axial, bending and shear loads on the open and closed section beams [1].The algebraic steps for this theory are long and laborious.

Ata and Loughlan [3] & [4] proposed the approach which simply makes use of existing theories of torsion for isotropic beams and modifying them suitably to account for the composite materials. It is basically intended for symmetrical laminates which exhibits membrane orthotropy that is $A_{16} = A_{26} = 0$ (No axial shear coupling). They compared their analytical solution with FEM as well as experimental results and found good correlations between all the 3 methods.

A simple methodology for analysis of thin walled composite beams subjected to bending, torsion, shear and axial forces was developed by Massa and Barbero [5].Geometric properties used in classical beam theory such as area, first moment of area, center of gravity etc were replaced by mechanical properties such as axial stiffness, mechanical 1st moment of area, mechanical center of gravity to incorporate both

geometry and material properties. The methodology takes into account the balanced and symmetrical configuration as they are widely used. They also included the assumptions of Wu and Sun for slender thin walled laminated beams in the formulation of the constitutive equation.

Salim and Davalos [6] expanded the Vlasov's theory to perform the linear analysis of open and closed sections composite sections. All the possible elastic couplings were taken into account and beam assumptions from Gjelsvik' book," The theory of thin walled bars" was used to derive the equations for N, V_x, V_y, T, M_x, M_y, and G_x and G_y defined by Chandra and Chopra by equating the strain energy per unit length. Warping effects were also studied and analytical solution for closed section was compared to the experimental results for the verification purpose.

Pultruded FRP bars with open section have relatively low transverse shear modulus in relation to their axial and flexural modulii. Thus it might be expected that shear deformation would influence the restrained torsional warping. But Roberts and Ubaidi [7] claims that their theory indicates that the influence of shear deformation on restrained warping torsional stiffness of such members is not significant. They developed an approximate theory based on Vlasov's thin walled elastic beam theory and compared the theoretical results with experimental results which support their claims of negligible influence of shear deformation. For the experiments they considered I-beam with equal flange width and thickness.

Ramesh Chandra and Inderjit Chopra [8] studied the static structural response of composite I-Beam with elastic couplings subjected to bending and torsional load by neglecting the shear deformation and an analytical solution developed on the basis of Vlasov's theory. They also studied the constrained warping effects, slenderness ratio and fiber orientation and stacking of plies of beam and validated the results with experiments.

According to the theory the bending torsion behavior of I-Beam is influenced by bending-twist and extension-twist couplings of plate segment, transverse shear deformation has a negligible influence on the structural behavior of symmetric I-Beam under bending and torsional loads and the torsional stiffness of I-beams is significantly influenced by restraining the warping deformation of the beams.

Jaehong Lee [9] combined the classical lamination theory with the Vlasov and Gjelsivk theory of thin walled elastic beam to find the closed form solution for center of gravity (C.G.) and shear center. The method is application to any arbitrary layup and cross-section. He showed that the location of C.G. and shear center is dependent on the fiber angle changes in flanges and web.

Skudra, Bulavs, Gurvich and Kruklinsh in their book [10] discussed about the free and pure torsion of a laminated beam considering the interply shear stresses thus including the edge effects. Using the basic equilibrium conditions and the Classical lamination theory they developed equations for torsional stiffness in free and pure torsion condition along with the expressions for stresses and strains

Gay, Hoa and Tsai have describes an equivalent Prandtl stress function for composite beams and developed the torsion equations of the laminated beams [11].

Chapter 2

Torsional Behavior of an Isotropic I-Beam

2.1 Overview

An aircraft is basically an assembly of stiffened shell structures ranging from the single cell closed section fuselage to multi-cellular wings and tail- surfaces each of them subjected to bending, shear, torsional and axial loads. It also consists of thin walled channel, T - , Z- , “top hat” or I – sections, which are used to stiffen the thin skins of cellular components and provide supports for internal loads from floors and engine mounting. Thin-walled structures have a high load-carrying capacity, despite their small thickness [12]. The flat plates develop shear forces, bending and twisting moments to resist transverse loads. The twisting rigidity in isotropic plates is quite significant and hence considered stiffer than a beam of comparable span and thickness. Thin plates combine light weight and form efficiency with high load-carrying capacity, economy and technological effectiveness. As a result of all these advantages thin walled structures are preferred in all fields of engineering. Structural members are normally classified as open section beams and closed section beams. I -, Z- , C – channel are examples of open section beams as shown in Figure 2-1 while box beam, hat section, tubular sections are all examples of closed section beams as in Figure 2-2.

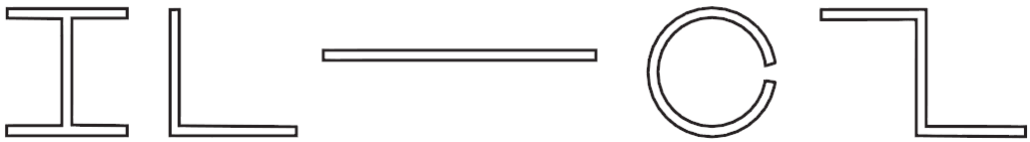

Figure 2-1 Open Section

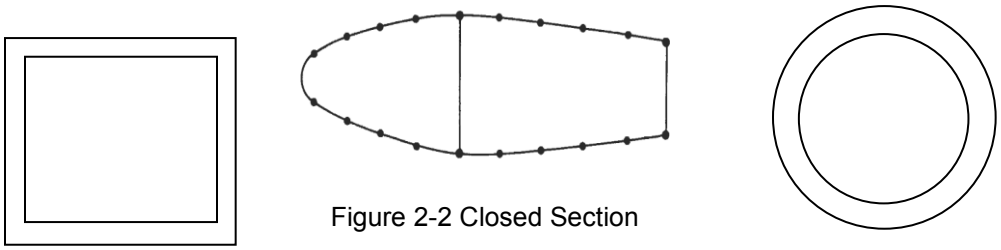

Figure 2-2 Closed Section

Usually closed sections are considered if the beam is to be designed for torsion as they have greater torsional stiffness and also less warping due to twisting. Any structural arrangement in which the loads are transferred to an open section by torsion is not an efficient design for resisting loads. In large number of practical designs, the loads are usually applied in such a manner that their resultant loads and forces pass through the centroid. If the sections are doubly symmetric than the shear center and centroid coincides thus eliminating torsional loads.

In some cases, it is inevitable and we have to ensure open sections can carry small magnitude of torsional loads.

2.2 Torsional behavior of noncircular and open sections

When a circular cross-section shaft is twisted and the deformations are small, the cross-section remains in the plane. The shearing stresses which are induced due to torsion acts only in the direction perpendicular to the radius vector and hence they only twist without any axial displacement. But this is only true for the circular sections. For other sections the shearing stress has component both perpendicular to the radius vector and in the direction of the radius vector. This extra shearing force results in a shearing strain both within the plane of the cross section and normal to it. This out- of -plane distortion is called as warping and it will exist for all but circular cross sections subjected to twisting [14].

For bars of non - circular sections subjected to twisting, two types of phenomena are observed. If the member is allowed to warp freely, then the applied torque is resisted

only by torsional shear stresses called as **St. Venant's torsional shear stresses**. If the member is not allowed to warp freely, that is if the cross section is axially constrained the applied torque is resisted by St. Venant's torsional shear stresses along with the **Wagner torsion bending torque** also called as **Warping Torsion** both exist in the section.

Cross-section of a thin walled beam subjected to a restrained torsion experiences two types of warping, one is the primary warping and other is the secondary warping. Warping of the mid-plane of the cross section which is assumed constant across the wall thickness is classified as primary warping. Warping of the section across its wall thickness is termed as secondary warping. A section undergoes primary warping if the constraints cause the development of two opposite flange shear forces which in turn reduces the effect of the torsional load applied. Cross-sections which possess primary warping are as shown below in Figure 2-3. Along with primary warping these sections also undergo secondary warping. The Figure 2-3 also shows the cross-sections which undergoes secondary warping only. In sections which possess primary warping, secondary warping and effects of restrained secondary warping are usually neglected as they are generally much less than primary warping and the effects of restrained primary warping. However if the section exhibits only secondary warping, then the effect of restrained secondary warping is quite significant and should not be ignored. For closed beams the warping displacements are considered to be of primary nature. For the analysis of I-beam we consider primary warping only.

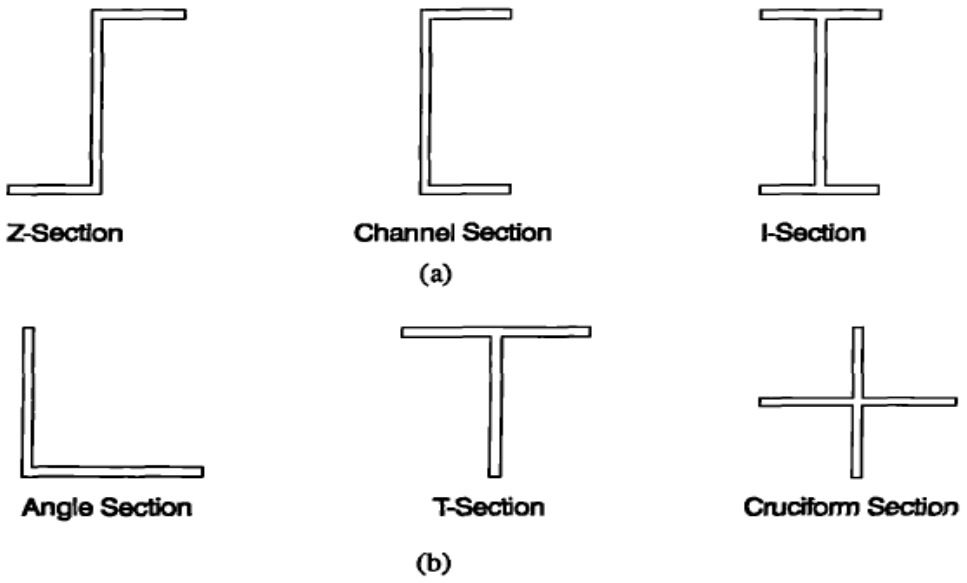

Figure 2-3 a) Open Sections possessing primary warping and secondary warping

b) Open sections possessing secondary warping only

The assumptions in evaluation of the theory of torsion of thin walled beams are as follows [3]:

1. Cross-section of any beam, whether of open or closed section, is stiffened against distortion, i.e., remains undistorted in their own plane after loading.
2. Shear stresses normal to beam surfaces are neglected
3. It is generally agreed that thin wall theory many be applied with reasonable accuracy to sections for which the ratio $\frac{t_{max}}{b} \leq 0.1$

where t_{max} is the maximum thickness in the section and *b* is a typical cross sectional dimension.

2.3 Calculation of Shear Center of I – Beam

Shear Center is defined as the point in the cross section where the bending and torsion are decoupled. That is if the lateral or transverse load pass through this point it produces only bending without twisting. It may also be shown by the use of reciprocal theorem that this point is also the center of twist of section subjected to torsion. In most of the cases it is difficult to guarantee that a shear load will act through the shear center. But the shear load may be represented by the combination of shear load through the shear center and torque. The stresses can then be super positioned. Therefore, it is essential to calculate and locate the shear center in the cross section. When a cross-section has an axis of symmetry the shear center must lie on that axis.

Thus if we assume that the cross section supports the shear loads V_z and V_y such that there is no twisting of the cross section and also as there are no hoop stresses in the beam the shear flow and direct stresses acting on an element of the beam wall are related by the below mentioned equilibrium equation [12]:

$$\frac{\partial q}{\partial s} + t\frac{\partial \sigma_x}{\partial x} = 0 \tag{2.1}$$

Where,

$$\sigma_x = \left(\frac{M_z I_y - M_y I_{yz}}{I_z I_y - I_{yz}^2}\right) y + \left(\frac{M_y I_z - M_z I_{yz}}{I_z I_y - I_{yz}^2}\right) z \tag{2.2}$$

q = shear flow = shear force per unit length = $\tau * t$

τ = shear force

t = thickness

σ_x = axial stress

M_z = Moment about z axis

M_y = Moment about y axis

I_y = Moment of Inertia about y –y Axis

I_z = Moment of Inertia about z –z Axis

I_{yz} = Product Moment of Inertia

V_y = Shear Force in y – direction

V_z = Shear Force in z - direction

Therefore we get,

$$\frac{\partial \sigma_x}{\partial x} = \left(\frac{\frac{\partial M_z}{\partial x} I_y - \frac{\partial M_y}{\partial x} I_{yz}}{I_z I_y - I_{yz}^2} \right) y + \left(\frac{\frac{\partial M_y}{\partial x} I_z - \frac{\partial M_z}{\partial x} I_{yz}}{I_z I_y - I_{yz}^2} \right) z \tag{2.3}$$

We also have

$$V_z = \frac{\partial M_y}{\partial x} \tag{2.4}$$

$$V_y = \frac{\partial M_z}{\partial x} \tag{2.5}$$

from Eqs. (2.3), (2.4) and (2.5) we get

$$\frac{\partial \sigma_x}{\partial x} = \left(\frac{V_y I_y - V_z I_{yz}}{I_y I_z - I_{yz}^2} \right) y + \left(\frac{V_z I_z - V_y I_{yz}}{I_y I_z - I_{yz}^2} \right) z \tag{2.6}$$

Substituting Eqs. (2.6) in (2.1) gives

$$\frac{\partial q}{\partial s} = - \left(\frac{V_y I_y - V_z I_{yz}}{I_y I_z - I_{yz}^2} \right) ty - \left(\frac{V_z I_z - V_y I_{yz}}{I_y I_z - I_{yz}^2} \right) tz \tag{2.7}$$

Integrating from s = 0 to s =s which would be the integration of complete cross – section we have,

$$\int_0^s \frac{\partial q}{\partial s} ds = - \left(\frac{V_y I_y - V_z I_{yz}}{I_y I_z - I_{yz}^2} \right) \int_0^s ty \, ds - \left(\frac{V_z I_z - V_y I_{yz}}{I_y I_z - I_{yz}^2} \right) \int_0^s tz \, ds \tag{2.8}$$

If the origin for s is taken at the open edge of the cross – section, then q = 0 when s = 0 and Eq (2.8) becomes,

$$q_s = - \left(\frac{V_y I_y - V_z I_{yz}}{I_y I_z - I_{yz}^2} \right) \int_0^s ty \, ds - \left(\frac{V_z I_z - V_y I_{yz}}{I_y I_z - I_{yz}^2} \right) \int_0^s tz \, ds \tag{2.9}$$

Now, considering I – Beam, as symmetrical about Z – axis I_{yz} = 0 and also to find the shear center we would apply only V_y. We assume that V_y is applied at shear center which is denoted by S.C in the Figure 2-4 and is z_{sc} away from the center of the I-beam Figure 2-4.

Now shear flow would be,

$$q_s = -\left(\frac{V_y}{I_z}\right)\int_0^s ty\, ds \tag{2.10}$$

I_z is moment of Inertia about the z – z axis and is of the form of:

$$I_z = \left(\frac{t_{f1}b_{f1}^3}{12}\right) + \left(\frac{t_{f2}b_{f2}^3}{12}\right) + \left(\frac{h_w t_w^3}{12}\right) \tag{2.11}$$

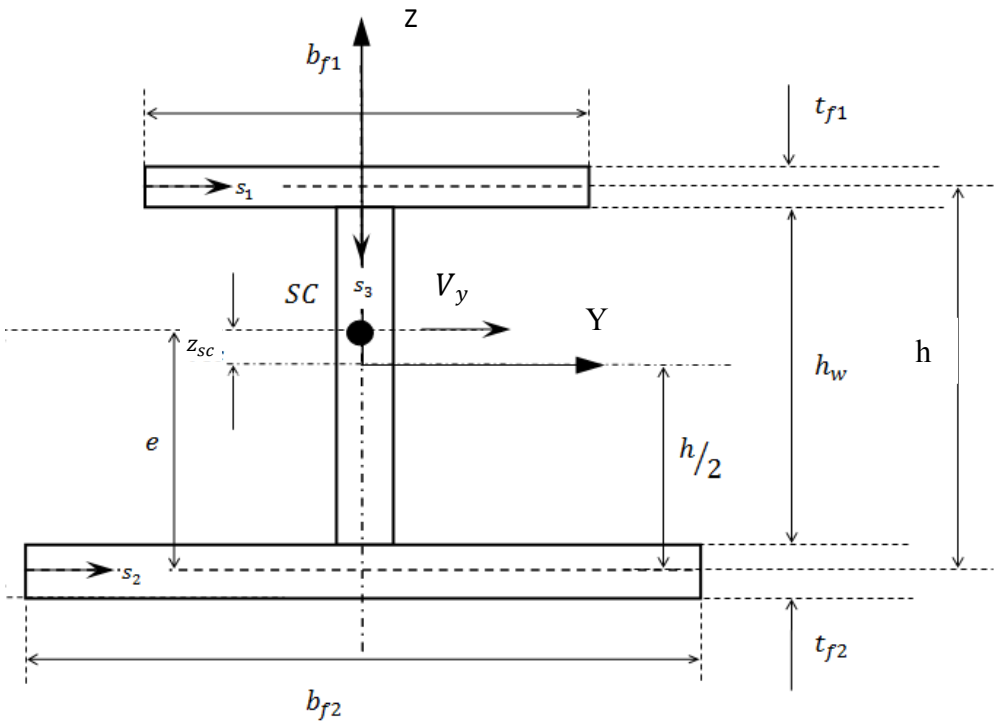

Figure 2-4 I-Beam

Calculating shear in each flange and web:

Top flange:

From Eq. (2.10) we can write the shear flow in the top flange as:

$$q_1 = -\left(\frac{V_y}{I_z}\right)\int_0^{s_1} t_{f1} y \, ds_1$$

$$y = \left(\frac{b_{f1}}{2} - s_1\right)$$

therefore,

$$q_1 = -\left(\frac{V_y}{I_z}\right) t_{f1}\left(\frac{b_{f1}}{2} - \frac{s_1}{2}\right) * s_1$$

$$q_1 = -\left(\frac{V_y}{I_z}\right) t_{f1}\left(\frac{b_{f1}s_1}{2} - \frac{s_1^2}{2}\right) \quad (2.12)$$

Similarly shear flow in the bottom flange can be written as:

$$q_2 = -\left(\frac{V_y}{I_z}\right) t_{f2}\left(\frac{b_{f2}s_2}{2} - \frac{s_2^2}{2}\right) \quad (2.13)$$

Shear flow for web would be zero (0).

Now considering the force balance at the center of the I beam we get

$$V_y z_{sc} = q_1 * \frac{h}{2} + q_2 * \left(-\frac{h}{2}\right) \quad (2.14)$$

Substituting Eqs (2.12) and (2.13) in (2.14) we get,

$$V_y z_{sc} = \int_0^{b_{f1}} \left(\frac{V_y}{I_z}\right) t_{f1}\left(\frac{b_{f1}s_1}{2} - \frac{s_1^2}{2}\right) * \frac{h}{2} ds_1 - \int_0^{b_{f2}} \left(\frac{V_y}{I_z}\right) t_{f2}\left(\frac{b_{f2}s_2}{2} - \frac{s_2^2}{2}\right) * \frac{h}{2} ds_2$$

Therefore	$z_{sc} = \frac{h}{2I_z}\left(\frac{t_{f1}b_{f1}^3}{12} - \frac{t_{f2}b_{f2}^3}{12}\right)$	(2.15)

The above shear center is at a distance of z_{sc} from the center of the I - beam.

Now, in the above case we did the force balance with respect to the midpoint of I- Beam, but if we take the force balance with respect to the mid-plane of the bottom flange and if e represents the distance of the shear center from that point, then we get the following equation

$$V_y\, e = \int_0^{b_{f1}} \left(\frac{V_y}{I_z}\right) t_{f1} \left(\frac{b_{f1} s_1}{2} - \frac{s_1^2}{2}\right) * h ds_1$$

Thus,	$e = \frac{h}{I_z}\left(\frac{t_{f1} b_{f1}^3}{12}\right)$	(2.16)

I_z can be calculated using Eq. (2.11).

Also, if we assume that the thickness of the plates considered are too thin we can ignore the higher powers of thickness in the moment of inertia.

$$I_z = \left(\frac{t_{f1} b_{f1}^3}{12}\right) + \left(\frac{t_{f2} b_{f2}^3}{12}\right) \quad (2.17)$$

Substituting Eq. (2.17) in Eq. (2.16),

$$e = \frac{h}{\left(\frac{t_{f1} b_{f1}^3}{12}\right) + \left(\frac{t_{f2} b_{f2}^3}{12}\right)} * \left(\frac{t_{f1} b_{f1}^3}{12}\right)$$

Thus,	$e = \frac{h t_{f1} b_{f1}^3}{t_{f1} b_{f1}^3 + t_{f2} b_{f2}^3}$	(2.18)

The above Eq (2.18) is similar to the equation of shear center mentioned in [15].

If $t_{f1} = t_{f2} = t$, then

$e = \frac{h b_{f1}^3}{b_{f1}^3 + b_{f2}^3}$	(2.19)

The above Eq (2.19) is similar to the equation of shear center mentioned in [16].

The comparison of the shear centers with different forms is as shown in the Table 2-2 for cases discussed in Table 2-1

Table 2-1 Description of Case 1, 2, 3

Table Dimensions (inches)	Case 1	Case 2	Case 3	Material Properties
Width of top flange	0.25	0.5	0.625	$\mathrm{E} = 1.02 \times 10^7$ psi, $\mathrm{G} = 4.08 \times 10^6$ psi, $\mathrm{v} = 0.25$,
Width of bottom flange	1.0	0.75	0.625	
Height of web	0.5	0.5	0.5	
Thickness of top flange	0.04	0.04	0.04	
Thickness of bottom flange	0.05	0.05	0.05	
Thickness of web	0.02	0.02	0.02	

The shear centers mentioned are measured from the base of the bottom flange.

Table 2-2 Isotropic Shear center comparison

Geometry	Shear center by ANSYS™ BEAM TOOL (inch)	Shear center by Eq. (2.15) (inch)	Shear center by Eq. (2.18) (inch)	Shear center by Eq. (2.19) (inch)
Case 1	0.0321	0.0317	0.0317	0.0333
Case 2	0.1297	0.1294	0.1294	0.1495
Case 3	0.2672	0.2672	0.2672	0.2975

2.4 Uniform Torsion in Rectangular Section

When a torque is applied to non- circular cross sections like the rectangular cross section in our case, the transverse section which are plane prior to twisting, warp in the axial direction and the plane section no longer remains plane after twisting. But as long as the warping is not constrained we can apply the same theory of St. Venant's Torsion (T_{sv}) which is for the circular cross-section by replacing it with the appropriate torsional constant (K) for the rectangular section.

$$T_{sv} = GK\frac{d\theta_{sv}}{dx} \tag{2.20}$$

Where

G = shear Modulus

θ_{sv} = the total angle of twist in free torsion case

K = polar moment of inertia / torsional constant

x = direction along the axis of the member

The behavior of I-Beam under free torsion condition is shown in Figure 2-5. It has been shown that when a cross – section is of the open type and consists of several thin plate elements rigidly attached with one another to form the “thin walled” shape, K can be taken as the sum of the torsional constants of each of the part. K is the factor dependent on the form and dimensions of the cross-section. For circular section, K is the polar moment of inertia equal to J; for other sections K is less than J and may be only a very small fraction of J. I-Beam is made of 3 rectangular sections viz. upper flange, bottom flange and web.

The torsional constant K, for a rectangular section is usually assumed to be:

$$K = \frac{bt^3}{3} \tag{2.21}$$

where,

b = width of the section and t = thickness

Thus, for I-beam the torsional constant would be:

Method 1	$K = \frac{b_{f1}{t_{f1}}^3}{3} + \frac{b_{f2}{t_{f2}}^3}{3} + \frac{h_w{t_w}^3}{3}$	(2.22)

But, this condition is true only if the ratio of $^b/_t$ approaches infinity or is very large; however for the ratio in excess of 10 the error is of the order of only 6 percent. Obviously the approximate nature of the solution increases as $^b/_t$ decreases. Therefore, in order to retain the usefulness of the analysis a factor μ is included in the torsional constant, viz.

$$K = \frac{\mu bt^3}{3} \tag{2.23}$$

Values of μ for different types of sections are found experimentally and quoted in various references [30] and listed below in Table 2-3:

Table 2-3 Width reduction factor table

b/t	1.0	1.5	2.0	2.5	3.0	4.0	5.0	6.0	10.0	∞
μ	0.423	0.588	0.687	0.747	0.789	0.843	0.873	0.897	0.936	0.999

Thus, for I-beam the torsional constant would be:

Method 2	$K = \frac{\mu_{f1} b_{f1} {t_{f1}}^3}{3} + \frac{\mu_{f2} b_{f2} {t_{f2}}^3}{3} + \frac{\mu_w h_w {t_w}^3}{3}$ (2.24)

Also, the width correction factor can be computed by the method mentioned below. The torsional constant for rectangular section as found in [15] can be used to calculate the K for overall I-Beam.

The equations mentioned are in a simplified form involving an approximation, with a resulting error no greater than 4 percent.

$$\mathrm{K_{f1}} = \frac{b_{f1}}{2} * \left(\frac{t_{f1}}{2}\right)^3 * \left[\frac{16}{3} - 3.36 * \frac{\left({t_{f1}}/{2}\right)}{\left({b_{f1}}/{2}\right)} * \left(1 - \frac{\left({t_{f1}}/{2}\right)^4}{12 * \left({b_{f1}}/{2}\right)^4}\right)\right] \quad (2.25)$$

$$\mathrm{K_{f2}} = \frac{b_{f2}}{2} * \left(\frac{t_{f2}}{2}\right)^3 * \left[\frac{16}{3} - 3.36 * \frac{\left({t_{f2}}/{2}\right)}{\left({b_{f2}}/{2}\right)} * \left(1 - \frac{\left({t_{f2}}/{2}\right)^4}{12 * \left({b_{f2}}/{2}\right)^4}\right)\right] \quad (2.26)$$

$$\mathrm{K_w} = \frac{h_w}{2} * \left(\frac{t_w}{2}\right)^3 * \left[\frac{16}{3} - 3.36 * \frac{\left({t_w}/{2}\right)}{\left({h_w}/{2}\right)} * \left(1 - \frac{\left({t_w}/{2}\right)^4}{12 * \left({h_w}/{2}\right)^4}\right)\right] \quad (2.27)$$

Method 3	$K = \mathrm{K_{f1}} + \mathrm{K_{f2}} + \mathrm{K_w}$ (2.28)

GK is also known as the Torsional rigidity of the section.

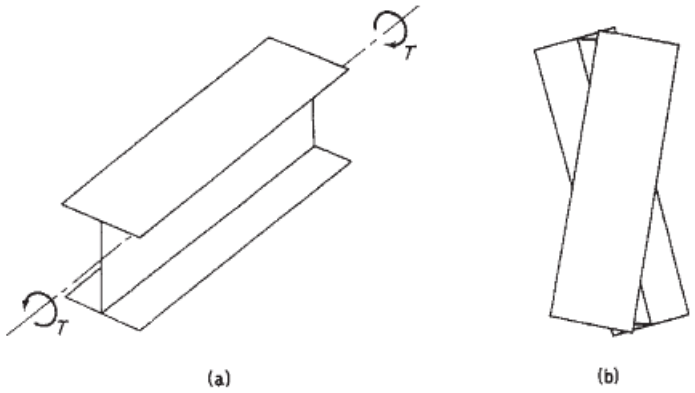

Figure 2-5 Free Torsion to I-Beam

A comparison of the Torsional stiffness GK for an isotropic I-Beam, where K is calculated by 3 different methods mentioned above is presented below in Table 2-4:

Table 2-4 Torsional Stiffness comparison for Isotropic I-Beam

Case	Torsional Stiffness, GK or GJ ($\mathrm{lb}-\mathrm{in}^2$)		
	Method 1 Eqs (2.22)	Method 2 Eqs (2.24)	Method 3 Eqs (2.28)
1	197.2	188.79	189.51
2	176.46	168.35	168.77
3	166.09	159.45	158.4

We observe that the torsional stiffness by method 2 and method 3 are quite comparable and hence we can use any of the width correction method to calculate the torsional stiffness.

2.5 Non-Uniform Torsion in Rectangular Section

When the warping deformation is constrained, the member undergoes non-uniform torsion. The presence of warping normal stresses in a thin walled, open cross-section member depends upon how the member is supported and how it is loaded. We will consider a cantilever type of arrangement where one end of the I-Beam is constrained and not allowed to warp while the other end is allowed to warp freely. The

warping restraint causes bending deformation of the flanges in their plane in addition to twisting. The Bending deformation is accompanied by a shear force in each flange.

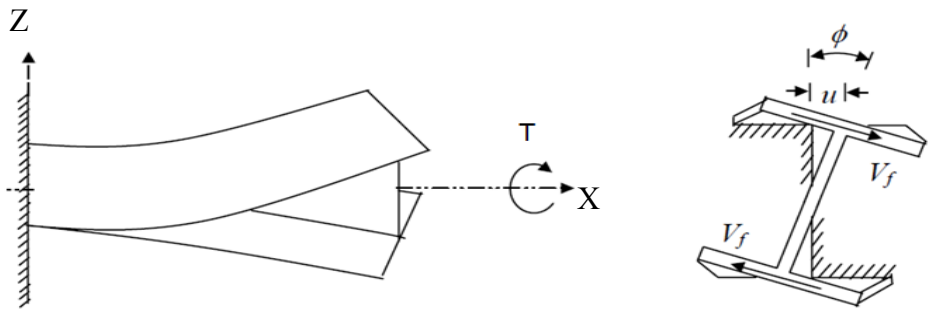

Figure 2-6 Restrained warping condition in I-Beam

Since, the flanges bend in opposite directions, the shear forces in two flanges are oppositely directed and form a couple. This couple, which acts to resist the applied torque, is called as the Warping torsion (T_w) as shown in Figure 2-6. This theory was originally developed by Wagner and Kappus, and is most generally known as the Wagner torsion bending theory. The complete derivation of T_w is very well documented in [12], [13], [14] and also [15].

$$T_w = -E\Gamma\frac{d^3\theta}{dx^3} \tag{2.29}$$

E = Axial Stiffness

Γ = Warping Constant, analogous to K, torsional constant

$E\Gamma$ = warping rigidity of the section, analogous to GK, St. Venant's torsional stiffness.

For I beam [15],

$$\Gamma = \frac{\mathrm{h}^2 * \mathrm{t_{f1}} * \mathrm{t_{f2}} * b_{f1}^3 * b_{f2}^3}{12\,(t_{f1}b_{f1}^3 + t_{f2}b_{f2}^3)} \tag{2.30}$$

The Torque will be resisted by a combination of St. Venant's shearing stresses and warping torsion. That is

$$T = T_{sv} + T_w \tag{2.31}$$

From Eqs. (2.20), (2.25) and (2.31) we have,

$$T = GK\frac{d\theta}{dx} - E\Gamma\frac{d^3\theta}{dx^3} \tag{2.32}$$

may now be solved for $\frac{d\theta}{dx}$. Rearranging and writing $\mu^2 = \frac{GK}{E\Gamma}$ we have,

$$\frac{d^3\theta}{dx^3} - \mu^2\frac{d\theta}{dx} = -\mu^2\frac{T}{GK} \tag{2.33}$$

Applying the boundary conditions

- The slope of the beam is zero when x = 0 and
- The Bending moment is zero at x = L

$$\frac{d\theta}{dx} = \frac{T}{GK}\left(1 - \frac{\cosh\mu\,(L-x)}{\cosh\mu L}\right) \tag{2.34}$$

The first term in Eq. (2.32) is seen to be the rate of twist derived from the St. Venant torsion theory. The hyperbolic second term is therefore the modification introduced by the axial constraint. The Eq. (2.32) can be further integrated to find the distribution of angle of twist θ, thus,

$$\theta = \frac{T}{GK}\left(x + \frac{\sinh\mu\,(L-x)}{\mu\cosh\mu L} - \frac{\sinh\mu\,L}{\mu\cosh\mu L}\right) \tag{2.35}$$

Thus we can also get the following,

$$\theta' = \frac{d\theta}{dx} = \frac{T}{GK}\left(1 - \frac{\cosh\mu\,(L-x)}{\cosh\mu L}\right) \tag{2.36}$$

$$\theta'' = \frac{d^2\theta}{dx^2} = \frac{T}{GK}\left(\frac{\mu\sinh\mu\,(L-x)}{\cosh\mu L}\right) \tag{2.37}$$

$$\theta''' = \frac{d^3\theta}{dx^3} = -\frac{T}{GK}\left(\frac{\mu^2\cosh\mu\,(L-x)}{\cosh\mu L}\right) \tag{2.38}$$

St. Venant Shearing stresses in flanges:

$$\tau_{sv} = 2Gn\frac{d\theta}{dx} \tag{2.39}$$

where n varies from -$^{t_{f1}}/_{2}$ to +$^{t_{f1}}/_{2}$ for upper flange and -$^{t_{f2}}/_{2}$ to +$^{t_{f2}}/_{2}$ for bottom flange. $\tau_{sv}\ is\ zero$ in the mid-plane of the flanges and maximum shear stresses occurs on the surface at the mid-point of the thickest part of the section. By Eq (2.35)and Eq (2.39) we get,

$$\tau_{sv} = 2Gn\frac{T}{GK}\left(1 - \frac{\cosh\mu\,(L-x)}{\cosh\mu L}\right) \tag{2.40}$$

Warping normal stresses:

In the presence of axial constraints, $\frac{d\theta}{dx}$ is no longer constant so that the longitudinal strains are not zero and direct stresses (σ_Γ) are induced and given by the below equation.

$$\sigma_\Gamma = -2A_R E\frac{d^2\theta}{dx^2} \tag{2.41}$$

where A_R is the area swept out by a generator, rotation about the center of twist, from the point of zero warping and given as below. Detailed description of A_R, p_R are avoided in this literature but described in detail in reference [12].

$$2A_R = \int_0^s p_R ds \tag{2.42}$$

$$p_{R\ above} = h - e \tag{2.43}$$

$$p_{R\ above} = \frac{ht_{f2}b_{f2}^3}{t_{f1}b_{f1}^3 + t_{f2}b_{f2}^3} \tag{2.44}$$

$$p_{R\ below} = e \tag{2.45}$$

$$p_{R\ below} = \frac{ht_{f1}b_{f1}^3}{t_{f1}b_{f1}^3 + t_{f2}b_{f2}^3} \tag{2.46}$$

$$s_{f1\,21} = -\frac{b_{f1}}{2}, s_{f1\,23} = \frac{b_{f1}}{2}, s_{f1\,54} = \frac{b_{f2}}{2}, s_{f1\,56} = -\frac{b_{f1}}{2} \tag{2.47}$$

From Eqs (2.37) (2.41) (2.42) (2.43) (2.44) (2.45) (2.46) & (2.47) we get,

$$\begin{aligned} \sigma_{\Gamma\,\mathrm{f1\,max}} &= \pm\left\{\frac{ht_{f2}b_{f2}^3}{t_{f1}b_{f1}^3 + t_{f2}b_{f2}^3} * \frac{b_{f1}}{2} * E\frac{T}{GK}\left(\frac{\mu \sinh \mu\,(L-x)}{\cosh \mu L}\right)\right\} \\ \sigma_{\Gamma\,\mathrm{f2\,max}} &= \pm\left\{\frac{ht_{f1}b_{f1}^3}{t_{f1}b_{f1}^3 + t_{f2}b_{f2}^3} * \frac{b_{f2}}{2} * E\frac{T}{GK}\left(\frac{\mu \sinh \mu\,(L-x)}{\cosh \mu L}\right)\right\} \end{aligned} \tag{2.48}$$

The above expression for stresses matches with the stress formulation in reference [15].

Warping

The expression for primary warping (w) is as below.

$$w = -2A_R\frac{d\theta}{dx} \tag{2.49}$$

From Eqs (2.35) (2.42) (2.43) (2.44) (2.45) (2.46) (2.47),

$$w_{21} = \frac{ht_{f2}b_{f2}^3}{t_{f1}b_{f1}^3 + t_{f2}b_{f2}^3} * s_{f1\,21} * \frac{T}{GK}\left(z + \frac{\sinh\mu\,(L-x)}{\mu\cosh\mu L} - \frac{\sinh\mu\,L}{\mu\cosh\mu L}\right)$$

$$w_{23} = \frac{ht_{f2}b_{f2}^3}{t_{f1}b_{f1}^3 + t_{f2}b_{f2}^3} * s_{f1\,23} * \frac{T}{GK}\left(z + \frac{\sinh\mu\,(L-x)}{\mu\cosh\mu L} - \frac{\sinh\mu\,L}{\mu\cosh\mu L}\right) \quad (2.50)$$

$$w_{21} = \frac{ht_{f1}b_{f1}^3}{t_{f1}b_{f1}^3 + t_{f2}b_{f2}^3} * s_{f1\,54} * \frac{T}{GK}\left(z + \frac{\sinh\mu\,(L-x)}{\mu\cosh\mu L} - \frac{\sinh\mu\,L}{\mu\cosh\mu L}\right)$$

$$w_{21} = \frac{ht_{f1}b_{f1}^3}{t_{f1}b_{f1}^3 + t_{f2}b_{f2}^3} * s_{f1\,56} * \frac{T}{GK}\left(z + \frac{\sinh\mu\,(L-x)}{\mu\cosh\mu L} - \frac{\sinh\mu\,L}{\mu\cosh\mu L}\right)$$

Shearing force:

The shearing force (V_F) induced in the flanges due to the constraints are given as,

$$V_F = \frac{dM_w}{dx} \quad (2.51)$$

$$V_F = E\Gamma\frac{d^3\theta}{dx^3} \quad (2.52)$$

$$V_F = -T\left(\frac{\cosh\mu\,(L-x)}{\cosh\mu L}\right) \quad (2.53)$$

Warping bending moment:

The expression for maximum bending moment which is creating in the flanges due to restrained torsion is as below:

$$M_{w\,f1\,max} = -E * \left(\frac{t_{f1} b_{f1}^3}{12}\right) * \frac{h t_{f2} b_{f2}^3}{t_{f1} b_{f1}^3 + t_{f2} b_{f2}^3} * \frac{d^2\theta}{dx^2} \tag{2.54}$$

$$M_{w\,f1\,max} = -E\Gamma \frac{T}{GK}\left(\frac{\mu \sinh \mu\,(L-x)}{\cosh \mu L}\right) \tag{2.55}$$

$$M_{w\,f1\,max} = -T\left(\frac{\sinh \mu\,(L-x)}{\cosh \mu L}\right) \tag{2.56}$$

$$M_{w\,f2\,max} = -T\left(\frac{\sinh \mu\,(L-x)}{\cosh \mu L}\right) \tag{2.57}$$

Chapter 3

Finite Element Method

3.1 Overview

Most of the real-world problems are too complicated to be solved analytically, because of various reasons like line geometry, boundary conditions, environmental conditions, etc. The complexity increases if we consider orthotropic material properties. If all these things are considered the analytical solutions are practically unreachable. Numerical Methods become the only feasible methods to solve those problems. The finite element method is one of the most successful numerical methods for boundary-value problems.

A basic idea of finite element method is to divide the entire structural body into many small and geometrically simple bodies, called elements, so that equilibrium equations can be written down and all the equilibrium equations are then solved simultaneously. The elements have finite size and hence the method is named Finite Element Methods (FEM). Nowadays, a large number of commercial programs exist with many finite element analysis capabilities for different engineering disciplines. They help solve a variety of problems from a simple linear static analysis to nonlinear transient analysis. A few of these codes, such as ANSYS™ or ABAQUS™, have special capabilities to analyze composite materials and they accept user programmed element formulations and custom constitutive equations. These softwares are commonly organized into three different blocks: the pre-processor, the processor and the post processor.

In the first block, commonly called pre-processor, we define the geometry, material properties and elements for the FEM. One should have good knowledge about these things as they have major contribution in the final results. With this information, the

processor computes the stiffness matrix of the model. In the second stage, we apply the boundary conditions and forces, which help in the formation of equilibrium equations that are later solved simultaneously. In the last block, the post processor, the derived results, such as strain, stress and failure ratios are computed and can be reviewed using graphic tools. We are going to use ANSYS™ 13 as the FEM tool to solve the isotropic and composite I – Beam problem.

3.2 Element Type

ANSYS™ has a variety of elements in its library. One should carefully select elements for modeling as it determines the element formulation used like the degree of freedom set, the interpolation functions, 1D, 2D or 3D space etc, Some of the element types are listed below which are used in ANSYS™ for composite modeling. For detailed understanding one can refer ANSYS™ help files [22]. Below are some highlights from the mentioned references.

1–Dimensional Elements:

BEAM188 and BEAM189 – These are 3-D finite strain beam elements. They are based on Timoshenko Beam Theory.

2–Dimensional Elements:

2-D elements are widely used in composite analysis. ANSYS™ offers a wide range of shell elements with different properties. Classical Lamination Theory of composites is based on Kirchhoff thin shell theory. In classical Kirchhoff thin shell theory it is difficult to derive finite element for other than very simple rectangular geometries. This is because to derive the bending strains we need to differentiate the transverse displacement twice. It is also difficult to derive shape function and Jacobian matrix for arbitrary shaped elements. So typically, to overcome the shortcomings of Kirchhoff theory

we use Mindlin theory. Mindlin theory takes transverse shear deformation into account. Also the Kirchhoff theory only provides acceptable deflections, natural frequencies and critical buckling loads for thin plates whose ratio of thickness to the characteristics dimension of mean surface is less than $^1/_{20}$. Mindlin theory, in which the transverse shear strains are constant through the plate thickness, gives satisfactory results for flexure, vibration and buckling of moderately thick plates whose ratio of thickness to the characteristic dimension of mean surface is between $^1/_5$ and $^1/_{20}$. Hence, shell elements in ANSYS™ are based on Mindlin theory. Also the elements can be layered or non-layered that is, one can specify individual layer properties or can specify the ABD matrices directly. All shell elements assumes plane stress condition.

SHELL93:

- It's a 4 node element
- Typically used for sandwitch applications
- Normally not a preferred type of element

SHELL181:

- Suitable for analyzing thin to moderately thick shell structures
- 4 node element with 6 degrees of freedom at each node
- Well suited for linear, large rotation and large strain non-linear applications
- Works on first order shear deformation theory (usually referred as Mindlin shell theory)
- Layered shell element and specific forms are highly accurate even in coarse mesh
- Includes linear effects of transverse shear deformation and also Interlaminar shear stresses evaluated at the layer interface are available

- A maximum of 250 elements are supported

SHELL281:

- Suitable for analyzing thin to moderately thick shell structures
- 8 node element with 6 degrees of freedom at each node
- Finite strain shell. Well suited for linear, large rotation and large strain non-linear applications
- Works on first order shear deformation theory (usually referred as Mindlin shell theory)
- Includes linear effects of transverse shear deformation and also Interlaminar shear stresses evaluated at the layer interface are available
- Layered shell element

Shell elements like SHELL91, SHELL99, and SHELL43 etc are no longer available in ANSYS™ 13.

3-Dimentional Elements;

A 2D element assumes plane stress conditions, so we will never be able to get the stress in the third direction. Also for thick composite laminates SHELL elements are normally avoided. 3-dimensional elements are preferred when we are modeling micromechanics model, when edge stresses are important as in the case of delamination analysis, also when we are interested in the stresses near the high stress concentration area, discontinuities etc. Use of 3D elements should be done wisely as they need high computer space to store the data, high computer configuration to solve the large amount of equations and thus directly related to cost of the analysis.

SOLID46:

- Layered version of 8-node 3D element SOLID45

- Can be used to model thick layered solids and allow 250 uniform thickness layers per element
- Finer meshes are necessary for accuracy

SOLID185:

- 3-D layered element with 8 nodes with 3 degrees of freedom on each node
- The element has plasticity, hyper-elasticity, stress stiffening, creep, large deflection and large strain capabilities
- Allows for prism and tetrahedral degenerations when used in irregular regions

SOLID186:

- Layered Solid with 20 node 3-D element with 3 degrees of freedom at each node
- Allow up to 250 layers and full nonlinear capabilities including large strain

SOLID191:

- Layered Solid with 20 node 3-D element with 3 degrees of freedom at each node
- Allows 100 layers per element
- Element does not support non linear materials or large deflections

3.3 Meshing

It is advisable to use mapped mesh for meshing the composite structure in ANSYS™. Also rectangular mesh should be used and triangular mesh should be avoided for composite modeling. The detailed explanations for this section can be found in the Master's thesis work of Farhan [21] and Chen [20]. Mesh density is also a critical aspect. It is normally preferred to have finer mesh in the region where load is applied, the region in which we are interested to get the stress and strain results and coarse mesh is acceptable in the other region of the structure. This can help to reduce the element numbers and make the model run faster and also cost effective.

In addition, the aspect ratio of the elements used is very critical. ANSYS™ recommends an aspect ratio of less than 10. Aspect Ratio of more than 20 could lead to inaccurate answers. But it is not easy to achieve aspect ratio of less than 10 always, so it is usually recommended to have it as low as possible. It is usually true that finer the mesh more accurate the solution [18]. Below are few points which validate the above statement.

- The nodal displacements are single valued, that is each node has a unique value. The displacement fields are continuous but not necessarily smooth. The use of continuous shape functions within the element guarantees the displacement fields piecewise smooth, but not necessarily smooth across the element boundaries. Stress values are calculated from strain and the calculations are element by element. The nodes may have multiple stress values, since the nodes may be connected to multiple elements and each element calculation results a value. Thus the stresses are not continuous across the element boundaries. By default, stresses are averaged in the nodes and the stress fields are recalculated. After that the stress values are continuous. Thus in general getting finer mesh, solution is more accurate and stress discontinuity is less.
- For an element, strain energies calculated using average stresses and un-averaged stresses respectively are different. The difference between these two energies is called as structural error of element. Finer the mesh, smaller the structural error. The structural error can be used for 2 purposes:
    - As an indicator of global mesh adequacy. In general, we want the values as small as possible.
    - As an indicator of local mesh adequacy. In general, we want the structural error distribution as uniform as possible to maximize the

efficiency of the computing resources. This implies that in the region of large values of structural error, we need to refine our mesh.

The final results are depended on the kind of elements used for the analysis. Always quadrilateral elements converge faster than triangular elements. Skewness is also one of the important mesh qualities. Skewness is calculated for each element according to the geometry. Definition of skewness can be found in the Help section of ANSYS™. But we can state that lower the skewness, better the answer. So as guideline, element skewness of more than 0.95 are considered un-acceptable.

3.4 Boundary Conditions

Type of boundary conditions (B.C) is specific to a particular composite problem. Symmetric B.C should be carefully enforced. It has been extensively studied by Chen [20] and Farhan [21] that if the symmetric conditions are applied to composite structures similar to that of isotropic material structures the results are not always correct. One should have an in-depth knowledge about composite materials and its axial-bending-torsional coupling behavior.

3.5 Geometry and Material Properties

Three cases of I-beam with different length of the flanges are considered for parametric study. However, all of the three I-beams have the same total length of laminates and with even and uneven top and bottom flanges. The dimensions and layup of the top, bottom flanges and web laminates are listed in Table 3-1.

Table 3-1 Dimensions and Stacking sequence of Flanges and Web of I-Beam for CASE 1, 2, 3

CASE	Width		Height
	Top Flange, in	Bottom Flange, in	Web, in
	$[\pm 45/0/90]_s$	$[\pm 45/0_2/90]_s$	$[\pm 45]_s$
1	0.25	1	0.5
2	0.5	0.75	0.5
3	0.625	0.625	0.5

The material used in this study is T300/977-2 graphite/epoxy laminate. The unidirectional layer orthotropic properties for the material are given as

$$E_1 = 21.75 \text{ x } 10^6 \text{ psi}, \quad E_2 = 1.595 \text{ x } 10^6 \text{psi}, \quad E_3 = 1.595 \text{ x } 10^6 \text{psi}$$

$$G_{12} = 0.8702 \text{ x } 10^6 \text{ psi}, \quad G_{23} = 0.5366 \text{ x } 10^6 \text{ psi}, \quad G_{13} = 0.8702 \text{ x } 10^6 \text{ psi}$$

$$\nu_{12} = 0.25, \qquad \nu_{23} = 0.45, \qquad \nu_{13} = 0.25, \qquad t_{ply} = 0.005\ in.$$

where E_1, E_2, and E_3 are the Young's moduli of the composite lamina along the material coordinates. G_{12}, G_{23}, and G_{13} are the Shear moduli and ν_{12}, ν_{23}, and ν_{13} are Poisson's ratio with respect to the 1-2, 2-3 and 1-3 planes, respectively and t_{ply} is the cured ply thickness.

The stacking sequences for the top and bottom flanges are $[\pm 45/0/90]_s$ and $[\pm 45/0_2/90]_s$ respectively.

3.6 Composite I-Beam Modeling in ANSYS

ANSYS™ Classic (APDL) version 13 is used to carry out all the FEM modeling and solutions in this thesis work. Simple steps are used to model the composite/isotropic I-Beam in ANSYS™ 13. Also the I-beam is considered to be an assembly of 3 rectangular cross section. The tool radius, ply drop-off and other features of a realistic I-beam are ignored. Details are as follows:

- Define Element type:

2D SHELL 181 is used for modeling the I-Beam. 3D elements are not used as 2D model will suffice our needs. In this thesis we are not interested in the 3D stresses, edge stresses and also the geometry is simple.

- Define Material type:

We will define orthotropic properties so that the same model can be used for isotropic and composite I-Beam by just modifying the material properties.

- Define Shell layup:

As we have different layups for bottom & top flange and web we will define all the 3 different types of layups. For converting composite model into isotropic we will just change all the angles to 0°.

- Define Keypoints:

As we are constructing 2D model, we need to create Areas and one of the simplest method is by defining the keypoints. The outer dimensions of the I-Beam would serve as the keypoints. For case 2, the keypoints are as listed in Table 3-2

Table 3-2 Keypoints for modeling I-Beam in ANSYS™

	Keypoints	X- Axis	Y- Axis	Z- Axis
Top Flange	1	0	0	0
	2	10	0	0
	3	0	-0.375	0
	4	10	-0.375	0
	5	0	0.375	0
	6	10	0.375	0
Web	7	0	0	-0.545
	8	10	0	-0.545
Bottom Flange	9	10	-0.25	-0.545
	10	10	0.25	-0.545
	11	0	0.25	-0.545
	12	0	-0.25	-0.545

As we are modeling 2D I-Beam, in ANSYS™ we define the midsection of web and flanges. So we need to modify the web height as it would be equal to

$$Modified\ web\ height = Original\ web\ height + \frac{Top\ flange\ thickness}{2} + \frac{Bottom\ flange\ thickness}{2}$$

Figure 3-1 below shows the Solid I-Beam and the Shell I-Beam.

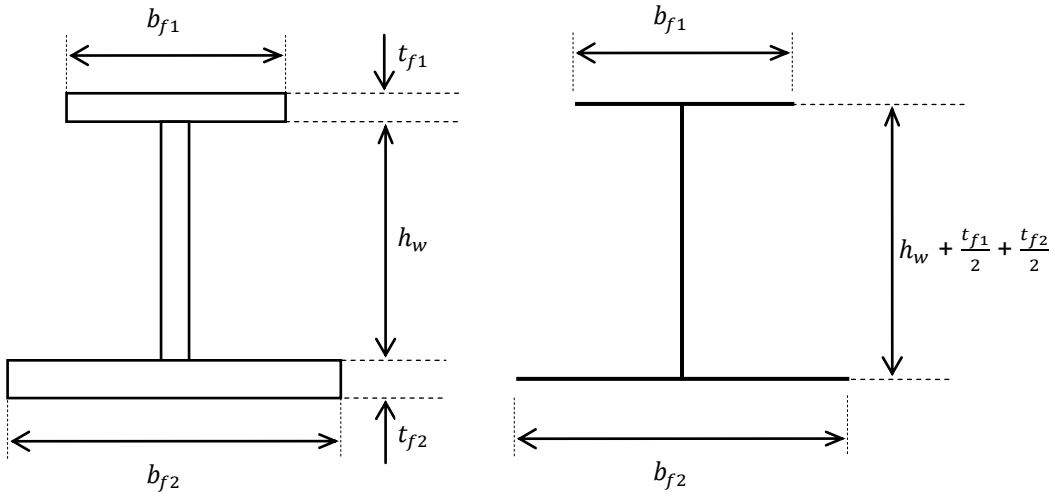

(a) Solid I-Beam Cross-Section (b) Shell I-Beam Cross- Section

Figure 3-1 2D I-Beam cross-section

- Define Areas:

We define areas by connecting the keypoints defined earlier. Figure 3-2 depicts the areas created with the help of keypoints to form I-Beam in ANSYS™ 13.

Table 3-3 shows the list of keypoints connected to form areas for I-Beam for Case 2.

Table 3-3 Areas created by connection key-points

Area	Keypoints connected
Top Flange	5, 1, 2, 6
	3, 1, 2, 4
Web	1, 7, 8, 2
Bottom Flange	11, 7, 8, 10
	12, 7, 8, 9

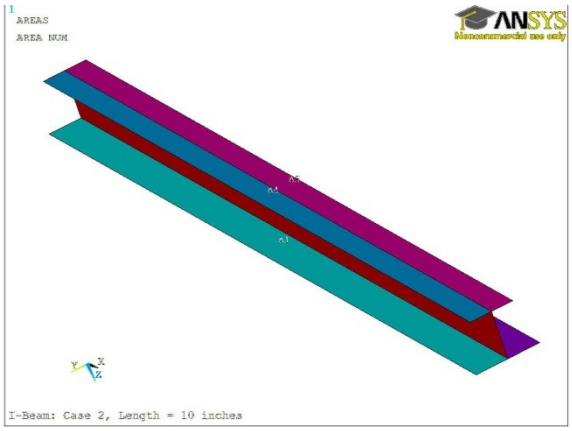

Figure 3-2 Different Areas created with the help of Keypoints to model I-Beam in ANSYS™ 13

- Define Local co-ordinate system:

The Global co-ordinate system is assigned to the flanges such that X-Axis represents the length of flange and Y-Axis will represent the width. But for the web we need to define a local co-ordinate system so that X-axis will be the length and Y-Axis will be the height. For doing this we rotate the co-ordinate system by -90° with respect to global X-axis. Figure 3-3 shows that different co-ordinate system are assigned to web and flanges

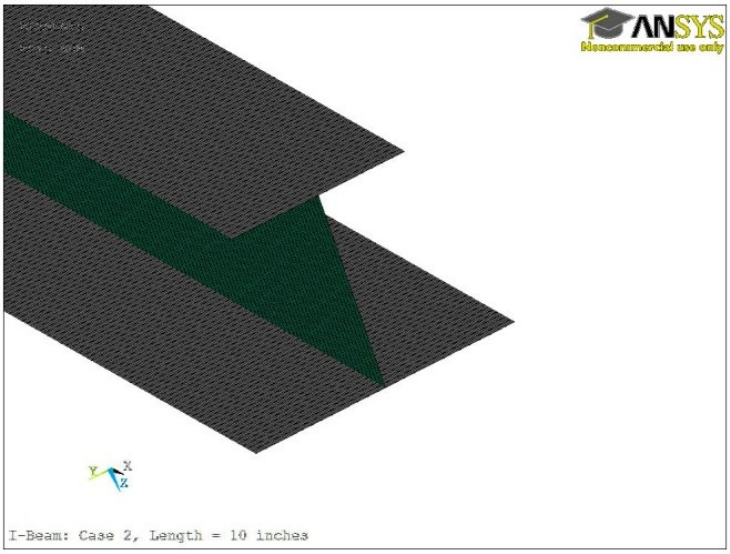

Figure 3-3 Flange Areas assigned global co-ordinate system and Web assigned local co-ordinate system

- Define Meshing Attributes:

This is the most important step. Here we assign properties like element type, material type, co-ordinate system, layup to the areas we modeled.

- Define element Size:

Element sizing will define our mesh which in turn will decide the accuracy of our results. To get good fine mesh manual meshing option is used. For case 2, the bottom flange is divided into 150 elements in width and 200 elements in length, top flange is divided into 100 elements in width and 200 elements in length and web is divided into 110 elements in height and 200 elements in length. This assures a very fine mesh with an Aspect ratio less than 10 all over the I-Beam. We can also use the smart size option where we ensure a dense mesh in the areas where loads are applied and results are recorded, and a coarse mesh in the remaining area. For the I-Beam with the number of elements chosen we do get satisfactory results and hence smart meshing is not used.

- Meshing

After defining the meshing attributes and element size, all the areas are meshed. As the element size is manually decided we do get a mapped mesh all over the I-Beam. Figure 3-4 shows the I-Beam with mesh generated with different meshing attributes.

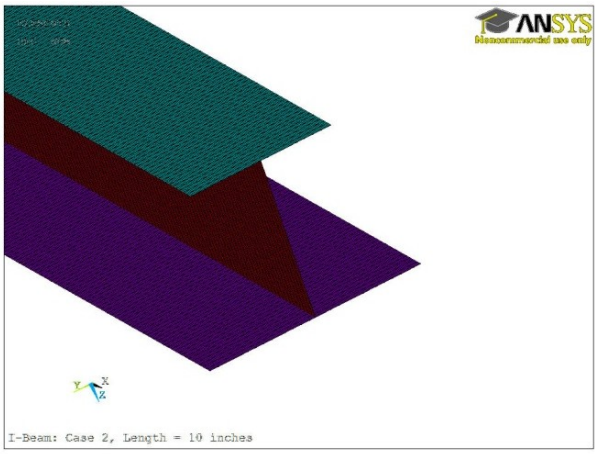

Figure 3-4 Mesh generated, different meshing attributes to all the 3 areas

- Define Loads and Boundary Conditions:

For Constrained torsion:

The load is the torsional moment for the I-Beam considered. So we apply moment in X-direction to all the nodes on one of the extreme cross-section. The Moment magnitude is specified as $\left({}^{1}/_{Number\ of\ Nodes\ in\ the\ cross\ section}\right)$ as shown in Figure 3-6. This ensures that the total torsional moment is 1 lb-in. To apply cantilever boundary conditions, we constrained all the degrees of freedom (DOF) of all the nodes on the other extreme cross-section as shown in Figure 3-5. This will ensure a constrained torsion condition.

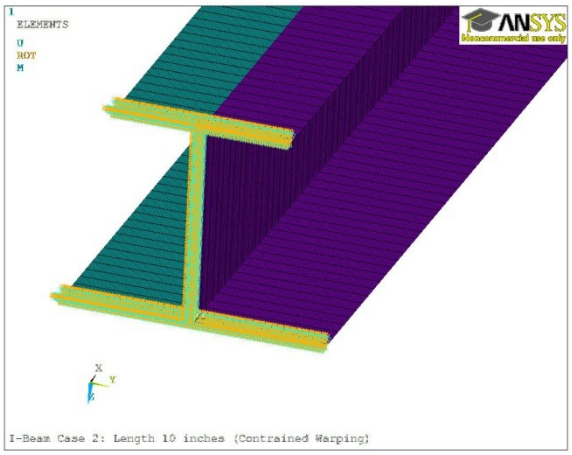

Figure 3-5 Constrain all DOF of nodes of one end of I-Beam

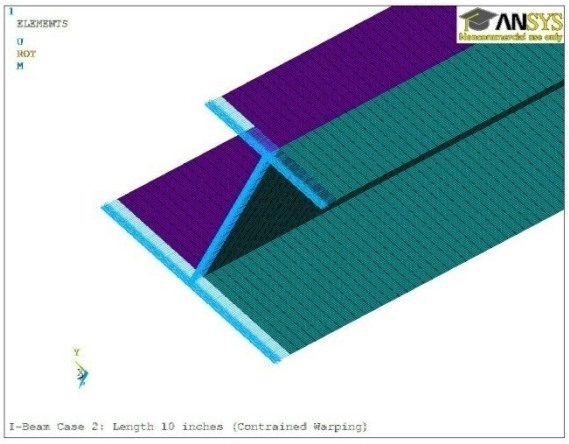

Figure 3-6 Torsional load applied to all the nodes of the I-Beam cross section on the other end

For Free Torsion (unrestrained torsion):

To get free torsion, we locate the shear center in the middle of beam length and constrain all the degrees of freedom of the node present there. We apply moment on the other two free ends as discussed above. On one side, torsional moment would be $\left({}^{1}/_{Number\ of\ Nodes\ in\ the\ cross\ section}\right)$ and on the other side it would be

$-\left({}^{1}/_{Number\ of\ Nodes\ in\ the\ cross\ section}\right)$. This loading and Boundary conditions will ensure a free torsion in I-Beam.

- Solve

After applying all the required loads and boundary conditions we give the solve command to ANSYS™ and get the desired results. Figure 3-7 shows the deformed I-beam.

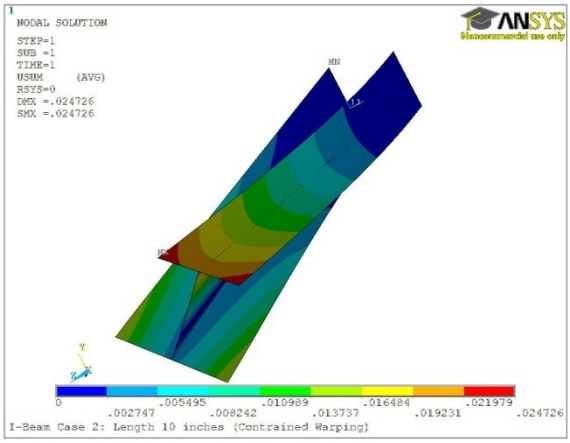

Figure 3-7 Deformed I-Beam under restrained Torsion

3.7 Validation of ANSYS™ I-Beam Model

We need to validate our ANSYS™ I-Beam Model. For this purpose we will compare our ANSYS™ results for the Isotropic I-Beam case. The closed form solution for Isotropic I-Beam is discussed in Chapter 2. The isotropic properties used for validation purpose are:

$$E = E_{11} = E_{22} = E_{33} = 1.02 \text{ x } 10^{7} \text{ psi}$$

$$\nu = \nu_{12} = \nu_{23} = \nu_{13} = 0.25$$

$$G = G_{12} = G_{23} = G_{13} = \frac{E}{2(1+\nu)} = 4.08 \text{ x } 10^{6} \text{ psi}$$

Length of the I-Beam considered for Free Torsion is 20 inches and for constrained condition it is 10 inches if not specified. At first, we will compare the following properties for all the 3 cases of I-Beam mentioned in Table 2-1:

K = Torsional constant

Γ = Warping Constant

GK = Torsional Rigidity

EΓ = Warping rigidity of the section

e = Shear Center

θ_{SV} = Angle of twist in free torsion case

θ_{warp} = Angle of twist in constrained torsion case

3.8 Methodology adapted to get the above mentioned properties:

The I-Beam is subjected to free torsion and the deformed shape is obtained. The shear center can be located as the point which has the least or no displacement that is, the point which remained stationary. Figure 3-8 shows the deformed and original I beam cross section. The Shear Center locations documented are all from the base of the bottom flange. So $\left(\frac{thickness\ of\ bottom\ flange}{2}\right)$ is added to the result obtained from the ANSYS™. The angle of twist is evaluated by applying the Pythagorean Theorem to the triangle formed as shown in Figure 3-8. 'A' is the point of intersection of web with bottom flange and A' denotes the displacement of point "A", SC denotes the Shear Center. We can also consider the other triangle but it was noticed that the error in calculating the θ_{SV} is less when considered the smaller triangle. Distance AA' is the displacement result by ANSYS™. Thus

$$\theta_{SV} = \tan^{-1}\left(\frac{displacement\ of\ point\ A}{Distance\ of\ point\ A\ from\ the\ Shear\ Center}\right) radians$$

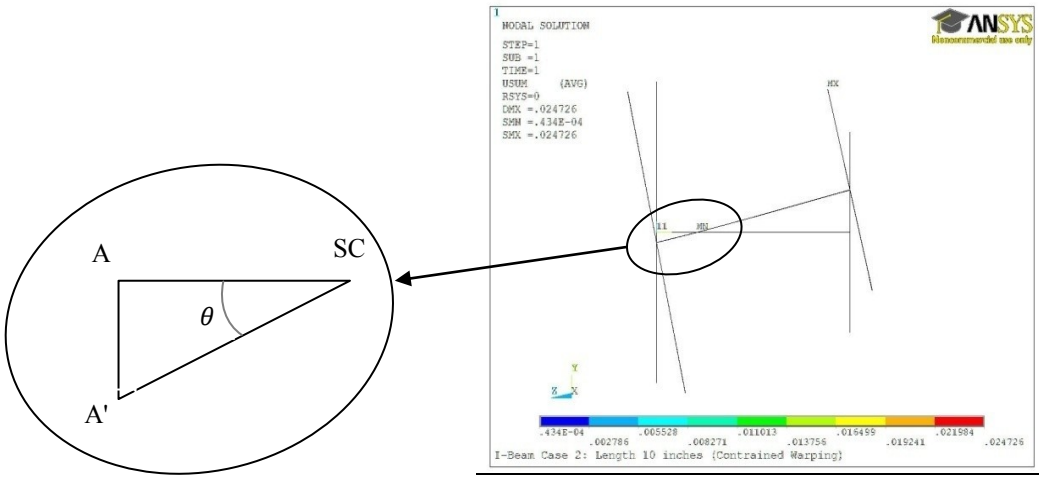

Figure 3-8 Cross section of I-Beam Twisting at its Shear Center

ANSYS™ FEM model would also give the angle of rotation of each node as part of result. One can directly use this rotation result as θ_{SV}. Once θ_{SV} is calculated we can calculate Torsional constant and Torsional Rigidity by applying the below given expressions respectively:

$$K = \frac{T * L}{G * \theta_{SV}}$$

$$GK = \frac{T * L}{\theta_{SV}}$$

To evaluate the warping constant and warping rigidity the I-Beam is given a constrained torsion and θ_{warp} is evaluated in the similar method as mentioned for θ_{SV}. Warping constant is evaluated by the using equation (2.35) for x = L, the equation simplifies to:

$$\theta_{warp} = \frac{T * L}{GK}\left(1 - \frac{\tanh(\mu\, L)}{(\mu\, L)}\right)$$

The only unknown in the above expression is μ, so it can be easily evaluated by solving the above expression.

$$\mu^2 = \frac{GK}{E\Gamma}$$

Thus warping constant and warping rigidity are calculated by using the relationship mentioned above.

We can also get the above properties from the BEAM TOOL in ANSYS™. So the result from the ANSYS™ BEAM TOOL, Analytical and from the ANSYS™ I-Beam model which is modeled are tabulated in Table 3-4, Table 3-5 & Table 3-6. By observing the data presented we can ensure that SHELL 2D ANSYS™ model gives satisfactory results and the same model can be used for the study of composite material I -Beam torsional analysis by making suitable modifications in material properties and defining the layups.

Also the analytical torsional stiffness GK values mentioned in the tables are the once which are calculated by method 3 in chapter 2 by Eqs (2.28). We conclude that the width correction is necessary to calculate the torsional constant K, so as to get better comparable results with ANSYS™ FEM model.

Table 3-4 Comparison of Torsional properties and angle of twist of Isotropic I-Beam with ANSYS™ results for CASE 1

Case 1: Isotropic material				
	ANSYS™ BEAM TOOL	Analytical	ANSYS™ I-BEAM Model	Difference % (Analytical and ANSYS™ model)
K (in^4) Torsional Constant	$4.7 \text{ x } 10^{-5}$	$4.645 \text{ x } 10^{-5}$	$4.6838 \text{ x } 10^{-5}$	-0.84
$\Gamma(\text{in}^4)$ Warping Constant	$1.61 \text{ x } 10^{-5}$	$1.528 \text{ x } 10^{-5}$	$1.4859 \text{ x } 10^{-5}$	2.75
$GK(\text{psi} - \text{in}^4)$ Torsional Rigidity	192.17	189.51	191.09	-0.84
$E\Gamma\ (\text{psi} - \text{in}^4)$ WARPING Rigidity	164.22	155.85	151.56	2.75
Shear Center(in)	0.0319	0.0317	0.0329 (constrained torsion)	-3.86
θ_{SV} (rad)	-	0.0528	0.0523	0.88
θ_{warp} (rad)	-	0.0480	0.0482	-0.41

Table 3-5 Comparison of Torsional properties and angle of twist of Isotropic I-Beam with ANSYS™ results for CASE 2

Case 2: Isotropic material				
	ANSYS™ BEAM TOOL	Analytical	ANSYS™ I-BEAM Model	Difference % (Analytical and ANSYS™ model)
K(in^4) Torsional Constant	$4.2 \text{ x } 10^{-5}$	$4.1366 \text{ x } 10^{-5}$	$4.1855 \text{ x } 10^{-5}$	-1.18
Γ(in^4) Warping Constant	$1.0 \text{ x } 10^{-4}$	$1.0005 \text{ x } 10^{-4}$	$9.4372 \text{ x } 10^{-5}$	5.67
GK $(\text{psi} - \text{in}^4)$ Torsional Rigidity	171.36	168.77	170.77	-1.19
EΓ $(\text{psi} - \text{in}^4)$ WARPING Rigidity	1020	1020.47	962.59	5.67
Shear Center(in)	0.1296	0.1295	0.1385 (constrained torsion)	-6.92
θ_{SV} (rad)	-	0.0593	0.0585	1.27
θ_{warp} (rad)	-	0.0447	0.0446	0.14

Table 3-6 Comparison of Torsional properties and angle of twist of Isotropic I-Beam with ANSYS™ results for CASE 3

Case 3: Isotropic material				
	ANSYS™ BEAM TOOL	Analytical	ANSYS™ I-BEAM Model	Difference % (Analytical and ANSYS™ model)
K (in^4) Torsional Constant	$3.94 \text{ x } 10^{-5}$	$3.8825 \text{ x } 10^{-5}$	$3.8395 \text{ x } 10^{-5}$	1.11
$\Gamma(\text{in}^4)$ Warping Constant	$1.34 \text{ x } 10^{-4}$	$1.3429 \text{ x } 10^{-4}$	$1.2536 \text{ x } 10^{-4}$	6.65
GK $(\text{psi} - \text{in}^4)$ Torsional Rigidity	160.75	158.4	156.65	1.10
EΓ $(\text{psi} - \text{in}^4)$ WARPING Rigidity	1366.8	1369.74	1278.72	6.65
Shear Center(in)	0.2673	0.2672	0.2757 (constrained torsion)	-3.18
θ_{SV} (rad)		0.0631	0.0638	-1.06
θ_{warp} (rad)		0.0446	0.0456	-2.23

Effect of Warping constraint on the twist angle was also studied. Comparison between angle of twist with free torsion and warping torsion with varying length of I-Beam for Case 2 is tabulated in Table 3-7. Observing the data we can conclude that:

The effect on twisting is significant in shorter I-Beams due to Constrained Warping as shown in Figure 3-9. Shear center results of ANSYS™ converges to the theoretical value when the I-Beam is longer as observed in

Figure 3-10.

Table 3-7 Comparison of angle of twist and shear center for Isotropic Case 2 with ANSYS™ results

Total length (Case 2)	θ_{warp} Analytical (rad)	θ_{SV} Analytical (Rad)	Effect of warping on I beam (%)	θ_{warp} ANSYS™ (rad)	Diff (θ_{warp} Analytical and θ_{warp} ANSYS™ (%)	Shear Center Analytical(inch)	Shear Center ANSYS ™ (inch)	Diff SC (%)
3	0.0055	0.0178	68.83	0.0054	2.00	0.1295	0.1216	6.09
4	0.0102	0.0237	56.90	0.0096	5.82		0.1365	-5.39
5	0.0155	0.0296	47.52	0.0149	4.35		0.1409	-8.83
7	0.0270	0.0415	34.89	0.0269	0.31		0.1399	-8.06
10	0.0447	0.0593	24.58	0.0451	-0.81		0.1375	-6.15
20	0.1039	0.1185	12.30	0.1039	-0.01		0.1335	-3.09

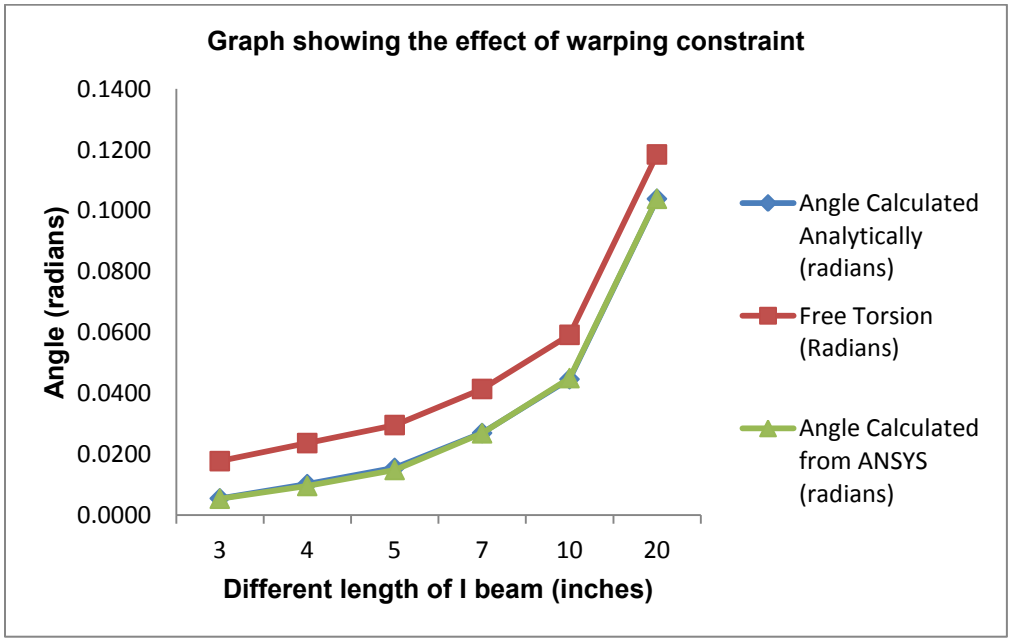

Figure 3-9 Graphical representation showing effect of warping constraint on the angle of twist

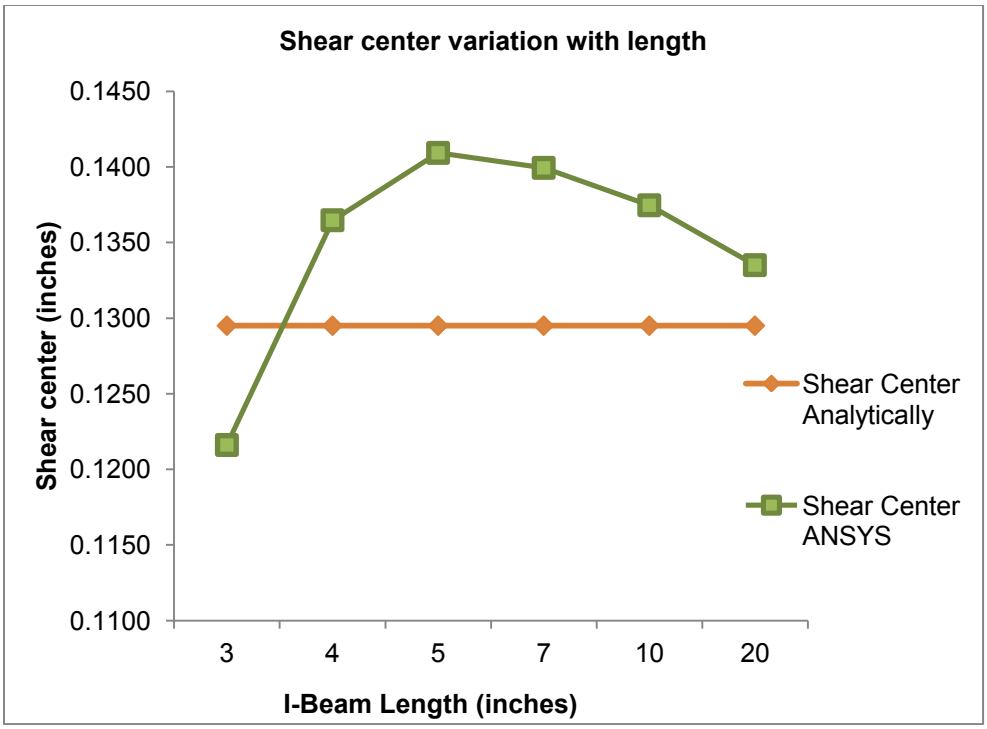

Figure 3-10 Graphical representation of Shear center variation with respect to length

Variation of twisting angle at different location lengthwise was also studied. For this purpose, a 20 inch long I-Beam with cross-sectional properties of case 2 was studied and it was found that the relationship is linear. ANSYS™ and theoretical results have a very good match after 3 inches from the constrained boundary. Results are tabulated in Table 3-8 and shown graphically in Figure 3-11. Also the variation in the shear center location at different length is plotted.

Table 3-8 Study of angle of twist variation along the I-Beam length

Study of angle of twist variation in a 20 inch long I beam (cantilever) Case 2 considered for this study				
Length variation (inches)	Angle in (radians) Analytical	Angle in (radians) ANSYS™	Difference in angle	Shear center (ANSYS™)
0	0.0000	0.0000	0.00	0.0000
1	0.0011	0.0018	-69.51	0.0869
2	0.0037	0.0047	-25.94	0.1087
3	0.0075	0.0084	-12.16	0.1191
4	0.0120	0.0128	-6.80	0.1241
5	0.0170	0.0177	-4.35	0.1266
6	0.0223	0.0230	-3.37	0.1276
7	0.0278	0.0287	-3.38	0.1276
8	0.0334	0.0340	-1.84	0.1291
9	0.0391	0.0398	-1.79	0.1291
10	0.0449	0.0457	-1.73	0.1291
11	0.0508	0.0514	-1.20	0.1295
12	0.0566	0.0573	-1.20	0.1295
13	0.0626	0.0633	-1.10	0.1295
14	0.0684	0.0693	-1.30	0.1295
15	0.0743	0.0754	-1.44	0.1295
16	0.0803	0.0816	-1.68	0.1295
17	0.0862	0.0876	-1.61	0.1300
18	0.0921	0.0931	-1.08	0.1310
19	0.0980	0.0992	-1.18	0.1315
20	0.1040	0.1039	0.05	0.1335

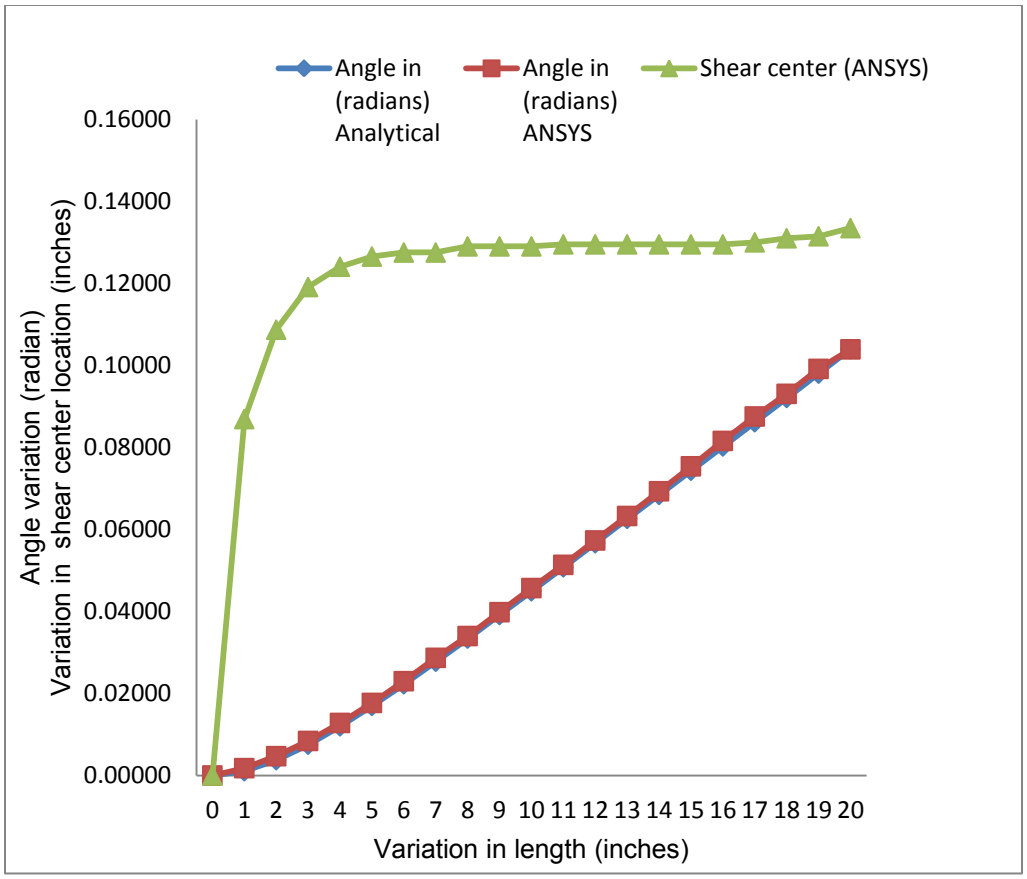

Figure 3-11 Graphical representation of shear center and angle of twist variation

Chapter 4

Torsional Behavior of a Composite I-Beam

4.1 Brief overview of lamination theory

Lamina Constitutive Equation:

Since composite lamina is very thin, a state of plane stress is assumed for the analysis purpose. Two co-ordinate systems as shown in Figure 4-1 are used to completely describe the properties of lamina

- 1-2-3 co-ordinates refer to the lamina (local co-ordinate system) where 1 is the fiber direction, 2 is the transverse direction and 3 is perpendicular to the ply plane.
- x-y-z co-ordinate system are the global co-ordinate system and are selected at mid-plane of laminates.

$$\sigma_3 = \tau_{13} = \tau_{23} = 0$$

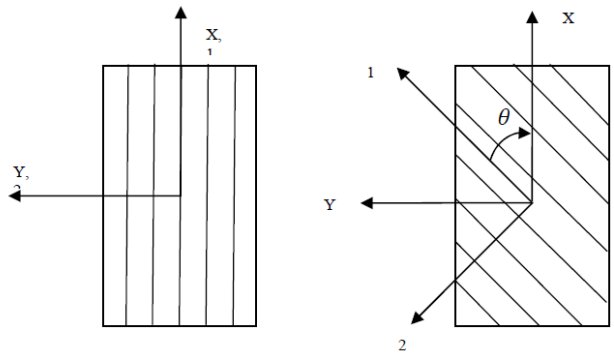

Figure 4-1 Local and Global co-ordinate system in lamina

Therefore, orthotropic stress strain relation reduces to 3 x 3 matrix in a composite lamina. The strain-stress relation is written as

$$[\varepsilon]_{1-2} = [S]_{1-2}[\sigma]_{1-2}$$

$$\begin{bmatrix}\varepsilon_1\\ \varepsilon_2\\ \gamma_{12}\end{bmatrix} = \begin{bmatrix}S_{11} & S_{12} & 0\\ S_{12} & S_{22} & 0\\ 0 & 0 & S_{66}\end{bmatrix}\begin{bmatrix}\sigma_1\\ \sigma_2\\ \tau_{12}\end{bmatrix} \quad (4.1)$$

and stress-strain relationship is

$$\begin{bmatrix}\sigma_1\\ \sigma_2\\ \tau_{12}\end{bmatrix} = \begin{bmatrix}Q_{11} & Q_{12} & 0\\ Q_{12} & Q_{22} & 0\\ 0 & 0 & Q_{66}\end{bmatrix}\begin{bmatrix}\varepsilon_1\\ \varepsilon_2\\ \gamma_{12}\end{bmatrix} \quad (4.2)$$

where,

$\varepsilon_1\ and\ \varepsilon_2$ = strain in 1 and 2 directions, respectively

γ_{12} = shear strain in 1-2 plane

$[S]_{1-2}$ = compliance matrix of the order 3 x 3 in 1-2 co-ordinate system

$[Q]_{1-2}$ = reduced stiffness matrix of the order 3 x 3 in 1-2 co-ordinate system

$$S_{11} = \frac{1}{E_1}\ ;\ S_{22} = \frac{1}{E_2}\ ;\ S_{12} = -\frac{\upsilon_{12}}{E_1} = -\frac{\upsilon_{21}}{E_2}\ ;\ S_{66} = \frac{1}{G_{12}}$$

$$Q_{11} = \frac{E_1}{1-\upsilon_{12}\upsilon_{21}}\ ;\ Q_{22} = \frac{E_2}{1-\upsilon_{12}\upsilon_{21}} \quad (4.3)$$

$$Q_{12} = \frac{\upsilon_{21}E_1}{1-\upsilon_{12}\upsilon_{21}} = \frac{\upsilon_{12}E_2}{1-\upsilon_{12}\upsilon_{21}}\ ;\ Q_{66} = G_{12}$$

where,

$E_1, E_2, \upsilon_{12}, G_{12}$ are 4 independent material constants.

Axis Transformation relationship:

The relationship of the compliance matrix in x-y co-ordinate system and 1-2 co-ordinate system is as follows:

$$[\bar{S}]_{x-y} = [T_\varepsilon(-\theta)][S]_{1-2}[T_\sigma(\theta)] \quad (4.4)$$

The relationship of the reduced stiffness matrix in x-y co-ordinate system and 1-2 co-ordinate system is as follows:

$$[\bar{Q}]_{x-y} = [T_\sigma(-\theta)][Q]_{1-2}[T_\varepsilon(\theta)] \tag{4.5}$$

where,

$[\bar{S}]_{x-y}$ = Compliance matrix in x-y co-ordinate system

$[\bar{Q}]_{x-y}$ = Reduced stiffness matrix in x-y co-ordinate system

$$[T_\varepsilon(\theta)] = \begin{bmatrix} m^2 & n^2 & mn \\ n^2 & m^2 & -mn \\ -2mn & 2mn & m^2 - n^2 \end{bmatrix}$$

$$[T_\sigma(\theta)] = \begin{bmatrix} m^2 & n^2 & 2mn \\ n^2 & m^2 & -2mn \\ -mn & mn & m^2 - n^2 \end{bmatrix} \tag{4.6}$$

$$m = cos\theta \; ; \; n = sin\theta$$

where,

θ = angle by which the axis is rotated about z-axis

Thus, the stress-strain relationship for angle ply with θ degree fiber orientation in x-y co-ordinate system is,

$$\begin{bmatrix} \sigma_x \\ \sigma_y \\ \tau_{xy} \end{bmatrix} = \begin{bmatrix} \overline{Q_{11}} & \overline{Q_{12}} & \overline{Q_{16}} \\ \overline{Q_{12}} & \overline{Q_{22}} & \overline{Q_{26}} \\ \overline{Q_{16}} & \overline{Q_{26}} & \overline{Q_{66}} \end{bmatrix} \begin{bmatrix} \varepsilon_x \\ \varepsilon_y \\ \gamma_{xy} \end{bmatrix} \tag{4.7}$$

or

$$[\sigma]_{x-y} = [\bar{Q}]_{x-y}\,[\varepsilon]_{x-y}$$

4.2 Classical Lamination Theory (CLT):

The gist of classical lamination theory is described below. For thorough understanding of CLT one can refer any textbook or reference books on the mechanics of composite materials. The theory provided below is from Ref. [23] and [24]. CLT is commonly used to analyze the behavior of laminated composite to evaluate stresses and strains in individual plies in the laminate. Following are the assumptions of CLT:

1. Each Layer of the laminate is quasi-homogeneous and orthotropic.

2. The laminate is thin with its lateral dimensions much larger than its thickness and is loaded in its plane only, i.e., the laminate and its layer (except for their edges) are in a state of plane stress.
3. All displacements are small compared with the thickness of the laminate.
4. Displacements are continuous throughout the laminate.
5. In-plane displacements vary linearly through the thickness of the laminate, i.e., u and v displacements in the x and y directions are linear functions of z.
6. Transverse shear strain γ_{xz} and γ_{yz} are negligible. This assumption and the preceding one imply that straight lines normal to the middle surface remain straight and normal to that surface after deformation.
7. Strain-displacement and stress-strain relations are linear.
8. Normal distances from the middle surface remain constant, i.e., the transverse normal strain ε_z is negligible (compared with the in-plane strains ε_x and ε_y).

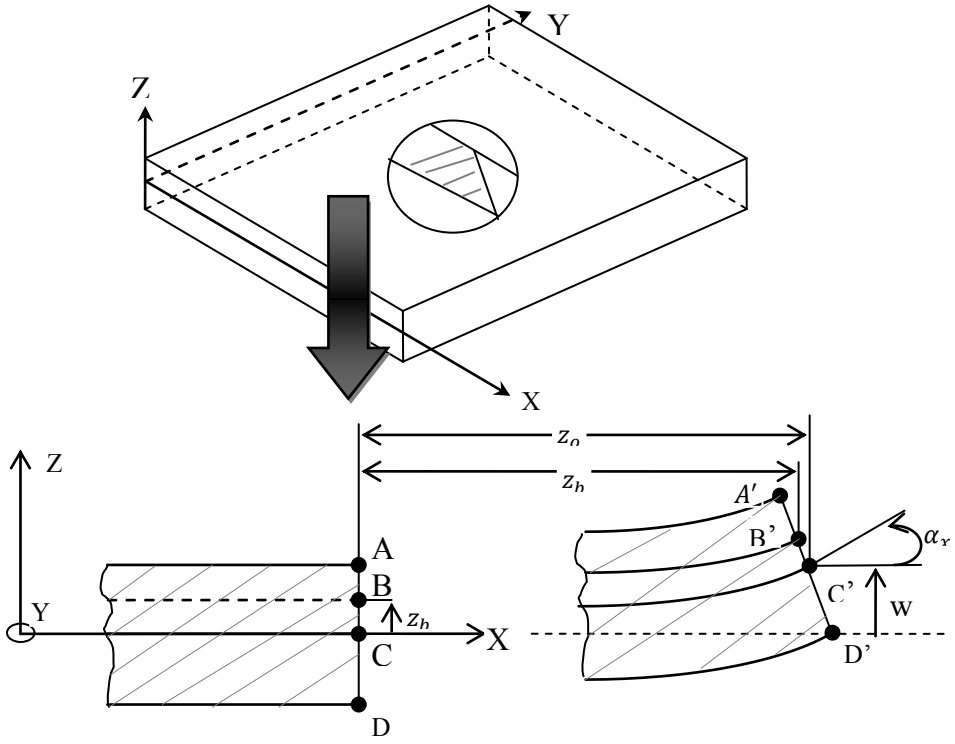

Figure 4-2 Laminate section before (ABCD) and after (A'B'C'D') deformation

The reference plane of laminated plate is located at the mid-plane of the plate as shown in Figure 4-2. The displacements of the mid-plane is assumed to be

$$u_0 = u_0(x,y);\ v_0 = v_0(x,y);\ w_0 = w_0(x,y) \tag{4.8}$$

The displacement of any points can be written as

$$u = u_0 - z\frac{\partial w}{\partial x}\ ; v = v_0 - z\frac{\partial w}{\partial y} \tag{4.9}$$

where, z is the co-ordinate variable of a general point of the cross section. For small displacements, the classical strain-displacement relations of elasticity yields,

$$\varepsilon_x = \frac{\partial u}{\partial x} = \frac{\partial u_0}{\partial x} - z\frac{\partial^2 w}{\partial x^2}$$

$$\varepsilon_y = \frac{\partial v}{\partial y} = \frac{\partial v_0}{\partial y} - z\frac{\partial^2 w}{\partial y^2} \tag{4.10}$$

$$\gamma_{xy} = \frac{\partial u}{\partial y} + \frac{\partial v}{\partial x} = \frac{\partial u_0}{\partial y} + \frac{\partial v_0}{\partial x} - 2z\frac{\partial^2 w}{\partial x \partial y}$$

Noting that the strain components on the reference plane are expressed as:

$$\varepsilon_x^0 = \frac{\partial u_0}{\partial x}\ ;\ \varepsilon_y^0 = \frac{\partial v_0}{\partial y}\ ;\ \gamma_{xy}^0 = \frac{\partial u_0}{\partial y} + \frac{\partial v_0}{\partial x} \tag{4.11}$$

And the curvatures of the laminate as:

$$\kappa_x = -\frac{\partial^2 w}{\partial x^2}\ ;\ \kappa_y = -\frac{\partial^2 w}{\partial y^2}\ ;\ \kappa_{xy} = -2\frac{\partial^2 w}{\partial x \partial y} \tag{4.12}$$

We can relate the strains at any point in the laminate Figure 4-3 to the reference plane strains and the laminate curvatures as follows:

$$\begin{bmatrix} \varepsilon_x \\ \varepsilon_y \\ \gamma_{xy} \end{bmatrix} = \begin{bmatrix} \varepsilon_x^0 \\ \varepsilon_y^0 \\ \gamma_{xy}^0 \end{bmatrix} + z\begin{bmatrix} \kappa_x \\ \kappa_y \\ \kappa_{xy} \end{bmatrix} \tag{4.13}$$

The stresses of the kth layer in the laminate can be written as

$$\left[\sigma_{x-y}\right]_{k^{th}} = \left[\bar{Q}_{x-y}\right]_{k^{th}}\left[\varepsilon_{x-y}\right]_{k^{th}}$$

i.e. (4.14)

$$\left[\sigma_{x-y}\right]_{k^{th}} = \left[\bar{Q}_{x-y}\right]_{k^{th}}\left(\left[\varepsilon^0{}_{x-y}\right] + z_{k^{th}}\left[\kappa_{x-y}\right]\right)$$

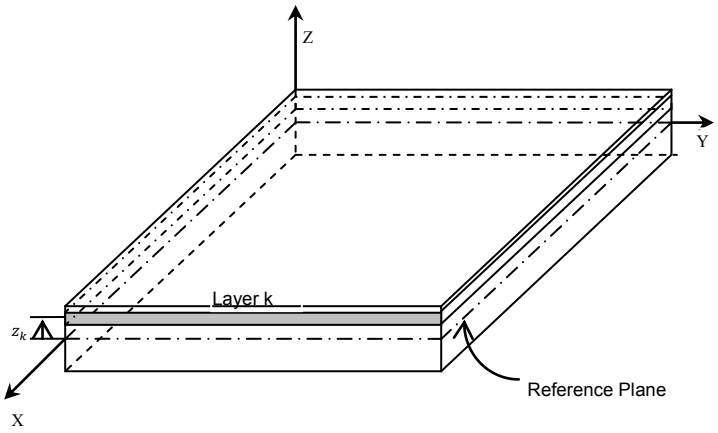

Figure 4-3 Layer k within laminate

Force and Moment resultant

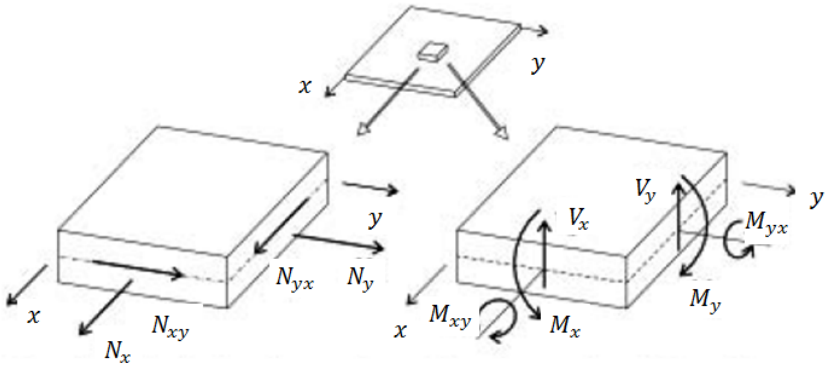

Figure 4-4 In-plane forces acting at the reference plane (left) and the moment and the transverse shear forces (right)

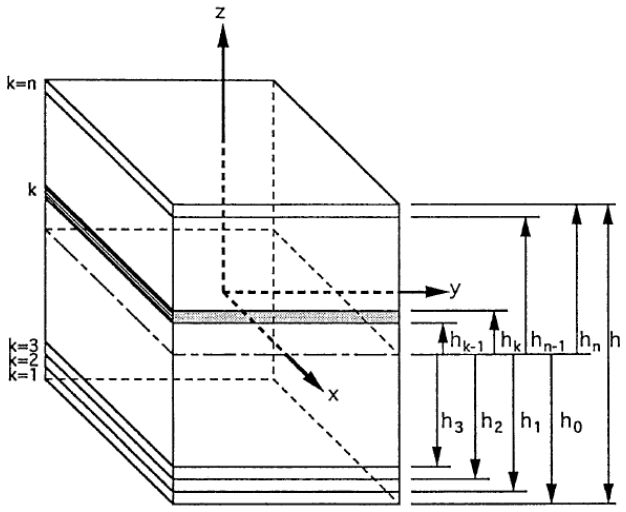

Figure 4-5 Multidirectional laminate with co-ordinate notation of individual plies

The sum of forces and moment in each layer Figure 4-4, Figure 4-5 is given as:

$$\begin{bmatrix} N_x \\ N_y \\ N_{xy} \end{bmatrix} = \sum_{k=1}^{n} \int_{h_{k-1}}^{h_k} \begin{bmatrix} \sigma_x \\ \sigma_y \\ \tau_{xy} \end{bmatrix}_k dz \quad (\frac{lb}{in})$$

$$\begin{bmatrix} M_x \\ M_y \\ M_{xy} \end{bmatrix} = \sum_{k=1}^{n} \int_{h_{k-1}}^{h_k} \begin{bmatrix} \sigma_x \\ \sigma_y \\ \tau_{xy} \end{bmatrix}_k z dz \quad (\frac{lb-in}{in}) \tag{4.15}$$

where,

z = The coordinate variable of a point in the cross section

t = Layer thickness

N_x , N_y = Normal forces per unit lenght

N_{xy} = Shear forces per unit lenght

M_x , M_y = Bending moments per unit lenght

M_{xy} = Twisting moment per unit lenght

The expanded form of the force moment – deformation relation can be stated as below:

$$\begin{bmatrix}[N]_{3x1}\\ [M]_{3x1}\end{bmatrix}_{6x1} = \begin{bmatrix}[A]_{3x3} & [B]_{3x3}\\ [B]_{3x3} & [D]_{3x3}\end{bmatrix}_{6x6} \begin{bmatrix}[\varepsilon^0]_{3x1}\\ [\kappa]_{3x1}\end{bmatrix}_{6x1}$$

or in expanded form as:

$$\begin{bmatrix}N_x\\ N_y\\ N_{xy}\\ M_x\\ M_y\\ M_{xy}\end{bmatrix} = \begin{bmatrix}A_{11} & A_{12} & A_{16} & B_{11} & B_{12} & B_{16}\\ A_{12} & A_{22} & A_{26} & B_{12} & B_{22} & B_{26}\\ A_{16} & A_{26} & A_{66} & B_{16} & B_{26} & B_{66}\\ B_{11} & B_{12} & B_{16} & D_{11} & D_{12} & D_{16}\\ B_{12} & B_{22} & B_{26} & D_{12} & D_{22} & D_{26}\\ B_{16} & B_{26} & B_{66} & D_{16} & D_{26} & D_{66}\end{bmatrix}\begin{bmatrix}\varepsilon_x^0\\ \varepsilon_y^0\\ \gamma_{xy}^0\\ \kappa_x\\ \kappa_y\\ \kappa_{xy}\end{bmatrix} \tag{4.16}$$

The above equation is the constitutive relation of the laminated plate where,

$$[A] = \sum_{k=1}^{n}\left[\bar{Q}_{x-y}\right]_k (h_k - h_{k-1})$$

$$[B] = \frac{1}{2}\sum_{k=1}^{n}\left[\bar{Q}_{x-y}\right]_k \left({h_k}^2 - {h_{k-1}}^2\right) \tag{4.17}$$

$$[D] = \frac{1}{3}\sum_{k=1}^{n}\left[\bar{Q}_{x-y}\right]_k \left({h_k}^3 - {h_{k-1}}^3\right)$$

where,

$[A]$ = Extensional stiffness matrix - Unit: lb/in

$[B]$ = Extensional-bending coupling stiffness matrix - Unit: lb

$[D]$ = Bending stiffness matix - Unit: $lb - in$

Also,

where,

$$\begin{bmatrix}\varepsilon^0\\ \kappa\end{bmatrix} = \begin{bmatrix}a & b\\ b^T & d\end{bmatrix}\begin{bmatrix}N\\ M\end{bmatrix}$$

$$\begin{bmatrix}a & b\\ b^T & d\end{bmatrix} = \begin{bmatrix}A & B\\ B & D\end{bmatrix}^{-1} \tag{4.18}$$

It should be noted that A, B and D as well as ‘a’ and ‘d’ are symmetrical matices while ‘b’ is not a symmetric.

4.3 Narrow Beam:

Though beams are classified as one dimensional body which has its length dimension quite larger than the other two dimensions viz, width and thickness, the beam behavior is also affected by the $^{width}/_{thickness}$ ratio. That is if $^{width}/_{thickness}$ is roughly less than 6 the beam is classified as *narrow beam* and if the ratio of $^{width}/_{thickness}$ is greater than 6 its considered as *wide beam.* This further classification of long beams as narrow beam and wide beams helps in understanding and analyzing the beam with more precision. For narrow beams only N_x and M_x acting in the axial direction are considered and loads & moments in other directions are neglected. The concept is explained in the Ref. [25].

I-Beam also falls under the category of narrow beams with an exception that due to the web the twisting κ_{xy} of the whole beam is quite negligile when the I-Beam is under axial or bending load and hence we have induced M_{xy}. For a narrow beam, the axial strain distribution gives rise to deformation of cross-section in transverse direction because of poisson's effect.

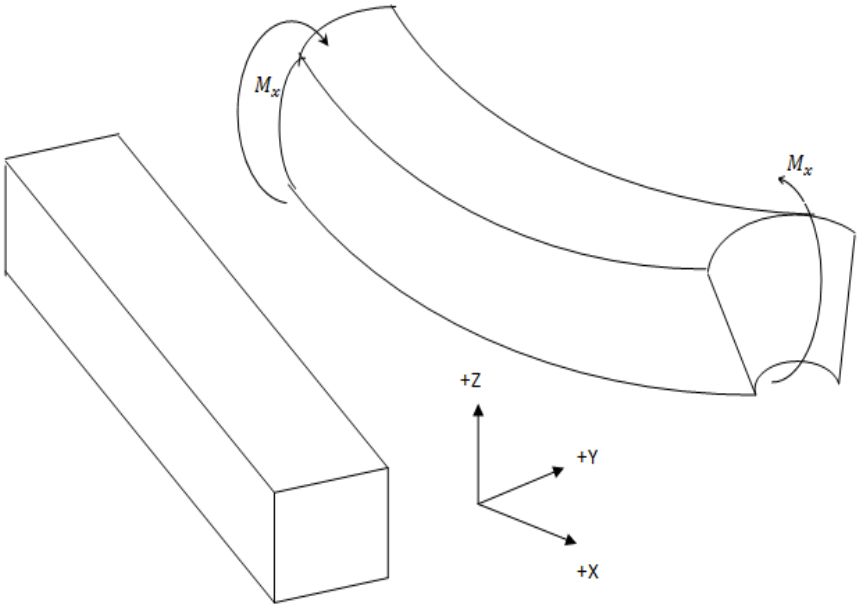

Figure 4-6 Narrow beam - before and after deformation

For narrow beam shown in Figure 4-6, considered for I-Beam we can assume the following things:

$$\begin{aligned} N_x &\neq 0 & \varepsilon_x &\neq 0 \\ N_y &= 0 & \varepsilon_y &\neq 0 \\ N_{xy} &= 0 & \gamma_{xy} &\neq 0 \\ M_x &\neq 0 & \kappa_x &\neq 0 \\ M_y &= 0 & \kappa_y &\neq 0 \\ M_{xy} &\neq 0 & \kappa_{xy} &= 0 \end{aligned} \tag{4.19}$$

This laminate constitutive equation for a narrow beam was originally developed in Ref.[25]:

$$\begin{bmatrix} N_x \\ M_x \end{bmatrix} = \begin{bmatrix} A^* & B^* \\ B^* & D^* \end{bmatrix} \cdot \begin{bmatrix} \varepsilon_x^0 \\ k_x \end{bmatrix} \tag{4.20}$$

A*, B* and D* are stiffnesses components defined below:

where

$$\begin{bmatrix} A^* & B^* \\ B^* & D^* \end{bmatrix} = \begin{bmatrix} a^* & b^* \\ b^* & d^* \end{bmatrix}^{-1} \tag{4.21}$$

$$a^* = a_{11} - \frac{b_{16}^2}{d_{66}} \; ; b^* = b_{11} - \frac{b_{16} d_{16}}{d_{66}} ; d^* = d_{11} - \frac{d_{16}^2}{d_{66}}$$

where ε_x^0 and κ_x are the mid-plane strain and curvature and a^*, b^* and d^* are the compliance, coupling and flexibility components of Narrow Beam laminate, respectively.

A*, B*, and D* refer to the axial, coupling and bending stiffnesses of a narrow beam. It is noted that B*≠0 if the cross-section of the beam is unsymmetrical.

4.4 Constitutive Equation for Sub-laminates

The constitutive equation for sub-laminates can be deduced from Eq (4.20). For sub-laminate i, we have

$$\mathrm{N_{xi}} = \mathrm{A^*_{1,fi}} \varepsilon^{\mathrm{o}}_{\mathrm{x,fi}} + \mathrm{B^*_{1,fi}} \kappa_{\mathrm{x,fi}} \tag{4.22}$$

$$\mathrm{M_{xi}} = \mathrm{B^*_{1,fi}} \varepsilon^{\mathrm{o}}_{\mathrm{x,fi}} + \mathrm{D^*_{1,fi}} \kappa_{\mathrm{x,fi}} \tag{4.23}$$

where i=1 and 2 refer to the top and bottom flange laminates , respectively.

And for web we have the constitutive equation as follows:

$$N_{xw} = A_w^* \varepsilon_{x,w}^0 + B_w^* \kappa_{x,w} \tag{4.24}$$

$$M_{xw} = B_w^* \varepsilon_{x,w}^0 + D_w^* \kappa_{x,w} \tag{4.25}$$

We do consider web as having a symmetric layup, hence B_w^* would be zero, flanges having arbitrary layup and the I-Beam symmetric with respect to z-z axis.

4.5 Centroid of Composite I-Beam:

The centroid is the average location of forces on each part of cross-section. Centroid is the location where axial and bending behavior is decoupled. That is if axial load is applied at centroid it would only give pure axial strain and if bending moment is

applied at centroid we will have the case of pure bending. The expression for the centroid of composite I-Beam is derived in [27] and is:

$$z_c = \frac{b_{f1}A^*_{1,f1}z_1 + b_{f2}A^*_{1,f2}z_2 + h_wA^*_{1,w}z_w}{b_{f1}A^*_{1,f1} + b_{f2}A^*_{1,f2} + h_wA^*_{1,w}} \tag{4.26}$$

The geometry of I-Beam is as shown in Figure 4-7. It should be noted that unlike isotropic materials, the centriod & shear center location of composite structure depends on the material properties and the laminate stacking sequence.

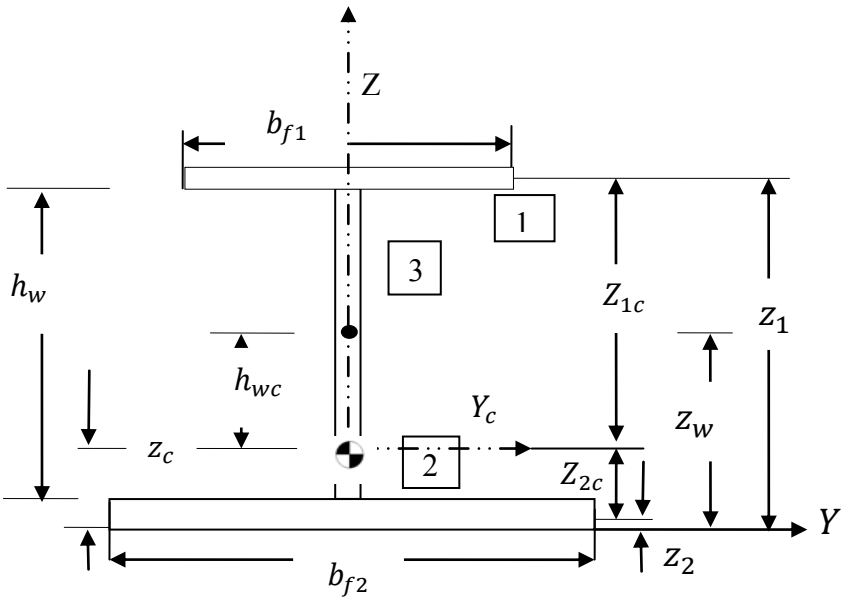

Figure 4-7 I-Beam cross-section

4.6 Bending stiffness about z axis for Composite I-Beam

We are interested in finding the bending stiffness of the Composite I-Beam with respect to z-z axis and for a given moment $\bar{M}_z$. Thus according to the mechanics theory we get the below relationship:

$$\bar{M}_z = D_y^c * \frac{1}{\rho_z^c} \tag{4.27}$$

where,

$\bar{M}_z =$ sum of the total moments components of each sub-laminate

$D_y^c = \overline{EI_{zz}} =$ equivalent bending stiffness of I-Beam with respect to z-z Axis

$\frac{1}{\rho_z^c} =$ Curvature at the centroid of I-Beam = $\frac{\partial^2 y}{\partial x^2}$

Now,

$$\bar{M}_z = (Total\ moment\ by\ top\ flange) + (Total\ moment\ by\ bottom\ flange) + (Total\ moment\ by\ web) \tag{4.28}$$

$$(Total\ moment\ by\ top\ flange) = \bar{M}_{z,f1} = \int_{-\left(b_{f1}/2\right)}^{\left(b_{f1}/2\right)} \{y * N_{x,f1}\}\, dy \tag{4.29}$$

$$(Total\ moment\ by\ bottom\ flange) = \bar{M}_{z,f2} = \int_{-\left(b_{f2}/2\right)}^{\left(b_{f2}/2\right)} \{y * N_{x,f2}\}\, dy \tag{4.30}$$

$$(Total\ moment\ by\ web\ flange) = \bar{M}_{z,w} = h_w * M_{x,w} \tag{4.31}$$

The web is considered symmetric in layup and hence $N_{x,w}$ will not contribute *but* if the web is not symmetric then we have to modify the above equation

If a beam is subjected to bending with respect to z-z axis the mid-plane strain can be adjusted to

$$\varepsilon_x = \varepsilon_x^0 + y\frac{1}{\rho_z^c} \tag{4.32}$$

Thus, considering the top flange,

$$N_{x,f1} = A_{1,f1}^* \varepsilon_{x,f1}^0 + B_{1,f1}^* \kappa_{x,f1} \tag{4.33}$$

$$M_{x,f1} = B^*_{1,f1}\varepsilon^0_{x,f1} + D^*_{1,f1}\kappa_{x,f1}$$

Also for top flange we have,

$$\varepsilon^0_{x,f1} = \varepsilon^0_x + y\frac{1}{\rho_{z,f1}} \tag{4.34}$$

As only bending moment in z axis is applied at centroid we have,

$$\begin{gathered}\varepsilon^0_x = 0 \\ \kappa_{x,f1} = 0 \\ \frac{1}{\rho_{z,f1}} = \frac{1}{\rho^c_z}\end{gathered} \tag{4.35}$$

From eqs. (4.35) (4.34) and (4.33) we have,

$$N_{x,f1} = A^*_{1,f1} * \left(y * \frac{1}{\rho^c_z}\right) + B^*_{1,f1} * 0 \tag{4.36}$$

From eqs. (4.36) and (4.29) we get,

$$\bar{M}_{z,f1} = \int_{-\left({}^{b_{f1}}/_{2}\right)}^{\left({}^{b_{f1}}/_{2}\right)} \left\{\left[y * A^*_{1,f1} * \left(y * \frac{1}{\rho^c_z}\right)\right]\right\} dy \tag{4.37}$$

Solving the above expression we get the following expression for top flange,

$$\bar{M}_{z,f1} = \left[A^*_{1,f1} * \left(\frac{{b_{f1}}^3}{12}\right)\right] * \frac{1}{\rho^c_z} \tag{4.38}$$

Similarly for bottom flange we get,

$$\bar{M}_{z,f2} = \left[A^*_{1,f2} * \left(\frac{{b_{f2}}^3}{12}\right)\right] * \frac{1}{\rho^c_z} \tag{4.39}$$

For web laminate the global and local co-ordinates are at different orientation, and hence we have the following relationship for web laminate

$$\varepsilon^0_{x,w} = \varepsilon^0_w + y\kappa_{x,w} \tag{4.40}$$

where,

$$\varepsilon_w^0 = 0$$
$$\kappa_{x,w} = \frac{1}{\rho_z^c} \tag{4.41}$$

From Eqs. (4.41) (4.40) (4.24) (4.25) & (4.31) we have,

$$\bar{M}_{z,w} = h_w * \left\{ B_w^* \left(\varepsilon_w^0 + y * \frac{1}{\rho_z^c} \right) + D_w^* * \left(\frac{1}{\rho_z^c} \right) \right\} \tag{4.42}$$

As web is considered having symmetric layup we get,

$$\bar{M}_{z,w} = h_w * \left\{ D_w^* * \left(\frac{1}{\rho_z^c} \right) \right\} \tag{4.43}$$

Substituting Eqs. (4.43) (4.39) (4.38) in (4.28) we get,

$$\bar{M}_z = \left\{ \left[A_{1,f1}^* * \left(\frac{{b_{f1}}^3}{12} \right) \right] + \left[A_{1,f2}^* * \left(\frac{{b_{f2}}^3}{12} \right) \right] + (h_w * D_w^*) \right\} * \frac{1}{\rho_z^c} \tag{4.44}$$

Comparing Eq. (4.44) with (4.27) we get the *equivalent bending stiffness* for a composite I-Beam as:

$$D_y^c = \overline{EI}_{zz} = \left\{ \left[A_{1,f1}^* \frac{{b_{f1}}^3}{12} \right] + \left[A_{1,f2}^* \frac{{b_{f2}}^3}{12} \right] + (h_w D_w^*) \right\} \tag{4.45}$$

4.7 Shear Center expression for Composite I-Beam:

Shear center is the location where bending and twisting behavior are uncoupled. The shear center expression of isotropic beams depends only on the geometry of the cross-section but for composite beams the shear center also depends on the material properties and the stacking sequence and it should include the relevant coupling behaviors.

To calculate the shear center we first need to understand and develop an expression for shear flow in the composite I-Beam.

Expression for shear flow in I-Beam:

If there is no load applied in the axial direction, the equilibrium equation is,

$$\frac{\partial q}{\partial s} + \frac{\partial N_x}{\partial x} = 0 \tag{4.46}$$

where,

q = Shear flow

s = Represents the shear flow direction

$N_x =$ Total force in x-direction, units (lb/in)

We are interested in shear force in y-direction V_y as the I-Beam is symmetric with respect to z axis. The procedure followed here has an approach similar to the one mentioned for the isotropic I-Beam with the introduction of material properties, stacking sequence and coupling effects.

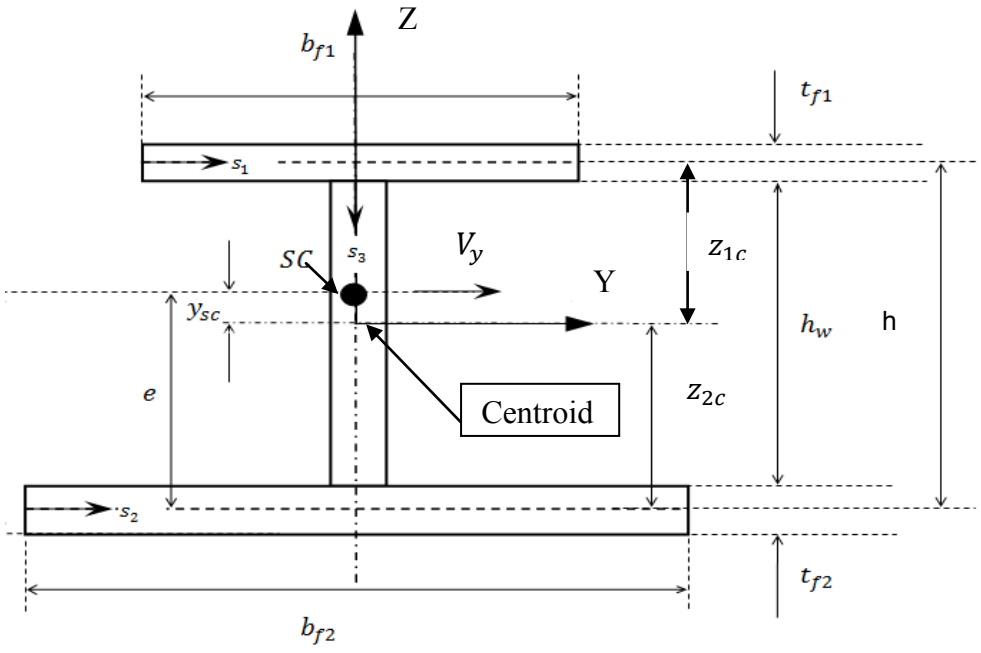

Figure 4-8 I-Beam cross-section with shear flow description

Shear flow in the top flange:

From Figure 4-8, we have to equation for $N_{x,f1}$ from eqs (4.33) for $\bar{N}_x$ & $\bar{M}_z$ applied at centroid of I-Beam,

$$\varepsilon_{x,f1}^{0} = \varepsilon_{x}^{0} + y\frac{1}{\rho_z^c}$$

$$\kappa_{x,f1} = 0 \tag{4.47}$$

$$\varepsilon_{x}^{0} = \frac{\bar{N}_x}{\overline{EA}} \; and \; \frac{1}{\rho_z^c} = \frac{\bar{M}_z}{D_y^c}$$

We apply only $\bar{M}_z$ as we need to create only shear force in y-direction.

$\overline{EA}$ = Equivalent axial stiffness of the composite I-Beam

Thus from eqs. (4.47) and (4.33) we get,

$$N_{x,f1} = A_{1,f1}^{*}\left(\frac{\bar{N}_x}{\overline{EA}} + y\frac{\bar{M}_z}{D_y^c}\right) \tag{4.48}$$

Differentiating eq (4.48) with respect to x, we get,

$$\frac{\partial N_{x,f1}}{\partial x} = \frac{\partial}{\partial x}\left\{A_{1,f1}^{*}\left(\frac{\bar{N}_x}{\overline{EA}} + y\frac{\bar{M}_z}{D_y^c}\right)\right\}$$

$$\frac{\partial \bar{N}_x}{\partial x} = 0; \; \frac{\partial \bar{M}_z}{\partial x} = V_y \; (shear \; force) \tag{4.49}$$

Thus we get,

$$\frac{\partial N_{x,f1}}{\partial x} = y * A_{1,f1}^{*} * \frac{V_y}{D_y^c} \tag{4.50}$$

From eqs. (4.50) and (4.46) we get,

$$\frac{\partial q_{f1}}{\partial s_1} = -\frac{\partial N_{x,f1}}{\partial x}$$

$$\frac{\partial q_{f1}}{\partial s_1} = -\left(y * A_{1,f1}^{*} * \frac{V_y}{D_y^c}\right) \tag{4.51}$$

Integrating both the sides,

$$q_{f1} = \int_{0}^{s_1} -\left(y * A_{1,f1}^{*} * \frac{V_y}{D_y^c}\right) ds_1 \tag{4.52}$$

y varies from 0 to $\frac{b_{f1}}{2}$ for top flange and hence,

$$q_{f1} = -\int_0^{s_1} \left\{ \left(\frac{b_{f1}}{2} - s_1 \right) * A^*_{1,f1} * \frac{V_y}{D^c_y} \right\} ds_1 \tag{4.53}$$

$$q_{f1} = -\left\{ \left(\frac{b_{f1}}{2} - \frac{s_1}{2} \right) * s_1 * A^*_{1,f1} * \frac{V_y}{D^c_y} \right\} \tag{4.54}$$

Also on the similar bases we can write the equation for bottom flange as,

$$q_{f2} = -\left\{ \left(\frac{b_{f2}}{2} - \frac{s_2}{2} \right) * s_2 * A^*_{1,f2} * \frac{V_y}{D^c_y} \right\} \tag{4.55}$$

For symmetric web

$$q_w = 0 \tag{4.56}$$

Now, the torque of the external forces about the centroid is equal to the torque produced by the internal shear flow and can be written as,

$$V_y * z_{sc} = -z_{1c} * \int_0^{b_{f1}} q_{f1}\, ds_1 + z_{2c} * \int_0^{b_{f2}} q_{f2}\, ds_2 \tag{4.57}$$

From Eqs (4.57) (4.54) (4.55) we get,

$$\begin{aligned} V_y * z_{sc} = z_{1c} * \int_0^{b_{f1}} \left\{ \left(\frac{b_{f1}}{2} - \frac{s_1}{2} \right) * s_1 * A^*_{1,f1} * \frac{V_y}{D^c_y} \right\} ds_1 \\ - z_{2c} \int_0^{b_{f2}} \left\{ \left(\frac{b_{f2}}{2} - \frac{s_2}{2} \right) * s_2 * A^*_{1,f2} * \frac{V_y}{D^c_y} \right\} ds_2 \end{aligned} \tag{4.58}$$

Thus we get the expression for the *shear center for composite I-Beam* from the centroid position as,

$$z_{sc} = \frac{z_{1c}}{D^c_y} \left(\frac{{b_{f1}}^3}{12} A^*_{1,f1} \right) - \frac{z_{2c}}{D^c_y} \left(\frac{{b_{f2}}^3}{12} A^*_{1,f2} \right)$$

or

$$z_{sc} = \frac{1}{D^c_y} \left(\frac{z_{1c} * A^*_{1,f1} * {b_{f1}}^3}{12} - \frac{z_{2c} * A^*_{1,f2} * {b_{f2}}^3}{12} \right) \tag{4.59}$$

where D^c_y is given by eq (4.45) and stated below:

$$D_y^c = EI_{zz} = \left\{\left[A_{1,f1}^* \frac{{b_{f1}}^3}{12}\right] + \left[A_{1,f2}^* \frac{{b_{f2}}^3}{12}\right] + (h_w D_w^*)\right\}$$

Smeared property approach for Shear center:

$$e = \frac{h * \left(\frac{1}{a_{11}}\right)_{f1} * b_{f1}^3}{\left(\frac{1}{a_{11}}\right)_{f1} * b_{f1}^3 + \left(\frac{1}{a_{11}}\right)_{f2} * b_{f2}^3} \tag{4.60}$$

The location of shear center calculated will be from the mid-plane of bottom flange

Overall ABD matrix approach for composite I-Beam:

The overall ABD matrix of the composite I-Beam can be easily derived by applying the axis translation laws:

$$[\bar{A}] = h_w[A]_w + b_{f1}[A]_{f1} + b_{f2}[A]_{f2}$$

$$[\bar{B}] = h_w[B]_w + b_{f1}\left([B]_{f1} + \rho_{f1}[A]_{f1}\right) + b_{f2}\left([B]_{f2} - \rho_{f2}[A]_{f2}\right)$$

$$[\bar{D}] = \left(h_w[D]_w + \frac{{h_w}^3}{12}[A]_w\right) + b_{f1}\left([D]_{f1} + 2 * \rho_{f1} * [B]_{f1} + \left(\rho_{f1}\right)^2[A]_{f1}\right) \tag{4.61}$$

$$+ b_{f2}\left([D]_{f2} - 2 * \rho_{f2} * [B]_{f2} + \left(\rho_{f2}\right)^2[A]_{f2}\right)$$

In the above expressions the overall ABD matrix is with respect to the center of the I-Beam and it has the width effect of the individual laminate.

The overall constitutive equation for the I-Beam can be written as,

$$\begin{bmatrix}\bar{N}\\ \bar{M}\end{bmatrix} = \begin{bmatrix}\bar{A} & \bar{B}\\ \bar{B} & \bar{D}\end{bmatrix} \cdot \begin{bmatrix}\varepsilon^0\\ k\end{bmatrix}$$

$$or \tag{4.62}$$

$$\begin{bmatrix}\varepsilon^0\\ k\end{bmatrix} = \begin{bmatrix}\bar{a} & \bar{b}\\ \bar{b}^T & \bar{d}\end{bmatrix}\begin{bmatrix}\bar{N}\\ \bar{M}\end{bmatrix}$$

And the expression of shear center as stated in [28] is

$$\overline{z_{sc}} = -\frac{\overline{b_{66}}}{\overline{d_{66}}} \tag{4.63}$$

where, $\overline{z_{sc}}$ is the measure of shear center from the center of the I-Beam. A similar method was employed by [29] to find the axial and bending stiffness of composite I-Beam and also the centroid location.

4.8 Results and verification for D_y^c and Shear Center

The bending stiffness formulation was verified by first applying it to the isotropic material and comparing the results with the mechanics and ANSYS™ model. Good agreement was found between all the results from all the 3 approaches as shown below in Table 4-1. The method to extract the bending stiffness from ANSYS™ is described in [26] and [25].

Hence, the formulation of D_y^c explained in Eqs (4.45) holds good and later applied to the composite I-Beam and compared with ANSYS™. The results are tabulated below in Table 4-1.

Table 4-1 Equivalent Bending stiffness verification

Case		Bending stiffness -D_y^c -(lb-in^2) w.r.t z-z Axis			Percentage differences		
		Mechanics Approach	Present formulae Eq (4.45)	ANSYS™ FEM model	Between ANSYS™ and Mechanics	Between ANSYS™ and Present formulae	Between Mechanics and Present formulae
Isotropic	1	43,035	43,035	43,011	0.06	0.06	0
	2	22,183	22,183	22,168	0.07	0.07	0
	3	18,680	18,680	18,692	-0.06	-0.06	0
Composite	1	-	46,870	46,874	-	-0.01	-
	2		23,128	23,137		-0.04	
	3		18,248	18,268		-0.11	

Later the shear center proposed in this thesis by Eq (4.59) was applied to the isotropic case and results were compared with ANSYS™, smeared property approach and complete ABD matrix approach. The shear formulation proposed in this thesis gives exactly the same results as the mechanics approach.

After the isotropic case verification, the formulation was applied to the composite I-Beam case and compared with the ANSYS™ and smeared property approach as tabulated in Table 4-2. We find a good correlation of the shear center found by the present approach and the ANSYS™ 2D model. Here also we find that complete ABD matrix approach fails to give a comparable answer.

Table 4-2 Verification of the composite shear center closed form expression by applying it for isotropic cases

Case		Shear Center				
		Mechanics Approach	Smeared Property Approach	Shear Center Present Formulae	Complete ABD matrix Approach	ANSYS™ FEM model
		Eq (2.15)	Eq (4.60)	Eq (4.59)	Eq (4.63)	
Isotropic	1	0.0317	0.0317	0.0317	0.1158	0.0329
	2	0.1294	0.1294	0.1294	0.2146	0.1385
	3	0.2672	0.2672	0.2672	0.2672	0.2757
Composite	1	-	0.0301	0.0301	0.1698	0.0319
	2		0.1084	0.1084	0.2505	0.1201
	3		0.2314	0.2314	0.2915	0.2381

We observe that the present formulation for shear center matches perfectly with the smeared shear center property and the essence of the present formulation to capture the coupling effect is not displayed. To do so, the following case studies are conducted and shear center results are compared with the ANSYS™ 2D model.

Case 4:

Table 4-3 I-Beam properties for Case 4

Geometry of composite I-Beam	Layup	Material Properties
Top flange width = 0.625 inch Bottom Flange width = 0.4 inch Web height = 0.8 inches	Top flange = $[\theta_2/-\theta_2]_T$ Bottom Flange = $[0_4]_T$ Web = $[0_4]_T$ $\theta\ varies\ from\ 0\ to\ 90$	$E_1 = 21.75 \text{ x } 10^6$ psi, $E_2 = 1.595 \text{ x } 10^6$psi, $G_{12} = 0.8702 \text{ x } 10^6$ psi , $\nu_{12} = 0.25, \quad t_{ply} = 0.005\ in.$

Table 4-4 Shear center calculated for Case 4

Case 4 ply orientation θ	Smeared Property Approach	Shear Center Present Formulae	ANSYS™ FEM model
	Eq (4.60)	Eq (4.59)	
0	0.6597	0.6597	0.6556
15	0.5531	0.6312	0.6079
30	0.3997	0.4884	0.4275
45	0.2685	0.2955	0.2560
60	0.2080	0.2121	0.1889
75	0.1918	0.1926	0.1755
90	0.1892	0.1897	0.1755

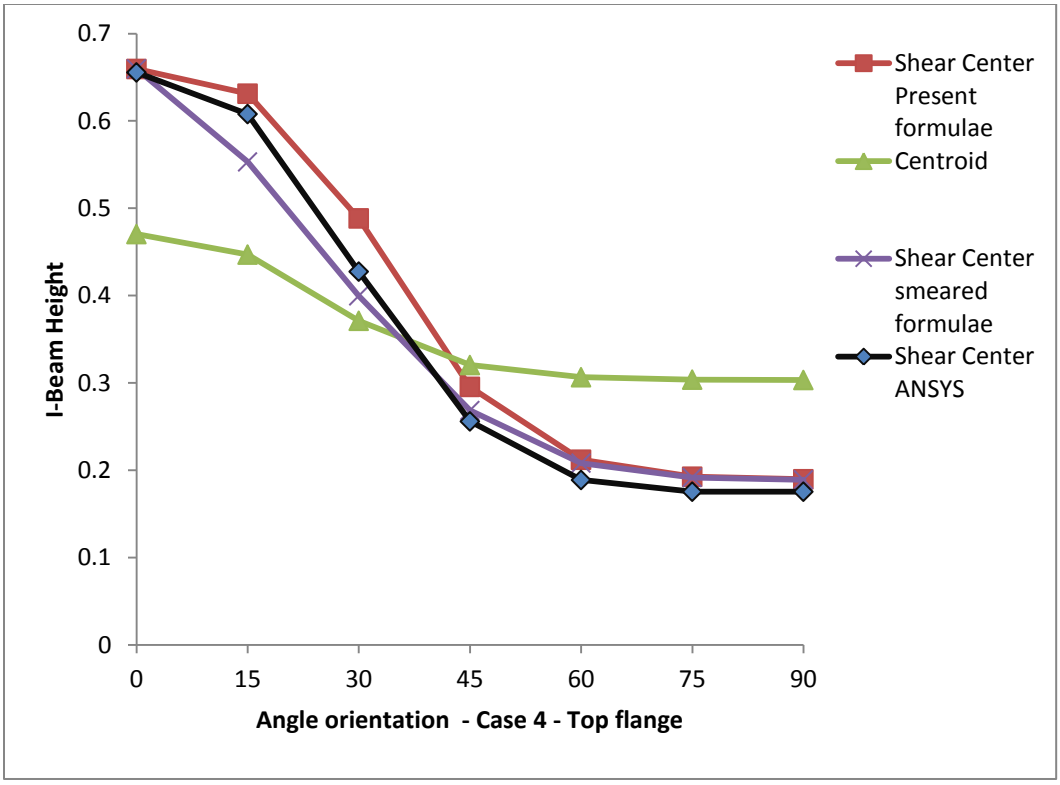

Figure 4-9 Variation of shear center location with respect to the fiber orientation for Case 4

Case 5:

Table 4-5 I-Beam properties for Case 5

Geometry of composite I-Beam	Layup	Material Properties
Top flange width = 0.625 inch Bottom Flange width = 0.4 inch Web height = 0.8 inches	Top flange = $[0_4]_T$ Bottom Flange =$[\theta_2/-\theta_2]_T$ Web = $[0_4]_T$ $\theta\ varies\ from\ 0\ to\ 90$	$E_1 = 21.75 \text{ x } 10^6$ psi, $E_2 = 1.595 \text{ x } 10^6$psi, $G_{12} = 0.8702 \text{ x } 10^6$ psi , $\nu_{12} = 0.25,\ t_{\ ply} = 0.005\ in.$

Table 4-6 Shear center calculated for Case 5

Case 5 ply orientation θ	Smeared Property Approach	Shear Center Present Formulae	ANSYS™ FEM model
	Eq (4.60)	Eq (4.59)	
0	0.6597	0.6597	0.6595
15	0.7326	0.6847	0.6997
30	0.7820	0.7577	0.7704
45	0.8049	0.8007	0.8017
60	0.8124	0.8117	0.8114
75	0.8143	0.8139	0.8129
90	0.8145	0.8142	0.8136

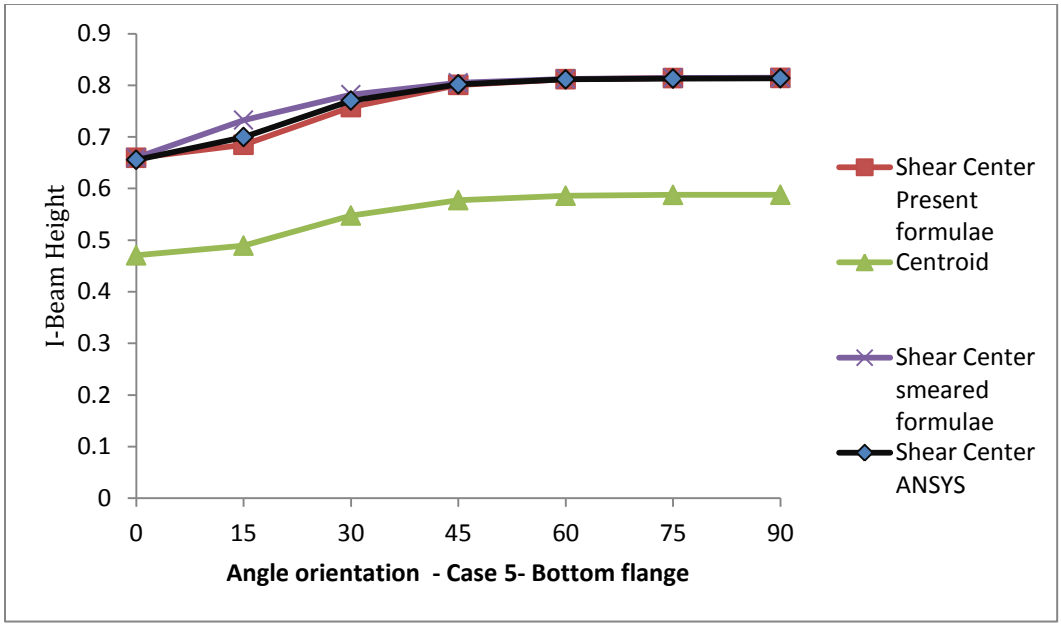

Figure 4-10 Variation of shear center location with respect to the fiber orientation for Case 5

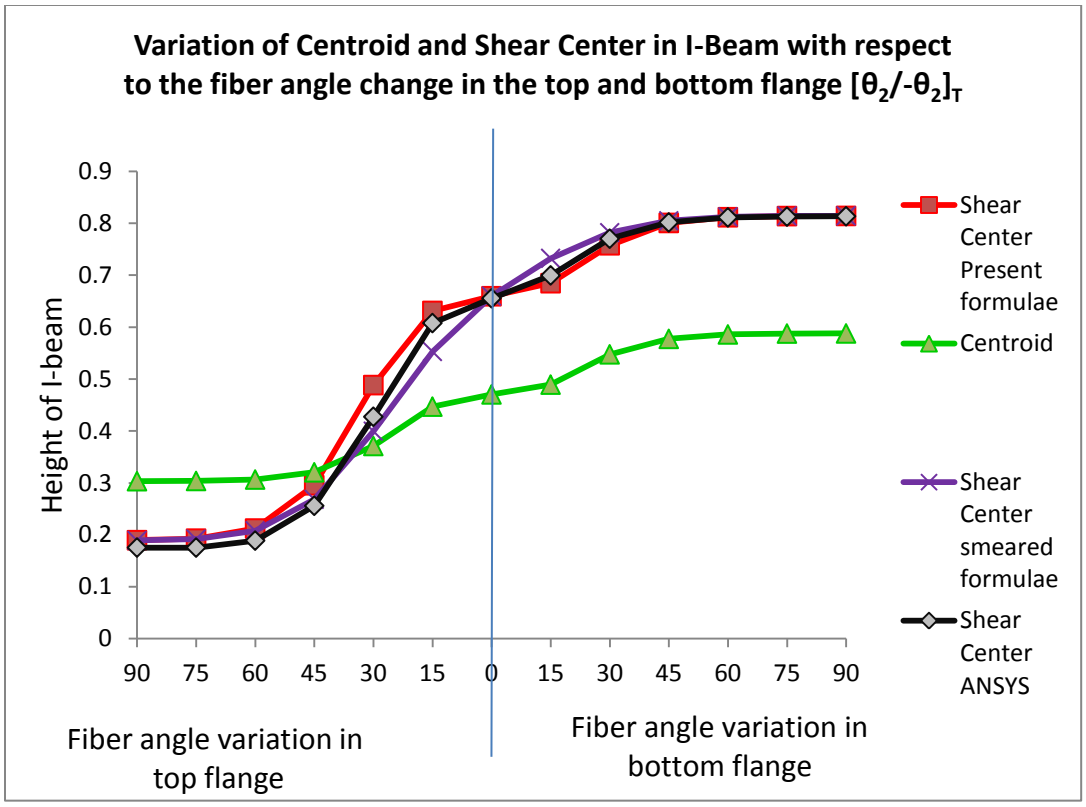

Figure 4-11 Variation of shear center location in Case 4 & Case 5 combined in one graph

Case 6:

Table 4-7 I-Beam properties for Case 6

Geometry of composite I-Beam	Layup	Material Properties
Top flange width = 0.625 inch Bottom Flange width = 0.4 inch Web height = 0.8 inches	Top flange = $[0_4]_T$ Bottom Flange =$[0_4]_T$ Web = $[\pm\theta]_S$ $\theta\ varies\ from\ 0\ to\ 90$	$E_1 = 21.75 \times 10^6$ psi, $E_2 = 1.595 \times 10^6$psi, $G_{12} = 0.8702 \times 10^6$ psi , $\nu_{12} = 0.25, \quad t_{ply} = 0.005\ in.$

Table 4-8 Shear center calculated for Case 6

Case 6 ply orientation θ	Smeared Property Approach	Shear Center Present Formulae	ANSYS™ FEM model
	Eq (4.60)	Eq (4.59)	
0	0.6597	0.6597	0.6556
15	0.6597	0.6595	0.6586
30	0.6597	0.6596	0.6735
45	0.6597	0.6597	0.6735
60	0.6597	0.6597	0.6682
75	0.6597	0.6597	0.6623
90	0.6597	0.6597	0.6548

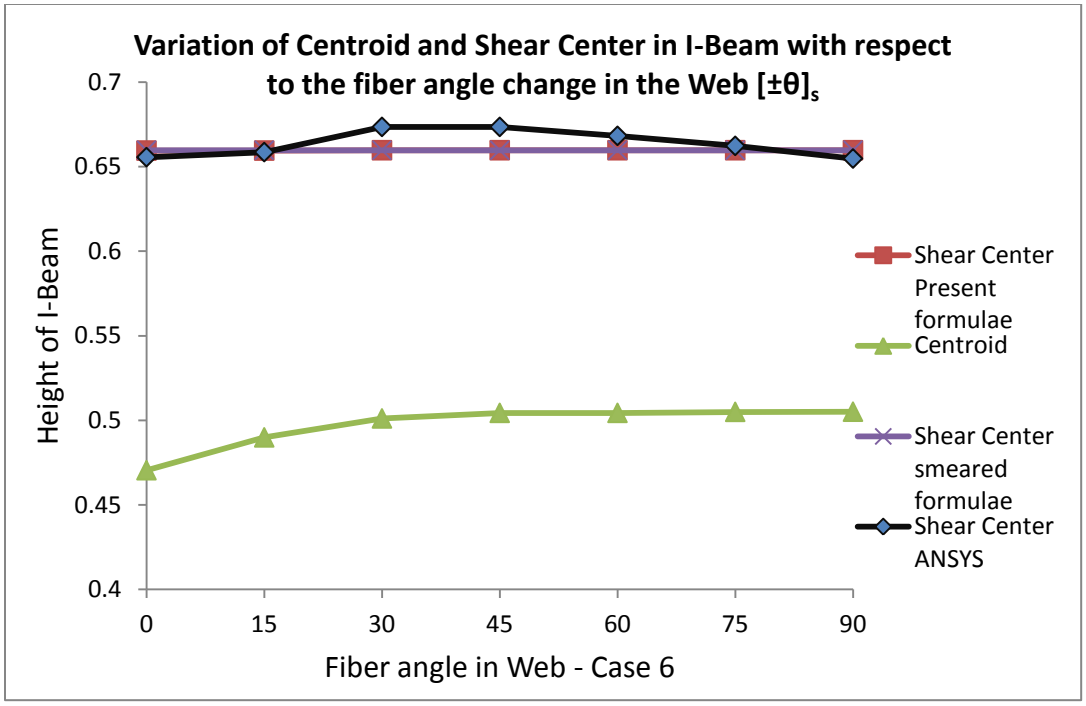

Figure 4-12 Variation of shear center location with respect to the fiber orientation for Case 6

Observations from the above 3 Case-Studies:

- From case 6 (Table 4-7, Table 4-8,Figure 4-12) we observe that the shear center is not affected by the change in the fiber orientation in web when the stacking sequence in the web is symmetric and top and bottom flanges have similar layup.
- Present formulation has a very good correlation with the smeared properties and ANSYS™ results if the fiber orientations are more than 45^0 ($45^0, 60^0, 75^0\ and\ 90^0$) and at 0^0 for case 4 (Table 4-3,
- Table 4-4) and case 5 (Table 4-5, Table 4-6).
- In the span of fiber orientation varying from 0^0 to 45^0 (i.e. $15^0, 30^0$) we observe a difference in the shear center results between ANSYS™, smeared property approach and present formulation for case 4 (
- Table 4-4, Figure 4-10) and case 5 (Table 4-6, Figure 4-10). ANSYS™ and present formulations are giving more comparable results while the results by smeared property approach are off. One of the reasons for this is the variation in shear coupling co-efficient $\eta_{xy,x}$.

$$\eta_{xy,x} = E_x\left[\left(\frac{2}{E_1}+\frac{2\nu_{12}}{E_1}-\frac{1}{G_{12}}\right)nm^3-\left(\frac{2}{E_2}+\frac{2\nu_{12}}{E_1}-\frac{1}{G_{12}}\right)mn^3\right]$$

where,

$$\frac{1}{E_x}=\frac{m^4}{E_1}+\frac{n^4}{E_2}-2m^2n^2\frac{\nu_{12}}{E_1}+\frac{m^2n^2}{G_{12}} \tag{4.64}$$

$$m = cos\theta, n = sin\theta$$

From the Figure 4-13, it is quite evident that $\eta_{xy,x}$ varies highly from fiber orientation between 0^0 – 45^0 and the variation is quite small for the 45^0 – 90^0 range. And hence

the coupling behavior is quite prominent for fiber orientation between $0^0 - 45^0$ for the material properties mentioned.

- Also as the ANSYS™ model is built with SHELL 181 which is a 2D model, it would be a good idea to extract the shear center result from 3D ANSYS™ model and compare the results.

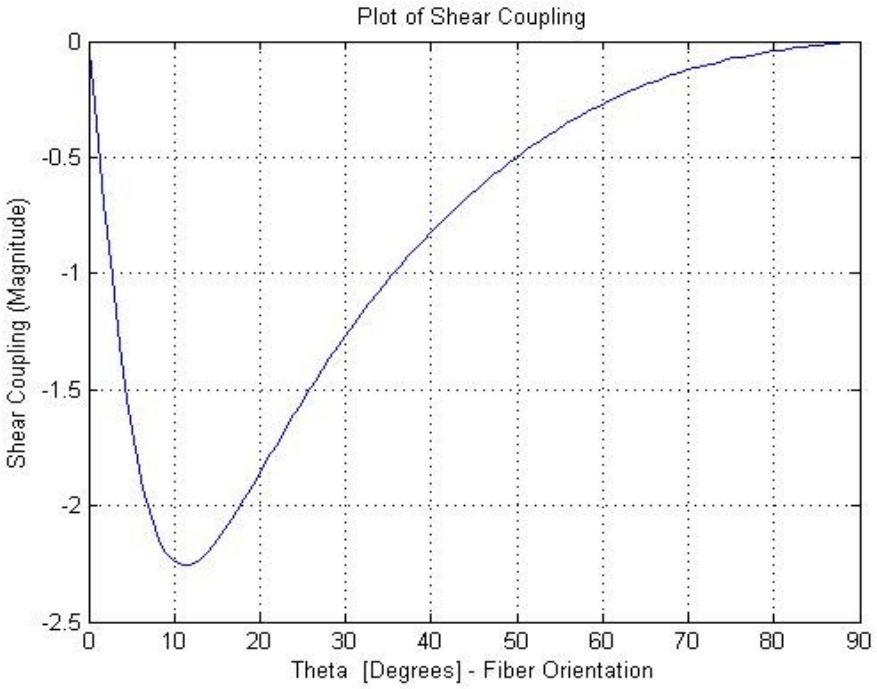

Figure 4-13 Shear coupling variation with respect to fiber orientation

4.9 Reasons for the failure of complete/overall ABD matrix approach to predict shear center:

It was observed that the shear center predicted by complete or overall ABD matrix approach presented by Syed [28] failed to predict the shear center for the I beam (isotropic and composite) and the error was huge. According to Syed [28], the overall ABD for the I-Beam structure is calculated by the following method:

$$[\bar{A}] = h_w[A]_w + b_{f1}[A]_{f1} + b_{f2}[A]_{f2}$$

$$[\bar{B}] = h_w[B]_w + b_{f1}\left([B]_{f1} + \rho_{f1}[A]_{f1}\right) + b_{f2}\left([B]_{f2} - \rho_{f2}[A]_{f2}\right)$$

$$[\bar{D}] = \left(h_w[D]_w + \frac{{h_w}^3}{12}[A]_w\right) + b_{f1}\left([D]_{f1} + 2 * \rho_{f1} * [B]_{f1} + \left(\rho_{f1}\right)^2[A]_{f1}\right) \quad (4.65)$$

$$+ b_{f2}\left([D]_{f2} - 2 * \rho_{f2} * [B]_{f2} + \left(\rho_{f2}\right)^2[A]_{f2}\right)$$

where,

$$[A]_w = \sum_{k=1}^{n}\left[\overline{Q''}_{x-y}\right]_k (h_k - h_{k-1})$$

$$[B]_w = \frac{1}{2}\sum_{k=1}^{n}\left[\overline{Q''}_{x-y}\right]_k \left({h_k}^2 - {h_{k-1}}^2\right)$$

$$[D]_w = \frac{1}{3}\sum_{k=1}^{n}\left[\overline{Q''}_{x-y}\right]_k \left({h_k}^3 - {h_{k-1}}^3\right)$$

$$\left[\overline{Q''}_{x-y}\right]_k = [T_\sigma(-\theta)]_z * [T_\sigma(-\beta)]_x * [Q]_{1-2} * [T_\varepsilon(\beta)]_x * [T_\varepsilon(\theta)]_z$$

$$\theta = fiber\ orientation;$$

$$\beta = orientation\ of\ web\ with\ respect\ to\ the\ global\ x-y\ plane, in\ case\ of\ I \quad (4.66)$$

$$-\ Beam\ \beta = 90^0 as\ web\ is\ vertical\ to\ the\ flanges.$$

$$[T_\sigma(\beta)]_x = \begin{bmatrix} 1 & 0 & 0 \\ 0 & cos^2\beta & 0 \\ 0 & 0 & cos\beta \end{bmatrix} = [T_\varepsilon(\beta)]_x$$

for I-Beam web $cos\beta = cos^2\beta = \cos 90 = cos^2 90 = 0$

$$\therefore [T_\sigma(\beta)]_x = \begin{bmatrix} 1 & 0 & 0 \\ 0 & 0 & 0 \\ 0 & 0 & 0 \end{bmatrix} = [T_\varepsilon(\beta)]_x$$

$$\rho_{f1} = \left(\frac{h_w}{2} + \frac{t_{f1}}{2}\right);\ \rho_{f2} = \left(\frac{h_w}{2} + \frac{t_{f2}}{2}\right)$$

Thus, for web the ABD matrix will have only 4 non-zero terms and will be as follows:

$$[ABD]_w = \begin{bmatrix} A_{11,w} & 0 & 0 & B_{11,w} & 0 & 0 \\ 0 & 0 & 0 & 0 & 0 & 0 \\ 0 & 0 & 0 & 0 & 0 & 0 \\ B_{11,w} & 0 & 0 & D_{11,w} & 0 & 0 \\ 0 & 0 & 0 & 0 & 0 & 0 \\ 0 & 0 & 0 & 0 & 0 & 0 \end{bmatrix} \quad (4.67)$$

On investigating, the following reasons were found because of which the overall ABD matrix theory fails to predict the correct or comparable shear center:

Reason 1:

In I-Beam the bending loads are resisted by the flanges and the shear loads by the web. Thus web contributes for the major percentage of the shear stiffness while the flanges contribute for the major part of the bending stiffness. In composites the different stiffness are given by the following elements of the ABD matrix;

$\mathrm{A}_{11} = \text{Axial Stiffness per unit width}$; $\mathrm{A}_{66} = \text{Shear Stiffness per unit width}$;

$\mathrm{D}_{11} = \text{Bending stiffness per unit width}$ & $\mathrm{D}_{66} = \text{Twisting stiffness per unit width}$

From Eqs(4.67) we observe that the web has only Axial stiffness and bending stiffness while the Shear stiffness and twisting stiffness are equal to zero. Thus there are some major errors in the method proposed by Syed [28].

Reason 2:

When the web ABD matrix is rotated by $(-90)^0$ with respect to global x- axis, the original (un-rotated) ABD matrix of the laminate should be achieved, but that is not the case with this method.

Reason 3:

As proposed the shear center depends on $b_{66}\, and\, d_{66}$ elements Eqs (4.63) but as the web does not contribute to the $b_{66}\, and\, d_{66}$ element, the shear center predicted is not correct.

However, centroid depends on the $b_{11}\ and\ d_{11}$ elements of the overall ABD matrix, where web and flanges both are contributing for the $b_{11}\ and\ d_{11}$ elements and hence the overall ABD matrix approach gives comparable centroid location with equation (4.26). Also as the logic of shifting the ABD matrix of flanges are correct and as flanges contribute the major percentage of the bending stiffness and the axial stiffness, the overall ABD matrix approach gives comparable results for both of them too.

$$centroid = -\frac{\overline{b_{11}}}{\overline{d_{11}}}$$
$$EA = \frac{\overline{d_{11}}}{\overline{a_{11}}\overline{d_{11}} - \overline{b_{11}}^2}\ ;\ EI = \frac{\overline{a_{11}}}{\overline{a_{11}}\overline{d_{11}} - \overline{b_{11}}^2} \tag{4.68}$$

Reason 4:

If we carefully observe $[ABD]_w$ in Eqs (4.67) we can deduce that the matrix is a singular matrix and hence we cannot have the constitutive relationship shown below:

$$\begin{bmatrix}\varepsilon^0\\ \kappa\end{bmatrix} = \begin{bmatrix}a & b\\ b^T & d\end{bmatrix}_w \begin{bmatrix}N\\ M\end{bmatrix}$$

where, (4.69)

$$\begin{bmatrix}a & b\\ b^T & d\end{bmatrix}_w = \begin{bmatrix}\bar{A} & \bar{B}\\ \bar{B} & \bar{D}\end{bmatrix}_w \ not\ possible\ due\ to\ singularity\ of\ \begin{bmatrix}\bar{A} & \bar{B}\\ \bar{B} & \bar{D}\end{bmatrix}_w$$

Reason 5:

Web should possess plane stress properties i.e. 2D properties as CLT is based on plane stress assumption. But looking at the $[ABD]_w$ in Eqs (4.67) we derive that web only has properties in global x-direction. Even though the web laminate is made of composite material, it losses all its coupling effects with the other direction which in our case is global z- axis.

4.10 Equivalent Torsional Stiffness for a Composite I-Beam

For a thin rectangular cross-section we have the following relationship:

$$\begin{bmatrix} \varepsilon_x^0 \\ \varepsilon_y^0 \\ \gamma_{xy}^0 \\ \kappa_x \\ \kappa_y \\ \kappa_{xy} \end{bmatrix} = \begin{bmatrix} a_{11} & a_{12} & a_{16} & b_{11} & b_{12} & b_{16} \\ a_{12} & a_{22} & a_{26} & b_{21} & b_{22} & b_{26} \\ a_{16} & a_{26} & a_{66} & b_{61} & b_{62} & b_{66} \\ b_{11} & b_{21} & b_{61} & d_{11} & d_{12} & d_{16} \\ b_{12} & b_{22} & b_{62} & d_{12} & d_{22} & d_{26} \\ b_{16} & b_{26} & b_{66} & d_{16} & d_{26} & d_{66} \end{bmatrix} \begin{bmatrix} N_x \\ N_y \\ N_{xy} \\ M_x \\ M_y \\ M_{xy} \end{bmatrix} \tag{4.70}$$

Definitions [15]:

Shear center / Flexural center – With reference to a beam, the flexural center of any section is that point in the plane of section through which a transverse load, applied at that section, must act if bending deflection only is to be produced, with no twist of section. i.e. bending – twist decoupled at shear center

Torsional center / Center of twist / Center of torsion / Center of shear – If a twisting couple is applied at a given section of a straight member, that section rotates about some point in its plane. This point which does not move when the member twist, is the torsional center of that section, i.e. twisting-shear decoupled at torsional center.

But one surprising thing though is, if the beam is only subjected to torsion, then the center of twist is same as the shear center i.e. bending – torsion – shear decoupled if only torsion applied to a beam at center of twist.

Thus for a thin rectangular composite section subjected to torsion we have,

$$\begin{bmatrix} \gamma_{xy}^0 \\ \kappa_x \\ \kappa_{xy} \end{bmatrix} = \begin{bmatrix} a_{66} & b_{61} & b_{66} \\ b_{61} & d_{11} & d_{16} \\ b_{66} & d_{16} & d_{66} \end{bmatrix} \begin{bmatrix} N_{xy} \\ M_x \\ M_{xy} \end{bmatrix} \tag{4.71}$$

As mentioned above at the center of twist which is also the shear center $\kappa_x = 0$.

Thus we have the following relationship:

$$\kappa_x = b_{61}N_{xy} + d_{11}M_x + d_{16}M_{xy} = 0$$

Thus,

$$M_x = -\left(\frac{b_{61}}{d_{11}}N_{xy} + \frac{d_{16}}{d_{11}}M_{xy}\right) \tag{4.72}$$

From Eqs. (4.71) and (4.72)

$$\gamma_{xy}^0 = \left(a_{66} - \frac{{b_{61}}^2}{d_{11}}\right)N_{xy} + \left(b_{66} - \frac{b_{61}d_{16}}{d_{11}}\right)M_{xy} \tag{4.73}$$

$$\kappa_{xy} = \left(b_{66} - \frac{b_{61}d_{16}}{d_{11}}\right)N_{xy} + \left(d_{66} - \frac{{d_{16}}^2}{d_{11}}\right)M_{xy} \tag{4.74}$$

From eqs. (4.73) and (4.74) we can write,

$$\begin{bmatrix}\gamma_{xy}^0 \\ \kappa_{xy}\end{bmatrix} = \begin{bmatrix}a_T^* & b_T^* \\ b_T^* & d_T^*\end{bmatrix}\begin{bmatrix}N_{xy} \\ M_{xy}\end{bmatrix} \tag{4.75}$$

where,

$$a_T^* = \left(a_{66} - \frac{{b_{61}}^2}{d_{11}}\right); b_T^* = \left(b_{66} - \frac{b_{61}d_{16}}{d_{11}}\right); d_T^* = \left(d_{66} - \frac{{d_{16}}^2}{d_{11}}\right) \tag{4.76}$$

Now, if $M_{xy} \neq 0$ & $N_{xy} = 0$ we have the following relationship from eqs. (4.75)

$$\begin{aligned}\gamma_{xy}^0 &= b_T^* M_{xy} \\ \kappa_{xy} &= d_T^* M_{xy}\end{aligned} \tag{4.77}$$

So at a distance ρ, we can write:

$$\gamma_{xy} = \gamma_{xy}^0 + \rho * \kappa_{xy} \tag{4.78}$$

Now, if $\gamma_{xy} = 0$, means that point is the center of twist, thus $\rho = \rho_{sc}$

$$\gamma_{xy}^0 + \rho_{sc}\,\kappa_{xy} = 0 \tag{4.79}$$

$$\rho_{sc} = -\frac{\gamma_{xy}^0}{\kappa_{xy}} = -\frac{b_T^* M_{xy}}{d_T^* M_{xy}} = -\frac{b_T^*}{d_T^*} \tag{4.80}$$

Thus we get the expression for center of twist, where if only torsion is applied, we will have pure twisting with no shear & bending taking place in the laminate. We can also write eqs (4.75) as

$$\begin{bmatrix} N_{xy} \\ M_{xy} \end{bmatrix} = \begin{bmatrix} A_T^* & B_T^* \\ B_T^* & D_T^* \end{bmatrix} \begin{bmatrix} \gamma_{xy}^0 \\ \kappa_{xy} \end{bmatrix}$$

$$\begin{bmatrix} A_T^* & B_T^* \\ B_T^* & D_T^* \end{bmatrix} = \begin{bmatrix} a_T^* & b_T^* \\ b_T^* & d_T^* \end{bmatrix}^{-1} \tag{4.81}$$

So we need to shift our stiffness to the center of twist location.

$$A_{T\_sc}^* = A_T^*$$

$$B_{T\_sc}^* = B_T^* - \rho_{sc} A_T^* = 0 \tag{4.82}$$

$$D_{T\_sc}^* = D_T^* - 2\rho_{sc} B_T^* + {\rho_{sc}}^2 A_T^*$$

Thus eqs (4.81) modifies to,

$$\begin{bmatrix} N_{xy} \\ M_{xy} \end{bmatrix} = \begin{bmatrix} A_{T\_sc}^* & 0 \\ 0 & D_{T\_sc}^* \end{bmatrix} \begin{bmatrix} \gamma_{xy}^0 \\ \kappa_{xy} \end{bmatrix} \tag{4.83}$$

So from the above relationship we derive:

$$N_{xy} = A_{T\_sc}^* * \gamma_{xy}^0$$

$$M_{xy} = D_{T\_sc}^* * \kappa_{xy} \tag{4.84}$$

Expression for κ_{xy} from eqs (4.12) is,

$$\kappa_{xy} = -2\frac{\partial^2 w}{\partial x \partial y} = -2\frac{\partial \frac{\partial w}{\partial y}}{\partial x} = -2\frac{\partial \theta}{\partial x} = -2\phi \tag{4.85}$$

where $\partial\theta/\partial x$ is rate of twist = ϕ

Also,

$$M_{xy} = -\frac{T}{2b} \tag{4.86}$$

where,

T = torsional load applied on the section

b = width of the laminate

Substituting eqs (4.85) (4.86) in (4.84) we get

$$-\frac{T}{2b} = D^*_{T\_sc}(-2\phi) \tag{4.87}$$

∴ we get,

$$\phi = \frac{T}{4b * D^*_{T\_sc}} \tag{4.88}$$

Thus, we can affirm that the torsional stiffness of the rectangular composite cross – section is

$$GK = 4b * D^*_{T\_sc} \tag{4.89}$$

Therefore, we can observe that the torsional stiffness of the composite rectangular cross-section depends on:

- Material properties
- Stacking sequence
- Ply orientation
- Geometry of the cross-section

If an open –section composite beam is made of thin wall segments, the torsional stiffness of the overall section can be approximated as shown below which is similar to the isotropic case.

$$GK_{total} = GK_1 + GK_2 + \ldots\ldots\ldots + GK_k \tag{4.90}$$

where k denotes the number of thin wall segments.

For a composite I-Beam the torsional stiffness can be approximated as:

$$GK_{total} = GK_{f1} + GK_{f2} + GK_w \tag{4.91}$$

where,

GK_{f1} = torsional stiffness of top flange

GK_{f2} = torsional stiffness of bottom flange

GK_w = torsional stiffness of the web section

$$GK_{f1} = 4b_{f1} * D^*_{T\_scf1}$$
$$GK_{f2} = 4b_{f2} * D^*_{T\_scf2} \quad (4.92)$$
$$GK_w = 4h_w * D^*_{T\_scw}$$

Thus from eqs. (4.92) and (4.91) we get:

Present approach	$GK_{total} = \left(4b_{f1} * D^*_{T\_scf1}\right) + \left(4b_{f2} * D^*_{T\_scf2}\right) + \left(4h_w * D^*_{T\_scw}\right)$	(4.93)

Smeared property approach to find the torsional stiffness of composite I-Beam

Smeared property approach	$GK_{total} = \frac{4b_{f1}}{d_{66f1}} + \frac{4b_{f2}}{d_{66f2}} + \frac{4h_w}{d_{66w}}$	(4.94)

4.11 Results and verification for Torsional stiffness expressions derived for Composite I-Beam

The above expression derived for the torsional stiffness of the composite I-Beam was applied to the isotropic cases described in Table 2-1 discussed in Chapter 2. In the results tabulated in Table 4-9 we observe that present approach mentioned above to find the GK_{total} gives the results which are similar to Eqs (2.22) i.e. without the width correction factor. To get comparable results we need to include the width correction factor in the method discussed above in eqs. (4.93). For composite the width correction factor should depend on the stacking sequence, ply orientation and the material properties, but at present we will use the width correction factor mentioned in chapter 2, Table 2-3. Therefore the modified expression for composite I-Beam GK would be:

Present approach	$GK_{total} = \left(4\mu_{f1}b_{f1} * D^*_{T\_scf1}\right) + \left(4\mu_{f2}b_{f2} * D^*_{T\_scf2}\right) + \left(4\mu_w h_w * D^*_{T\_scw}\right)$	(4.95)

where

μ_{f1} = width correction factor for top flange

μ_{f2} = width correction factor for bottom flange

μ_w = width correction factor for web

and all the width correction factors depend on the $^{width}/_{laminate\ thickness}$ ratio and selected from the table mentioned in chapter 2, Table 2-3.

Table 4-9 Composite equivalent Torsional stiffness verification for isotropic material properties

Cases Isotropic material properties	Torsional Stiffness, GK or GJ ($\mathrm{lb-in^2}$)					
	Mechanics approach			Composite formulation		ANSYS™ I-Beam Model
	Method 1 Eqs (2.22)	Method 2 Eqs (2.24)	Method 3 Eqs (2.28)	Present approach Eqs (4.93)	Present approach Eqs (4.95)	
1	197.2	188.79	188.51	197.20	188.79	191.09
2	176.46	168.35	168.77	176.46	168.57	170.77
3	166.09	159.45	158.4	166.09	159.45	156.65

We observe that the composite GK formulation with width correction gives comparable results with the GK calculated by the mechanics approach and the ANSYS™ FEM model.

Now, the composite GK formulation is applied to the composite cases discussed below:

CASE A:

Symmetric and Balanced stacking sequence

Equal top flange and bottom flange width

Equal top flange and bottom flange thickness

Table 4-10 Configuration for Case A

Geometry of composite I-Beam	Layup	Material Properties
Top flange width = 0.625 inch Bottom Flange width = 0.625 inch Web height = 0.5 inches	Top flange = $[\pm\theta/0/90]_s$ Bottom Flange =$[\pm\theta/0/90]_s$ Web = $[\pm 45]_S$ θ takes the values of 0, 15, 30, 45, 60, 75, 90.	$E_1 = 21.75 \times 10^6$ psi, $E_2 = 1.595 \times 10^6$psi, $G_{12} = 0.8702 \times 10^6$ psi , $\nu_{12} = 0.25$ $t_{ply} = 0.005$ in.

Table 4-11 Torsional Stiffness comparison for case A without width reduction factor

CASE A	Torsional Stiffness - GK ($lb - in^2$)			% Difference	
θ	Smeared property approach Eqs (4.94)	Present formulation Eqs (4.93)	ANSYS™ I-beam model	Between ANSYS™ and Smeared property approach	Between ANSYS™ Present formulation
0	27.59	27.98	27.53	-0.20	-1.65
15	53.21	55.73	52.98	-0.43	-5.18
30	104.74	108.35	98.46	-6.38	-10.04
45	130.27	131.60	116.72	-11.61	-12.75
60	104.07	104.55	93.91	-10.82	-11.33
75	52.97	53.37	50.23	-5.46	-6.26
90	27.59	27.98	27.28	-1.13	-2.59

Table 4-12 Torsional Stiffness comparison for case A with width reduction factor

CASE A	Torsional Stiffness - GK $(\mathrm{lb}-\mathrm{in}^2)$ WIDTH REDUCTION		% Difference
θ	Present formulation Eqs (4.95)	ANSYS™ I-beam model	Between ANSYS™ Present formulation
0	26.50	27.53	3.74
15	52.68	52.98	0.57
30	101.94	98.46	-3.53
45	123.80	116.72	-6.06
60	98.38	93.91	-4.75
75	50.26	50.23	-0.07
90	26.50	27.28	2.85

CASE B:

Anti-symmetrical stacking sequence for the flanges

Equal top flange and bottom flange width

Equal top flange and bottom flange thickness

Table 4-13 Configuration for Case B

Geometry of composite I-Beam	Layup	Material Properties
Top flange width = 0.625 inch Bottom Flange width = 0.625 inch Web height = 0.5 inches	Top flange = $[\pm\theta/0/90]_{2T}$ Bottom Flange =$[\pm\theta/0/90]_{2T}$ Web = $[\pm 45]_S$ θ takes the values of 0, 15, 30, 45, 60, 75, 90.	$E_1 = 21.75 \times 10^6$ psi, $E_2 = 1.595 \times 10^6$psi, $G_{12} = 0.8702 \times 10^6$ psi , $\nu_{12} = 0.25$ $t_{ply} = 0.005\ in.$

Table 4-14 Torsional Stiffness comparison for case B without width reduction factor

CASE B	Torsional Stiffness - GK $(\mathrm{lb}-\mathrm{in}^2)$			% Difference	
θ	Smeared property approach Eqs (4.94)	Present formulation Eqs (4.93)	ANSYS™ I-beam model	Smeared property approach Eqs (4.94)	Present formulation Eqs (4.93)
0	27.59	27.98	27.42	-0.59	-2.04
15	41.79	42.30	40.67	-2.75	-4.02
30	68.08	68.65	64.11	-6.20	-7.09
45	80.96	81.43	74.76	-8.30	-8.93
60	67.97	68.37	63.34	-7.31	-7.94
75	41.74	42.14	40.16	-3.93	-4.93
90	27.59	27.98	27.23	-1.32	-2.78

Table 4-15 Torsional Stiffness comparison for case B with width reduction factor

CASE B	Torsional Stiffness - GK $(\mathrm{lb}-\mathrm{in}^2)$ WIDTH REDUCTION		% Difference
θ	Present formulation Eqs (4.95)	ANSYS™ I-beam model	Between ANSYS™ Present formulation
0	26.50	27.42	3.37
15	39.86	40.67	1.98
30	64.63	64.11	-0.82
45	76.63	74.76	-2.51
60	64.36	63.34	-1.61
75	39.70	40.16	1.15
90	26.40	27.23	3.04

CASE C:

Symmetric and Balanced stacking sequence

Unequal top flange and bottom flange width

Unequal top flange and bottom flange thickness

Table 4-16 Configuration for Case C

Geometry of composite I-Beam	Layup	Material Properties
Top flange width = 0.25 inch Bottom Flange width = 1 inch Web height = 0.5 inches	Top flange = $[\pm\theta/0/90]_s$ Bottom Flange =$[\pm\theta/0_2/90]_s$ Web = $[\pm 45]_S$ θ takes the values of 0, 15, 30, 45, 60, 75, 90.	$E_1 = 21.75 \text{ x } 10^6$ psi, $E_2 = 1.595 \text{ x } 10^6$psi, $G_{12} = 0.8702 \text{ x } 10^6$ psi , $\nu_{12} = 0.25$ $t_{ply} = 0.005\ in.$

Table 4-17 Torsional Stiffness comparison for case C without width reduction factor

CASE C	Torsional Stiffness - GK ($\text{lb} - \text{in}^2$)			% Difference	
θ	Smeared property approach Eqs (4.94)	Present formulation Eqs (4.93)	ANSYS™ I-beam model	Smeared property approach Eqs (4.94)	Present formulation Eqs (4.93)
0	45.28	45.68	44.37	-2.05	-2.95
15	87.87	90.20	85.14	-3.21	-5.95
30	173.25	176.36	163.71	-5.83	-7.73
45	215.25	216.34	198.27	-8.57	-9.11
60	172.05	172.51	159.41	-7.93	-8.22
75	87.41	87.81	82.32	-6.19	-6.67
90	45.28	45.68	44.03	-2.83	-3.74

Table 4-18 Torsional Stiffness comparison for case C without width reduction factor

CASE C	Torsional Stiffness - GK $(\mathrm{lb}-\mathrm{in}^2)$ WIDTH REDUCTION		% Difference
θ	Present formulation Eqs (4.95)	ANSYS™ I-beam model	Between ANSYS™ Present formulation
0	43.28	44.37	2.46
15	85.94	85.14	-0.95
30	168.00	163.71	-2.62
45	206.06	198.27	-3.93
60	164.33	159.41	-3.09
75	83.67	82.32	-1.64
90	43.55	44.03	1.10

CASE D:

Anti-symmetrical stacking sequence for the flanges

Unequal top flange and bottom flange width

Unequal top flange and bottom flange thickness

Table 4-19 Configuration for Case D

Geometry of composite I-Beam	Layup	Material Properties
Top flange width = 0.25 inch Bottom Flange width = 1 inch Web height = 0.5 inches	Top flange = $[\pm\theta/0/90]_{2T}$ Bottom Flange =$[\pm\theta/0_2/90]_{2T}$ Web = $[\pm 45]_S$ θ takes the values of 0, 15, 30, 45, 60, 75, 90.	$E_1 = 21.75 \times 10^6$ psi, $E_2 = 1.595 \times 10^6$psi, $G_{12} = 0.8702 \times 10^6$ psi , $\nu_{12} = 0.25$ $t_{ply} = 0.005\ in.$

Table 4-20 Torsional Stiffness comparison for case D without width reduction factor

CASE D	Torsional Stiffness - GK $(\mathrm{lb}-\mathrm{in}^2)$			% Difference	
θ	Smeared property approach Eqs (4.94)	Present formulation Eqs (4.93)	ANSYS™ I-beam model	Smeared property approach Eqs (4.94)	Present formulation Eqs (4.93)
0	45.28	45.68	44.36	-2.08	-2.98
15	66.97	67.53	65.14	-2.82	-3.67
30	105.84	106.46	101.06	-4.73	-5.34
45	124.44	124.92	117.35	-6.04	-6.45
60	105.54	105.94	99.96	-5.58	-5.98
75	66.84	67.24	64.40	-3.80	-4.42
90	45.28	45.68	44.24	-2.35	-3.24

Table 4-21 Torsional Stiffness comparison for case D with width reduction factor

CASE D	Torsional Stiffness - GK $(\mathrm{lb}-\mathrm{in}^2)$ WIDTH REDUCTION		% Difference
θ	Present formulation Eqs (4.95)	ANSYS™ I-beam model	Between ANSYS™ Present formulation
0	43.56	44.36	1.79
15	64.36	65.14	1.19
30	101.38	101.06	-0.32
45	118.94	117.35	-1.35
60	100.89	99.96	-0.93
75	64.07	64.40	0.51
90	43.59	44.24	1.48

Observations from the above case studies:

- Torsional stiffness given by Present formulation Eqs (4.93) and Smeared property approach Eqs (4.94) are quite comparable for composite cases A, B, C and D (Table 4-10, Table 4-13, Table 4-16, Table 4-19), but present formulation fulfills the requirement of no bending and shear for pure torsion while smeared property approach doesn't.
- Analytical Torsional stiffness Eqs (4.93) when compared with ANSYS™ result (Table 4-11, Table 4-14, Table 4-17, Table 4-20) has some percentage of difference and this is because of the analytical approach not having the width correction factor included.
- Analytical Torsional stiffness Eqs (4.95) which includes the width correction factor gives quite comparable results with the ANSYS™ result (Table 4-12, Table 4-15, Table 4-18, Table 4-21) for GK.
- Width correction factor used for composite in Eqs (4.95) is basically for the isotropic case Table 2-3, which are found experimentally and tabulated in [30].
- Width correction factor for composite depends on stacking sequence, material properties and ply orientation, *but in this thesis isotropic width correction factor is applied for the composite case.*

4.12 Equivalent Warping Stiffness for a Composite I-beam

As explained in Chapter 2, when the beam is axially constrained at one of its cross-section, then at this cross-section warping cannot occur. The effect of restrained warping are more pronounced for thin-walled open section beams than the thin walled closed section beams. As a summary, we know that when the composite beam is subjected to pure torsion the expression is:

Free torsion expression	$\bar{T} = (GK) * \emptyset$	(4.96)

And if the composite beam is axially constrained, the restrained torsion expression modifies to:

Beam under restrained warping	$\bar{T} = (GK)\ \emptyset\ - (E\Gamma)\frac{d^2\emptyset}{dx^2}$	(4.97)

where,

GK = Equivalent torsional stiffness of the composite I-Beam eqs (4.95)

EΓ = Equivalent warping stiffness of the composite I-Beam

$\bar{T}$ = Total torsional load applied

$\emptyset =$ Rate of twist of composite I-Beam = $^{d\theta}/_{dx}$

The expression for (EΓ) for a composite I-Beam can be approximated by the method described below:

When the cross-section of beam is axially restrained we have axial forces N_x introduced and these axial forces create a bending moment which acts on the individual flange with respect to z-z axis. The forces created due to restrained warping as clearly shown in Figure 4-14 below:

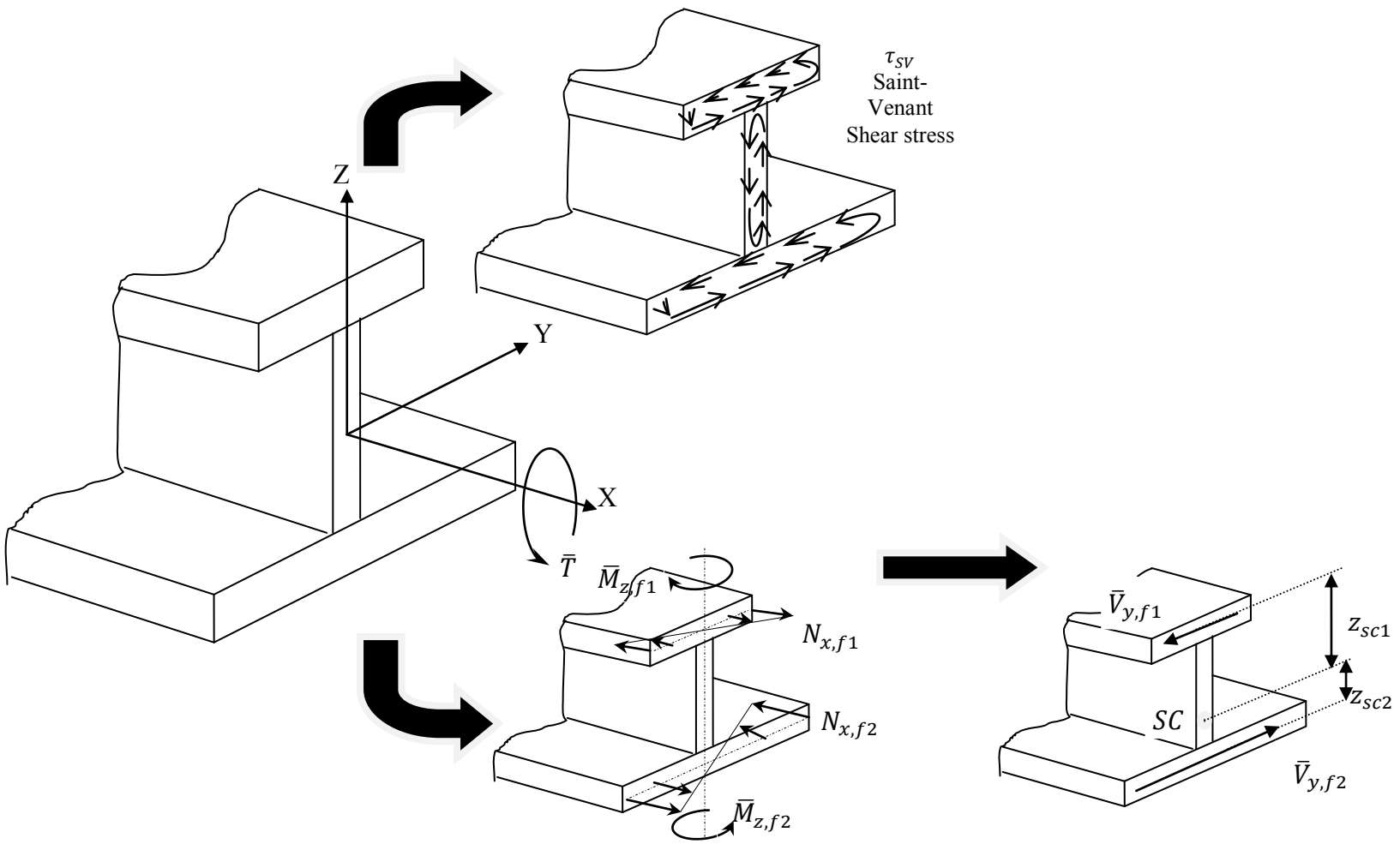

Figure 4-14 I-Beam under pure torsion with axial constraints

From Eqs (4.38) and (4.39) we can write the expression for the bending moments created in top and bottom flange due to the axial force as:

$$\bar{M}_{z,f1} = -\left(A^*_{1,f1} * \frac{{b_{f1}}^3}{12}\right) * \frac{d^2 v_{f1}}{dx^2}$$
$$\bar{M}_{z,f2} = \left(A^*_{2,f2} * \frac{{b_{f2}}^3}{12}\right) * \frac{d^2 v_{f2}}{dx^2} \quad (4.98)$$

Where,

v_{f1} = Displacement of top flange due to rotation about x-axis

$v_{f2} =$ Displacement of bottom flange due to rotation about x-axis

The expression for the displacements are as described below which can be easily derived by looking at the Figure 4-15:

$$v_{f1} = \theta * z_{sc1}$$
$$v_{f2} = \theta * z_{sc2} \quad (4.99)$$

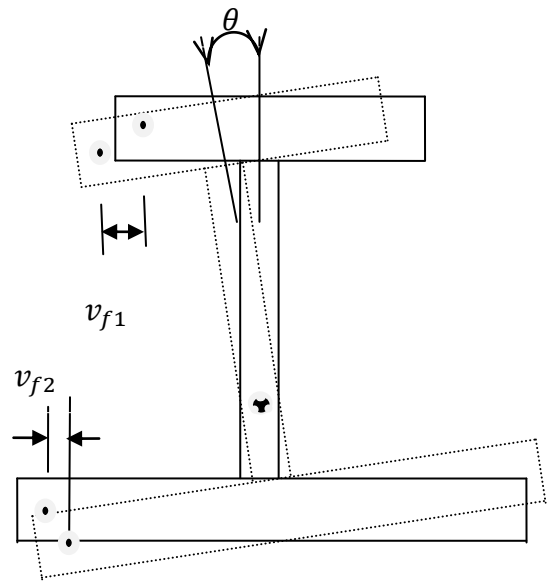

Figure 4-15 Rotation of I-Beam about x-axis

Also,

$$\frac{\mathrm{d}v_{f1}}{\mathrm{dx}} = \frac{\mathrm{d}}{\mathrm{dx}}(\theta * \mathrm{z_{sc1}}) = \mathrm{z_{sc1}} * \emptyset$$
$$\frac{dv_{f2}}{dx} = \frac{d}{dx}(\theta * z_{sc2}) = z_{sc2} * \emptyset \tag{4.100}$$

Thus from eqs (4.100) (4.98) we get,

$$\bar{M}_{z,f1} = -\left(A^*_{1,f1} * \frac{{b_{f1}}^3}{12}\right) * z_{sc1} * \frac{d\emptyset}{dx}$$
$$\bar{M}_{z,f2} = -\left(A^*_{1,f2} * \frac{{b_{f2}}^3}{12}\right) * z_{sc2} * \frac{d\emptyset}{dx} \tag{4.101}$$

Now these moments develops shear forces in the individual flanges as shown in the Figure 4-14.

$$\bar{V}_{y,f1} = \frac{d\,\bar{M}_{z,f1}}{dx} = -\left(A^*_{1,f1} * \frac{{b_{f1}}^3}{12}\right) * z_{sc1} * \frac{d^2\emptyset}{dx^2}$$
$$\bar{V}_{y,f2} = \frac{d\bar{M}_{z,f2}}{dx} = -\left(A^*_{1,f2} * \frac{{b_{f2}}^3}{12}\right) * z_{sc2} * \frac{d^2\emptyset}{dx^2} \tag{4.102}$$

Now the shear forces results in a torque $\bar{T}_w$, defined by,

$$\bar{T}_w = \bar{V}_{y,f1} * z_{sc1} + \bar{V}_{y,f2} * z_{sc2} \tag{4.103}$$

Thus from eqs (4.103) (4.102) we get,

$$\bar{T}_w = -\underbrace{\left[A^*_{1,f1} * \frac{{b_{f1}}^3}{12} * {z_{sc1}}^2 + A^*_{1,f2} * \frac{{b_{f2}}^3}{12} * {z_{sc2}}^2\right]}_{\text{Equivalent Warping stiffness for composite I-Beam}} * \frac{d^2\emptyset}{dx^2} \tag{4.104}$$

∴

Warping stiffness for composite I-Beam	$\bar{T}_w = -(E\Gamma) * \frac{d^2\emptyset}{dx^2}$ $E\Gamma = \left[A^*_{1,f1} * \frac{{b_{f1}}^3}{12} * {z_{sc1}}^2 + A^*_{1,f2} * \frac{{b_{f2}}^3}{12} * {z_{sc2}}^2\right]$	(4.105)

Therefore for a composite I-Beam:

$$\bar{T} = \bar{T}_{sv} + \bar{T}_w \tag{4.106}$$

Where,

$\bar{T}$ = Total torque applied to composite I-Beam

$\bar{T}_{sv}$ = Saint –Venant torque

$\bar{T}_w$ = Restrained warping induced torque

Summary:

Approach proposed in this thesis (present work)	$\bar{T} = \bar{T}_{sv} + \bar{T}_w$ $\bar{T}_{sv} = (GK)\phi$ $GK = \left(4\mu_{f1}b_{f1} * D^*_{T_{scf1}}\right) + \left(4\mu_{f2}b_{f2} * D^*_{T_{scf2}}\right)$ $+ \left(4\mu_w h_w * D^*_{T_{scw}}\right)$ $\bar{T}_w = -(E\Gamma) * \frac{d^2\emptyset}{dx^2}$ $E\Gamma = \left[A^*_{1,f1} * \frac{{b_{f1}}^3}{12} * {z_{sc1}}^2 + A^*_{1,f2} * \frac{{b_{f2}}^3}{12} * {z_{sc2}}^2\right]$	(4.107)

Also, similar to isotropic theory Eqs (2.31) we can write the expression for angle of twist θ as,

For composite I-Beam	$\theta_{total} = \frac{T}{GK}\left(x + \frac{\sinh \mu\,(L-x)}{\mu \cosh \mu L} - \frac{\sinh \mu\, L}{\mu \cosh \mu L}\right)$ Where, $\mu^2 = \left(\frac{GK}{E\Gamma}\right)$	(4.108)

L = Total length of I-Beam

x = Length of interest

x = 0 at constrained edge

$x = L\ at\ free\ edge$

Thus at free end,

$$\theta_{total} = \frac{T}{GK}\left(1 - \frac{\tanh(\mu L)}{(\mu L)}\right) \quad (4.109)$$

Smeared property approach	$\bar{T} = \bar{T}_{sv} + \bar{T}_w$ $\bar{T}_{sv} = (GK)\phi$ $GK = \left[\frac{4b_{f1}}{d_{66f1}} + \frac{4b_{f2}}{d_{66f2}} + \frac{4h_w}{d_{66w}}\right]$ $\bar{T}_w = -(E\Gamma) * \frac{d^2\emptyset}{dx^2}$ $E\Gamma = \left[\frac{h^2 * \left(\frac{1}{a_{11}}\right)_{f1} * \left(\frac{1}{a_{11}}\right)_{f2} * b_{f1}^3 * b_{f2}^3}{\left(\frac{1}{a_{11}}\right)_{f1} * b_{f1}^3 + \left(\frac{1}{a_{11}}\right)_{f2} * b_{f2}^3}\right]$	(4.110)

4.13 Results and Verification of Equivalent Warping stiffness expression and total angle of twist expression derived for Composite I-Beam

The composite formulation for equivalent warping stiffness was compared for the 3 cases discussed in Chapter 2, Table 2-1 for isotropic properties. The results are as tabulated in Table 4-22:

Table 4-22 Composite equivalent Torsional stiffness verification for isotropic material properties

Case - Isotropic Material properties	Warping Rigidity – $E\Gamma$ - (lb-in^2)				% Difference	
		Composite Formulation				
	Mechanics Approach Eq (2.25)	Present formulation Eq (4.105)	Smeared property approach Eq (4.110)	ANSYS™ results Chapter 3	Between Mechanics and present formulation	Between ANSYS™ and present formulation
1	155.85	155.85	155.85	151.56	0.00	2.83
2	1020.47	1020.47	1020.47	962.59	0.00	6.01
3	1369.74	1369.74	1369.74	1278.72	0.00	7.12

The results of warping stiffness by the composite formulation match perfectly with the warping stiffness computed by the mechanics approach and ANSYS and hence we can apply the formulation for the composite cases too.

Later, total angle of twist at free edge for a cantilever I-Beam were calculated by using eqs (4.109) and compared with the isotropic material properties and tabulated below:

Table 4-23 Composite Angle of twist expression verified for isotropic material properties

Case - Isotropic Material properties	Total Angle of twist- θ_{total} - (radians)				% Difference	
	Mechanics Approach Eq (2.31)	Composite Formulation		ANSYS results Chapter 3		
		Present formulation Eq (4.109)	Smeared property approach		Between Mechanics and present formulation	Between ANSYS and present formulation
1	0.048	0.048	0.0462	0.0482	0.00	-0.41
2	0.0447	0.0447	0.043	0.0446	0.00	0.22
3	0.045	0.045	0.043	0.0456	0.00	-1.32

From the above comparison we conclude that the angle of twist approximated by composite formulation for an isotropic material property I-beam works good and hence it was applied for the 4 cases (A, B, C, and D) discussed earlier in the chapter (Table 4-10, Table 4-13, Table 4-16 & Table 4-19) and compared with the ANSYS™ results.

Table 4-24 Comparison of Angle of twist for Case A

Case - A Composite Properties θ variation	Total Angle of twist (radians)			% Difference	
	Present formulation Eq (4.109)	Smeared property approach	ANSYS™ result	Between ANSYS™ and present formulation	Between ANSYS™ and Smeared property
0	0.1097	0.1080	0.1147	-4.36	-5.84
15	0.0855	0.0849	0.0872	-1.95	-2.64
30	0.0621	0.0608	0.0642	-3.20	-5.23
45	0.0578	0.0554	0.0615	-6.02	-9.92
60	0.0722	0.0690	0.0757	-4.65	-8.87
75	0.1210	0.1166	0.1218	-0.67	-4.29
90	0.1821	0.1776	0.1818	0.15	-2.33

Table 4-25 Comparison of Angle of twist for Case B

Case - B Composite Properties θ variation	Total Angle of twist (radians)			% Difference	
	Present formulation Eq (4.109)	Smeared property approach	ANSYS™ result	Present formulation Eq (4.109)	Smeared property approach
0	0.1097	0.1110	0.1157	-5.19	-4.06
15	0.0983	0.0981	0.1009	-2.55	-2.75
30	0.0857	0.0832	0.0869	-1.43	-4.30
45	0.0843	0.0813	0.0864	-2.43	-5.90
60	0.1002	0.0969	0.1018	-1.54	-4.79
75	0.1419	0.1388	0.1414	0.35	-1.84
90	0.1820	0.1800	0.1816	0.22	-0.88

Table 4-26 Comparison of Angle of twist for Case C

Case - C Composite Properties θ variation	Total Angle of twist (radians)			% Difference	
	Present formulation Eq (4.109)	Smeared property approach	ANSYS™ result	Present formulation Eq (4.109)	Smeared property approach
0	0.1739	0.1683	0.1663	4.57	1.20
15	0.0971	0.0952	0.0968	0.36	-1.61
30	0.0533	0.0518	0.0542	-1.71	-4.48
45	0.0447	0.0428	0.0461	-3.09	-7.20
60	0.0559	0.0535	0.0572	-2.24	-6.44
75	0.1063	0.1020	0.1067	-0.36	-4.39
90	0.1944	0.1877	0.1884	3.20	-0.36

Table 4-27 Comparison of Angle of twist for Case D

Case – D Composite Properties θ variation	Total Angle of twist (radians)			% Difference	
	Present formulation Eq (4.109)	Smeared property approach	ANSYS™ result	Present formulation Eq (4.109)	Smeared property approach
0	0.1739	0.1694	0.1660	4.73	2.02
15	0.1258	0.1220	0.1226	2.58	-0.52
30	0.0857	0.0824	0.0845	1.43	-2.47
45	0.0754	0.0723	0.0754	0.01	-4.10
60	0.0889	0.0854	0.0884	0.60	-3.36
75	0.1363	0.1314	0.1344	1.41	-2.24
90	0.1944	0.1882	0.1879	3.44	0.14

Observations from above tabulated values:

1. Present method of angle of twist, torsional stiffness and warping stiffness gives a better match with the ANSYS™ results

Later the equivalent torsional stiffness, warping stiffness, angle of twist in free torsion and angle of twist in restrained torsion for a composite I-beam were compared and the graphs were plotted to get a better understanding of the relationship of fiber angle with the above mentioned properties.

Table 4-28 Torsional Properties of Composite I-beam Case A

Case - A Composite Properties θ variation	Analytically calculated properties – present method			
	GJ (lb-in^2) Eqs (4.93)	EΓ (lb-in^2) Eq (4.105)	θ (restrained warping) - radians Eq (4.109)	θ (Free torsion) - radians
0	26.50	1989.10	0.1097	0.3774
15	52.68	1822.80	0.0855	0.1898
30	101.94	1400.90	0.0621	0.0981
45	123.80	1007.50	0.0578	0.0808
60	98.38	831.80	0.0722	0.1016
75	50.26	792.47	0.1210	0.1990
90	26.50	789.60	0.1821	0.3774

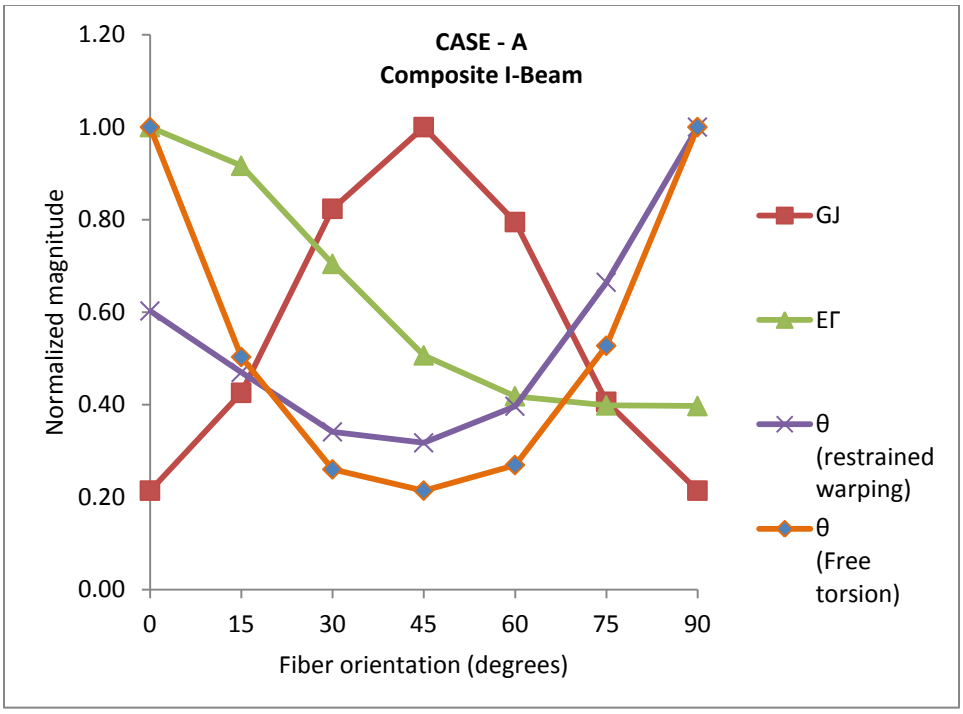

Figure 4-16 Variation of Torsional properties of Composite I-beam Case A

Table 4-29 Torsional Properties of Composite I-beam Case B

Case – B Composite Properties θ variation	Analytically calculated properties – present method			
	GJ (lb-in^2) Eqs (4.93)	EΓ (lb-in^2) Eq (4.105)	θ (restrained warping) - radians Eq (4.109)	θ (Free torsion) - radians
0	26.50	1988.50	0.1097	0.2311
15	39.86	1812.30	0.0983	0.1164
30	64.63	1355.10	0.0857	0.0595
45	76.63	973.14	0.0843	0.0485
60	64.36	824.28	0.1002	0.0609
75	39.70	792.15	0.1419	0.1195
90	26.40	789.63	0.1820	0.2296

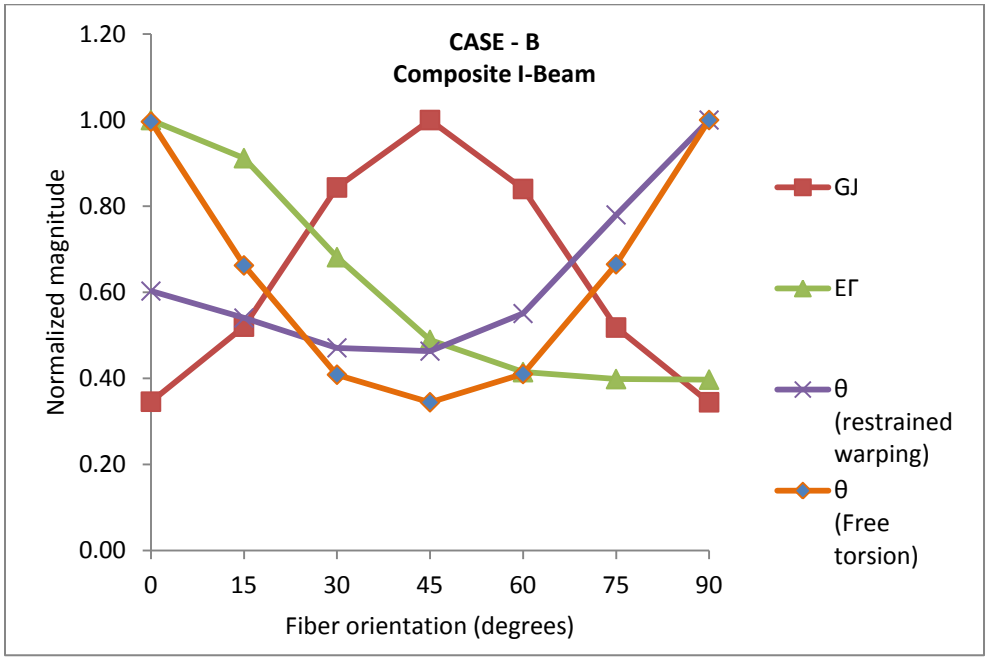

Figure 4-17 Variation of Torsional properties of Composite I-beam Case B

Table 4-30 Torsional Properties of Composite I-beam Case C

Case – C Composite Properties θ variation	Analytically calculated properties – present method			
	GJ ($lb\text{-}in^2$) Eqs (4.93)	EΓ ($lb\text{-}in^2$) Eq (4.105)	θ (restrained warping) - radians Eq (4.109)	θ (Free torsion) - radians
0	43.28	256.32	0.1739	0.2311
15	85.94	234.95	0.0971	0.1164
30	168.00	180.72	0.0533	0.0595
45	206.06	130.12	0.0447	0.0485
60	164.33	107.51	0.0559	0.0609
75	83.67	102.44	0.1063	0.1195
90	43.55	102.07	0.1944	0.2296

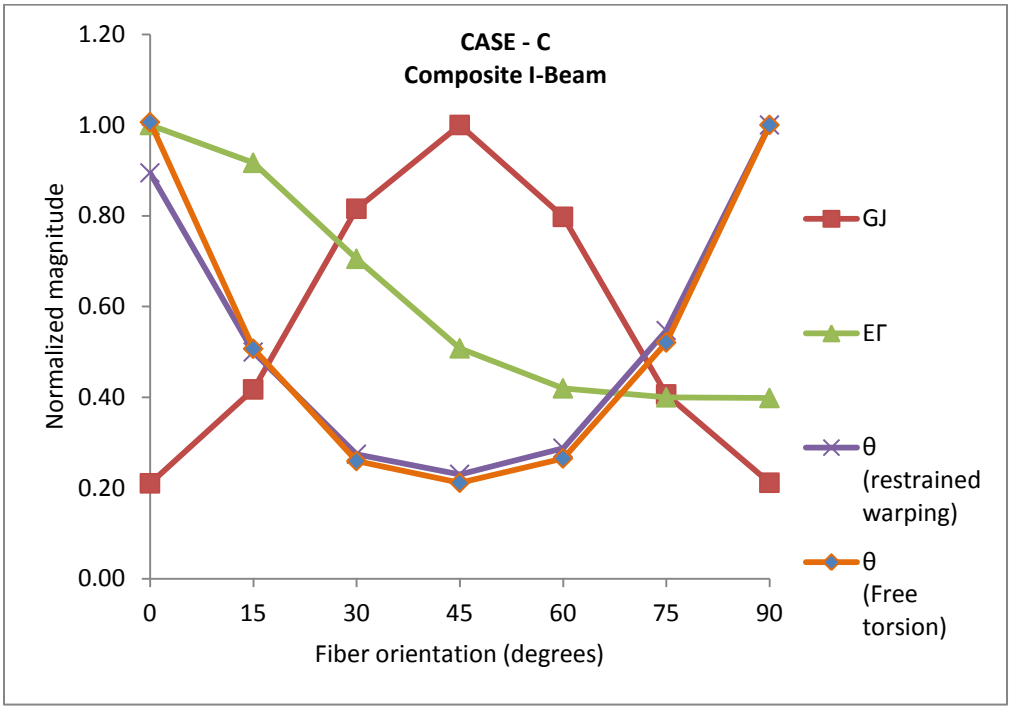

Figure 4-18 Variation of Torsional properties of Composite I-beam Case C

Table 4-31 Torsional Properties of Composite I-beam Case D

Case – D Composite Properties θ variation	Analytically calculated properties – present method			
	GJ (lb-in^2) Eqs (4.93)	EΓ (lb-in^2) Eq (4.105)	θ (restrained warping) - radians Eq (4.109)	θ (Free torsion) - radians
0	43.56	256.60	0.1739	0.2296
15	64.36	233.82	0.1258	0.1554
30	101.38	174.82	0.0857	0.0986
45	118.94	125.78	0.0754	0.0841
60	100.89	106.70	0.0889	0.0991
75	64.07	102.57	0.1363	0.1561
90	43.59	102.25	0.1944	0.2294

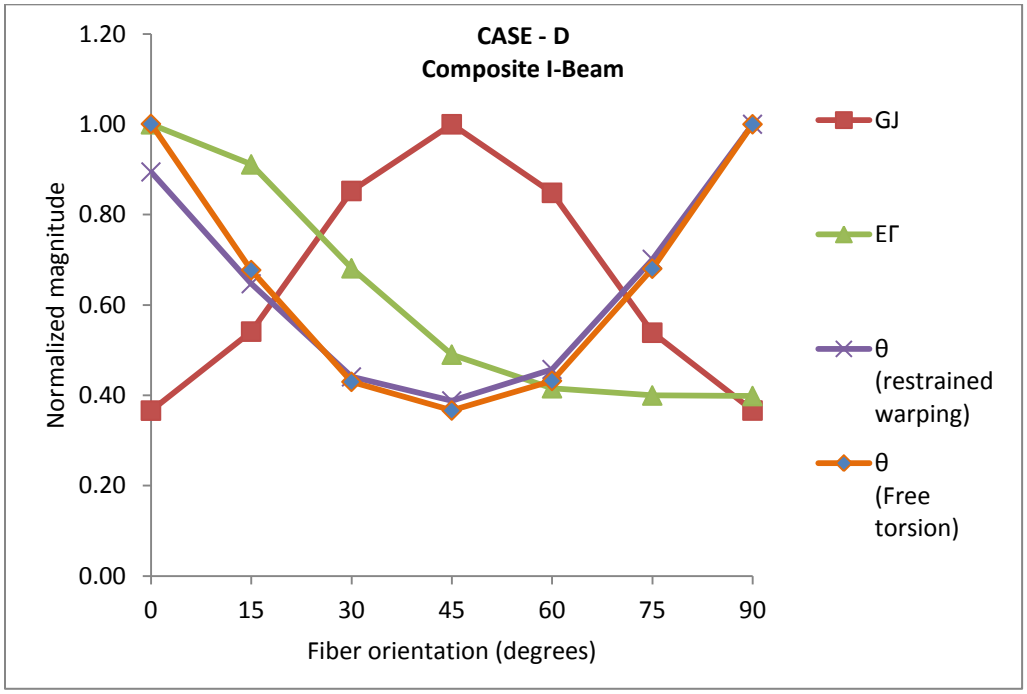

Figure 4-19 Variation of Torsional properties of Composite I-beam Case D

Observations from the above graphs and tabulated values:

Table 4-32 Observation for the Torsional Properties of a Composite I-Beam

Equivalent Properties	Maximum (at fiber orientation)	Minimum (at fiber orientation)	Variation pattern with respect to fiber orientation
Torsional Stiffness	45 degree	0 & 90 degrees	Increases from 0 – 45 and decreases from 45 – 90 degrees. It follows a bell shaped curve which is symmetric with respect to 45 degree
Warping stiffness	0 degree	90 degree	Decreases continuously from 0 – 90 degree. The reduction in stiffness is more severe from 0 – 45 and minimal from 45 – 90
Angle of twist – free torsion	0 & 90 degrees	45 degree	It is inversely related to the torsional stiffness. It follows an inverted bell shaped curve which has a maximum at 0 and reduced continuously till 45, where it holds the minimum value and then again increases till 90 degree.
Angle of twist – restrained warping	Depends	45 degree	Warping constrain will restrict the rotation of I-beam under torsion. Case A and B: As warping stiffness is comparatively quite higher than the torsional stiffness it has a prominent effect in reducing the angle of twist. Case C and D: Warping stiffness has minimal effect on the angle of twist and can be easily observed from the variation of angle of twist curve.

4.14 Comparison and study of variation of Equivalent Stiffness of Composite I-Beam

The variation of Equivalent axial stiffness, bending stiffness with respect to y-axis and z-axis, torsional stiffness and warping stiffness with respect to the fiber orientation in Case A, B, C and D are shown below in Figure 4-20, Figure 4-21, Figure 4-22, Figure 4-23, Table 4-33, Table 4-34 & Table 4-36 .

The expressions for equivalent axial stiffness and bending stiffness with respect to y-axis are derived in [27].

Equivalent Axial Stiffness is given by:

$$\overline{EA} = b_{f1}\left(A^*_{1,f1}\right) + b_{f2}\left(A^*_{1h,f2}\right) + h_w\left(A^*_{1,w}\right)$$

Equivalent Bending Stiffness with respect to Y-axis is given by:

$$D_x^c = \sum_{i=1}^{2} b_{fi}\left(A^*_{1,fi}z_{ic}^2 + 2B^*_{1,fi}z_{ic} + D^*_{i,fi}\right) + A^*_{1,w}\left(\frac{1}{12}h_w^3 + h_w h_{wc}^2\right)$$

Table 4-33 Equivalent Stiffness of composite I-beam Case A

Case – A Composite properties θ variation	Analytically calculated properties				
	EA (lb)	$(EI)_{yy}$ (lb-in^2)	$(EI)_{zz}$ (lb-in^2)	GJ (lb-in^2)	EΓ (lb-in^2)
0	868,000	61,820	27,286	26.50	1989.10
15	798,500	56,700	25,005	52.68	1822.80
30	620,790	43,738	19,218	101.94	1400.90
45	455,010	31,621	13,822	123.80	1007.50
60	380,960	26,214	11,411	98.38	831.80
75	364,399	25,005	10,872	50.26	792.47
90	363,180	24,916	10,832	26.50	789.60

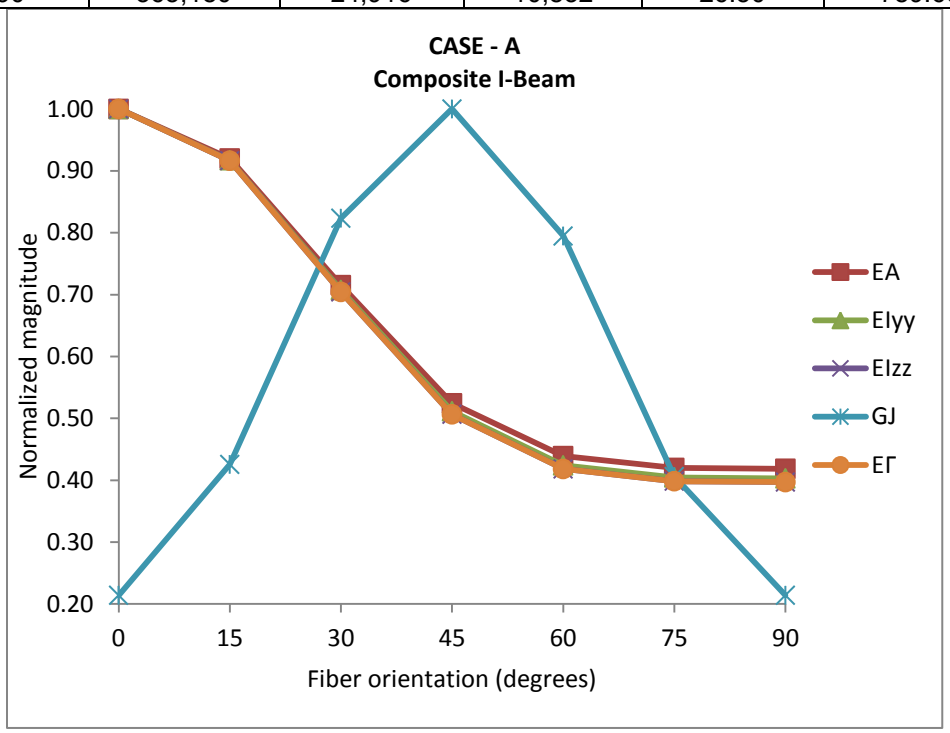

Figure 4-20 Variation of Equivalent stiffness properties with respect to fiber orientation for Case A

Table 4-34 Equivalent Stiffness of composite I-beam Case B

Case – B Composite properties θ variation	Analytically calculated properties				
	EA (lb)	$(EI)_{yy}$ (lb-in^2)	$(EI)_{zz}$ (lb-in^2)	GJ (lb-in^2)	EΓ (lb-in^2)
0	868,320	61,821	27,276	26.50	1988.50
15	794,080	56,399	24,859	39.86	1812.30
30	601,460	42,331	18,589	64.63	1355.10
45	440,500	30,577	13,350	76.63	973.14
60	377,780	25,995	11,308	64.36	824.28
75	364,260	25,006	10,867	39.70	792.15
90	363,170	24,929	10,832	26.40	789.63

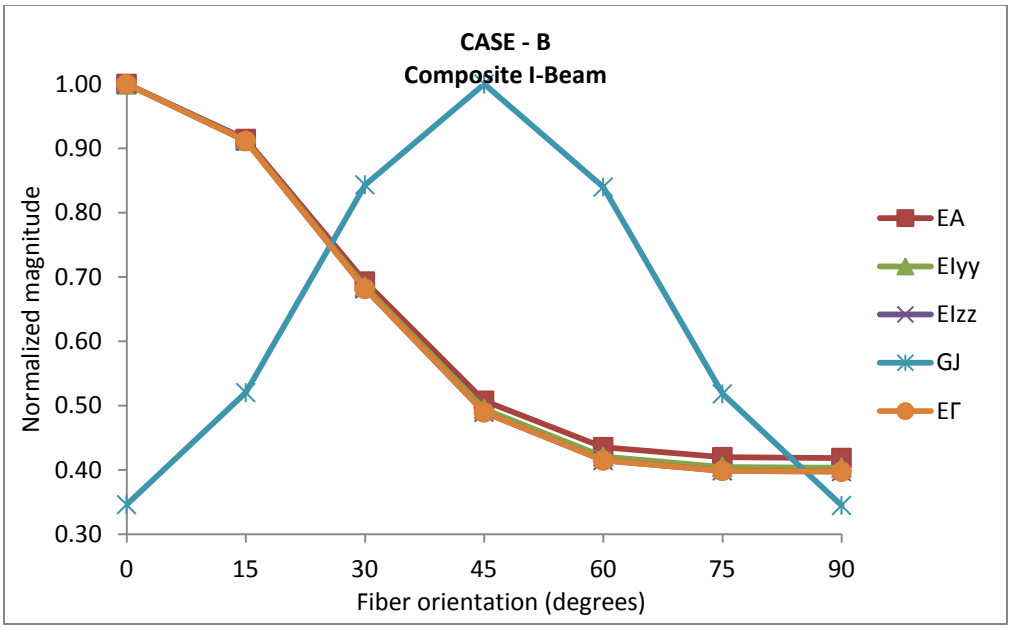

Figure 4-21 Variation of Equivalent stiffness properties with respect to fiber orientation for Case B

Table 4-35 Equivalent Stiffness of composite I-beam Case C

Case – C Composite properties θ variation	Analytically calculated properties				
	EA (lb)	$(EI)_{yy}$ (lb-in^2)	$(EI)_{zz}$ (lb-in^2)	GJ (lb-in^2)	EΓ (lb-in^2)
0	1,086,700	43,830	74,925	43.28	256.32
15	1,016,200	40,440	70,148	85.94	234.95
30	838,330	31,830	58,101	168.00	180.72
45	672,550	23,798	46,876	206.06	130.12
60	598,540	20,202	41,866	164.33	107.51
75	582,430	19,399	40,782	83.67	102.44
90	581,480	19,341	40,722	43.55	102.07

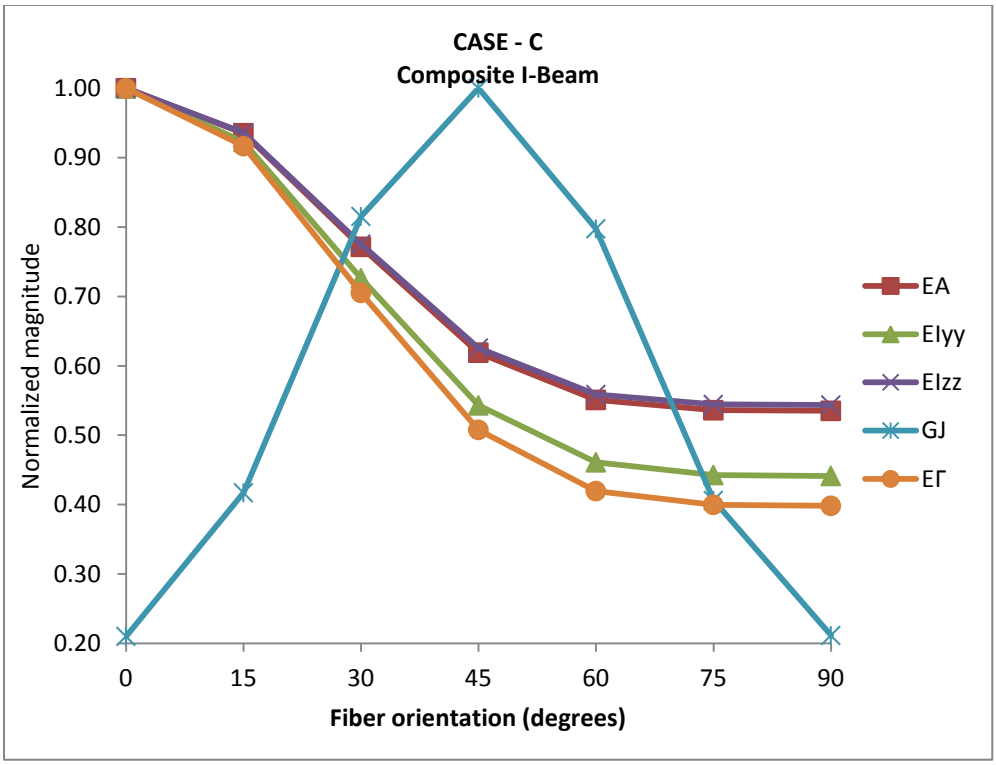

Figure 4-22 Variation of Equivalent stiffness properties with respect to fiber orientation for Case C

Table 4-36 Equivalent Stiffness of composite I-beam Case D

Case – D Composite properties θ variation	Analytically calculated properties				
	EA (lb)	$(EI)_{yy}$ (lb-in^2)	$(EI)_{zz}$ (lb-in^2)	GJ (lb-in^2)	EΓ (lb-in^2)
0	1,086,200	43,702	74,893	43.56	256.60
15	1,011,000	40,167	69,788	64.36	233.82
30	816,790	30,958	56,608	101.38	174.82
45	656,340	23,197	45,752	118.94	125.78
60	594,980	20,151	41,619	100.89	106.70
75	582,270	19,494	40,771	64.07	102.57
90	581,470	19,443	40,721	43.59	102.25

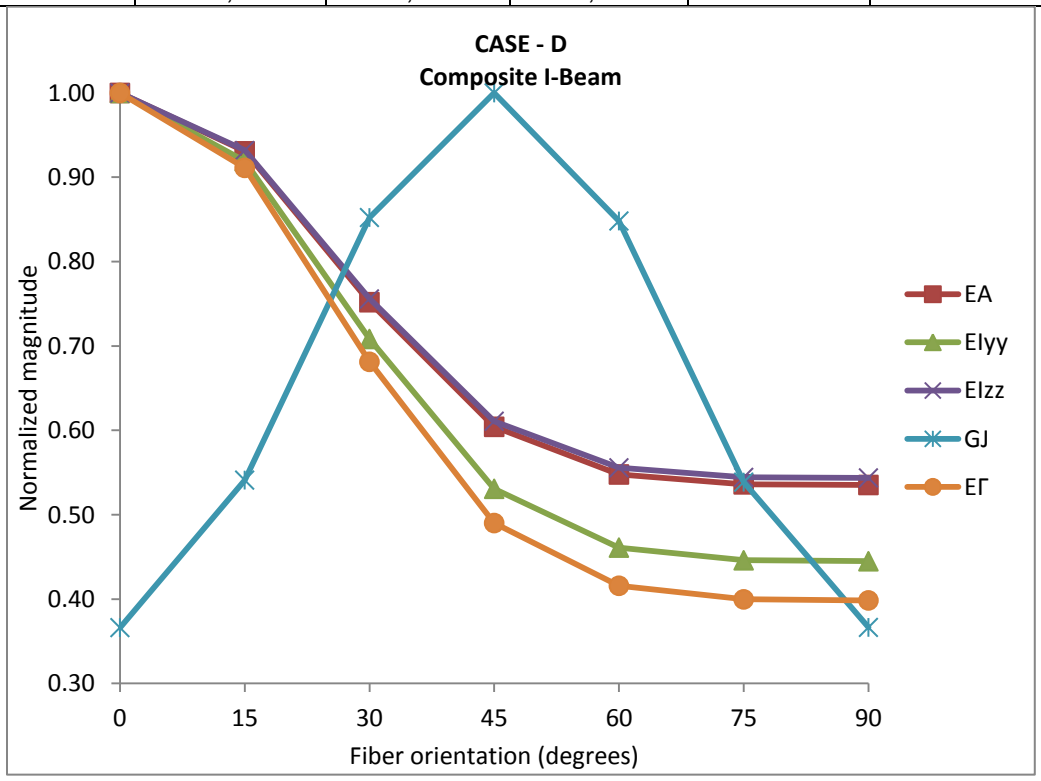

Figure 4-23 Variation of Equivalent stiffness properties with respect to fiber orientation for Case D

Table 4-37 Observation for the Equivalent stiffnesses of a Composite I-Beam

Equivalent Properties	Maximum (at fiber orientation)	Minimum (at fiber orientation)	Variation pattern with respect to fiber orientation
Torsional Stiffness	45 degree	0 & 90 degrees	Increases from 0 – 45 and decreases from 45 – 90 degrees. It follows a bell shaped curve which is symmetric with respect to 45 degree
Warping stiffness	0 degree	90 degree	Decreases continuously from 0 – 90 degree. The reduction in stiffness is more severe from 0 – 45 and minimal from 45 – 90
Axial Stiffness			
Bending Stiffness (EI)zz and (EI)yy			

Chapter 5

Conclusive Summary and Future Work

Analytical method to calculate:

1. Shear Center
2. Equivalent torsional stiffness
3. Equivalent warping stiffness
4. Equivalent bending stiffness with respect to z-z axis

for a mono-symmetric composite I-beam were developed and the results were compared with the smeared property approach and the result from the ANSYS™ 2D model.

Following conclusions can be drawn on the basis of this study

Shear Center:

- Shear center of a composite I-beam depends upon the material properties, stacking sequence, fiber orientation and geometry.
- The formulation proposed in this study gives better agreement with ANSYS™ results.
- The composite formulation when applied to isotropic material properties gives same results as the mechanics approach.
- The formulation also captures the coupling behavior. As shown, for angle plies with high shear coupling variation, present formulation predicts better results than smeared property approach.
- Also it was highlighted that if the stacking sequence is symmetrical in web, the change in fiber orientation in web does not affect the shear center location.
- The variation of shear center with respect to the fiber orientation in flanges and web were discussed.

- The study also highlights the loopholes in the complete ABD matrix approach and suggests that this approach should be avoided to calculate the shear center and torsional stiffness for an open section.

Equivalent Torsional stiffness:

- Equivalent Torsional stiffness of a composite I-beam depends upon the material properties, stacking sequence, fiber orientation and geometry.
- The composite formulation when applied to isotropic material properties gives same results as the mechanics approach.
- The formulation proposed in this study suppresses the curvature and shear in the composite I-beam when subjected to pure torsion which is not the case with the smeared property approach.
- It was observed that if width reduction factor is not applies, we get high differences between the results obtained from ANSYS and analytical calculation.
- The study also highlights the need to incorporate the width correction factor similar to an isotropic case while calculating the torsional stiffness of the laminate.
- In this literature, the isotropic width reduction factor is used to calculate the equivalent torsional stiffness and it was observed that it gives better co-relation with ANSYS™ results than the one with no width reduction factor.
- Torsional stiffness can be maximized by including 45 degree plies and minimized by using 0 or 90 degree plies.
- It the torsional load application in ANSYS should be distributed equally to all the nodes at the cross-section rather than making a master node. Making a master

node and applying torsional load only to it would have a restrain effect which will in turn not capture the free torsion condition.

Equivalent Warping stiffness:

- Equivalent Warping stiffness of a composite I-beam depends upon the material properties, stacking sequence, fiber orientation and geometry.
- The composite formulation when applied to isotropic material properties gives same results as the mechanics approach.
- Primary Warping is only considered as secondary warping effect will be very low and can be neglected for thin walled beams.
- The method proposed in this work to deduce Warping stiffness ($E\Gamma$) from ANSYS is an indirect method and hence a pure $E\Gamma$ is not extracted from ANSYS. There is a need to find a method to directly get $E\Gamma$ from ANSYS
- Warping stiffness can be maximized by including 0 degree plies and it goes on reducing when other angle plies are included.

Also the angle of twist was calculated and it gives good agreement with the angle of twist calculated by ANSYS™ model. The variation of equivalent torsional, warping, axial, bending stiffness and angle of twist (free torsion and restrained torsion) were also discussed.

Future work

The topic of torsion is vast like an ocean and this thesis work is just a droplet of that vast deep ocean. Numerous studies can be done on the torsional response of the open and closed section beam. Following topics can serve as future work:

- Predicting the width reduction factor
- Analysis of the effect of secondary warping
- Stresses and strains in each ply
- Torsional analysis of other open sections
- Study of behavior of warping and more accurate prediction of stiffness by incorporating some modifications to the present formulations
- Comparing the results with 3D model in ANSYS™
- Hygrothermal analysis
- Torsional analysis when torsion is applied at location other than shear center/ torsional center
- Experimental verification of the results
- Modification of the formulation for a more realistic I-beam (which includes the ply drop off, tool radius, spool ply effect, etc…)
- Comparing the formulation with other analytical approaches
- Effect of inter-laminar shear stress

Appendix A

MATLAB™ code used for this study

```
%% Matlab program for I-Beam (composite/isotropic)

%% By Vishal Sanghavi

%% program calculates Centroid, Axial Stiffness, Bending
Stiffness with
% respect to y axis and z- axis,
% Shear center (3 approaches), Torsional Stiffness (3
approaches), angle of
% twist (3 approaches),

%% last modified on 28 October 2012

clc
clear

prompt = {'Enter E1(psi):','Enter E2(psi):', 'Enter G12(psi):' ,
'Enter \nu 12 (psi):', 'Enter ply thickness tply (in):'};
dlg_title = 'Input for material properties for Q matrix';
num_lines = 1;
def = {'21.75*10^6','1.595*10^6','0.8702*10^6','0.25','0.005' };
%%def = {'1.02*10^7','1.02*10^7','4.08*10^6','0.25','0.005' };
%%def = {'18.2*10^6','1.41*10^6','0.92*10^6','0.274','0.005' };
a  = inputdlg(prompt,dlg_title,num_lines,def);
answer = [a(1),a(2),a(3),a(4),a(5)];
%a = str2num(answer{1}
S11=1/str2num(a{1}) ;
S22 = 1/str2num(a{2});;
S12 = -str2num(a{4})/str2num(a{1});
S66 = 1/str2num(a{3});
s = [S11,S12,0;S12,S22,0;0,0,S66];
%pretty (s);
Q = inv(s);
%pretty (Q);

% TOP FLANGE PLY INPUT %

prompt = {'Enter no of plies for the top most flange:'};
dlg_title = 'No of ply';
num_lines = 1;
def = {'1'};
b  = inputdlg(prompt,dlg_title,num_lines,def);
b = str2num(b{1});
ply_f1 = b;
thickness_top = b * str2num(a{5});
% TOP FLANGE PLY angle INPUT %

for i=1:b,
```

```
prompt = {'Enter thetha in degrees (start with first ply- top
most ply)for top most flange :'};
dlg_title = 'thetha';
num_lines = 1;
def = {'0'};
c(i) = inputdlg(prompt,dlg_title,num_lines,def);
end
c;
c_f1 = c
h = [0:b];
for i=0:b
    if i < b/2
        k = 0+i;
        j = 1+i;
        h(1,j) = (-b/2)+k;
   else
     k = i;
     j = 1+i;
     h(1,j) = h(1,j-1)+1;
    end
end
h = str2num(a{5})*h;
h_f1 = h
% CALCULATION OF ABBD MATRIX OF TOP FLANGE
A0 = zeros(3);
B0 = zeros(3);
D0 = zeros(3);

e = 0;
for j=1:b

     angle = str2num(c{b-e});
      e = e+1;
     theta = angle * pi / 180
     n = sin(-theta);
     m = cos(-theta);
     Tsigma = [m^2 , n^2 , 2*m*n ; n^2 , m^2 , -2*m*n ; -m*n ,
m*n , m^2 - n^2];
     n = sin(theta);
     m = cos(theta);
     Tepsilon = [m^2 , n^2 , m*n ; n^2 , m^2 , -m*n ; -2*m*n ,
2*m*n , m^2 - n^2];
     Qbar = Tsigma * Q * Tepsilon;
     n = sin(-theta);
     m = cos(-theta);
     TepsilonN = [m^2 , n^2 , m*n ; n^2 , m^2 , -m*n ; -2*m*n ,
2*m*n , m^2 - n^2];

     A = A0 + Qbar*(h(1,j+1) - h(1,j));
     f = ((h(1,j+1)*h(1,j+1)) - ((h(1,j)*h(1,j))));
```

```
format short
     B = B0 + (Qbar*f)/2;
format short
     D = D0 + (Qbar*(h(1,j+1)^3 - h(1,j)^3))/3;
     A0 = A;
     B0 = B;
     D0 = D;
end
A;
B;
D;
ABBD=[A,B;B,D];
Abarf1 = A;
Bbarf1 = B;
Dbarf1 = D;

%CALCULATION OF A*B*B*D* matric

abbd_t = inv(ABBD);
Etf1_smeared = (1 / abbd_t(1,1));

Eft1_warp = (1/( abbd_t(1,1) - ( (abbd_t(1,4)^2)/abbd_t(4,4)) )
);
astar = abbd_t(1,1) - (abbd_t(1,6)^2/abbd_t(6,6));
bstar = abbd_t(1,4) - (abbd_t(1,6)*abbd_t(4,6)/abbd_t(6,6));
dstar = abbd_t(4,4) - (abbd_t(4,6)^2/abbd_t(6,6));

astarbstardstar_t = [astar , bstar ; bstar , dstar ];
centroid_top = (-bstar / dstar )
thickness_top

ABBDstar_t = inv(astarbstardstar_t);
Af1 = ABBDstar_t(1,1);
Bf1 = ABBDstar_t(2,1);
%%-----------------------------------------------------------------
---
%%calculation for torsional stiffness elements by method 1
(smeared)
d66f1_1 = abbd_t(6,6);
GJf1_1 = 1/d66f1_1
%%-----------------------------------------------------------------
---
%%calculation for torsional stiffness elements by method 2
abdbarf1_2 = [abbd_t(1,1), abbd_t(1,4), abbd_t(1,6);
            abbd_t(1,4), abbd_t(4,4), abbd_t(4,6);
            abbd_t(1,6), abbd_t(4,6), abbd_t(6,6)];
ABDbarf1_2 = inv(abdbarf1_2);
```

```
GJf1_2 = ((ABDbarf1_2(3,3))/(1-(ABDbarf1_2(1,3)*abbd_t(1,6))-
(ABDbarf1_2(2,3)*abbd_t(4,6))))

%%-----------------------------------------------------------------
---
%%calculation for torsional stiffness elements by method 3

%%GJf1_3 = 1 / ( abbd_t(6,6) - ((abbd_t(4,6)^2)/abbd_t(4,4)));

astarf1_t = abbd_t(3,3) - (abbd_t(3,4)^2/abbd_t(4,4));
bstarf1_t = abbd_t(3,6) - (abbd_t(3,4)*abbd_t(4,6)/abbd_t(4,4));
dstarf1_t = abbd_t(6,6) - (abbd_t(4,6)^2/abbd_t(4,4));
astarbstardstarf1_t = [astarf1_t , bstarf1_t ; bstarf1_t ,
dstarf1_t ];

rho_sc_f1 = -(bstarf1_t/dstarf1_t)
ABBDstarf1_t = inv(astarbstardstarf1_t);

Astar_t_f1sc = ABBDstarf1_t(1,1);
Bstar_t_f1sc = ABBDstarf1_t(1,2) - rho_sc_f1 * ABBDstarf1_t(1,1);
Dstar_t_f1sc = ABBDstarf1_t(2,2) - 2 * rho_sc_f1 *
ABBDstarf1_t(1,2) + (rho_sc_f1^2) * ABBDstarf1_t(1,1);

D66f1_t = Dstar_t_f1sc

%%
% BOTTOM FLANGE PLY angle INPUT %

% BOTTOM FLANGE PLY INPUT %

prompt = {'Enter no of plies for the bottom most flange:'};
dlg_title = 'No of ply';
num_lines = 1;
def = {'1'};
b  = inputdlg(prompt,dlg_title,num_lines,def);
b = str2num(b{1});
ply_f2 = b;
thickness_bottom = b * str2num(a{5});
for i=1:b,
prompt = {'Enter thetha in degrees (start with first ply)for
bottom most flange :'};
dlg_title = 'thetha';
num_lines = 1;
def = {'0'};
c(i) = inputdlg(prompt,dlg_title,num_lines,def);
end
c;
c_f2 = c
```

```
h = [0:b];
for i=0:b
    if i < b/2
        k = 0+i;
        j = 1+i;
        h(1,j) = (-b/2)+k;
   else
     k = i;
     j = 1+i;
     h(1,j) = h(1,j-1)+1;
    end
end
h = str2num(a{5})*h;
h_f2 = h

% CALCULATION OF ABBD MATRIX OF bottom FLANGE

A0 = zeros(3);
B0 = zeros(3);
D0 = zeros(3);
e = 0;
for j=1:b

     angle = str2num(c{b-e});
      e = e+1;
     theta = angle * pi / 180;
     n = sin(-theta);
     m = cos(-theta);
     Tsigma = [m^2 , n^2 , 2*m*n ; n^2 , m^2 , -2*m*n ; -m*n ,
m*n , m^2 - n^2];
     n = sin(theta);
     m = cos(theta);
     Tepsilon = [m^2 , n^2 , m*n ; n^2 , m^2 , -m*n ; -2*m*n ,
2*m*n , m^2 - n^2];
     Qbar = Tsigma * Q * Tepsilon;
     n = sin(-theta);
     m = cos(-theta);
     TepsilonN = [m^2 , n^2 , m*n ; n^2 , m^2 , -m*n ; -2*m*n ,
2*m*n , m^2 - n^2];
     A = A0 + Qbar*(h(1,j+1) - h(1,j));
     f = ((h(1,j+1)*h(1,j+1)) - ((h(1,j)*h(1,j))));
format short
     B = B0 + (Qbar*f)/2;
format short
     D = D0 + (Qbar*(h(1,j+1)^3 - h(1,j)^3))/3;
     A0 = A;
     B0 = B;
     D0 = D;
```

```
end
A;
B;
D;
ABBD=[A,B;B,D];
Abarf2 = A;
Bbarf2 = B;
Dbarf2 = D;

%CALCULATION OF A*B*B*D* matric

abbd_b = inv(ABBD);
Etf2_smeared = (1 / abbd_b(1,1));

Eft2_warp = (1/( abbd_b(1,1) - ( (abbd_b(1,4)^2)/abbd_b(4,4))));

astar = abbd_b(1,1) - (abbd_b(1,6)^2/abbd_b(6,6));
bstar = abbd_b(1,4) - (abbd_b(1,6)*abbd_b(4,6)/abbd_b(6,6));
dstar = abbd_b(4,4) - (abbd_b(4,6)^2/abbd_b(6,6));

astarbstardstar_b = [astar , bstar ; bstar , dstar ];
centroid_bottom = (-bstar / dstar )
thickness_bottom

ABBDstar_b = inv(astarbstardstar_b);
Af2 = ABBDstar_b(1,1);
Bf2 = ABBDstar_b(2,1);

%%-----------------------------------------------------------------
---
%calculation for torsional stiffness elements by method 1
(smeared)

d66f2_1 = abbd_b(6,6);

%%-----------------------------------------------------------------
---
%%calculation for torsional stiffness elements by method 2
abdbarf2_2 = [abbd_b(1,1), abbd_b(1,4), abbd_b(1,6);
              abbd_b(1,4), abbd_b(4,4), abbd_b(4,6);
              abbd_b(1,6), abbd_b(4,6), abbd_b(6,6)];
ABDbarf2_2 = inv(abdbarf2_2);

GJf2_2 = ((ABDbarf2_2(3,3))/(1-(ABDbarf2_2(1,3)*abbd_b(1,6))-
(ABDbarf2_2(2,3)*abbd_b(4,6))));

%%-----------------------------------------------------------------
---
```

```
%%calculation for torsional stiffness elements by method 3

%GJf2_3 = 1 / ( abbd_b(6,6) - ((abbd_b(4,6)^2)/abbd_b(4,4)));
astarf2_t = abbd_b(3,3) - (abbd_b(3,4)^2/abbd_b(4,4));
bstarf2_t = abbd_b(3,6) - (abbd_b(3,4)*abbd_b(4,6)/abbd_b(4,4));
dstarf2_t = abbd_b(6,6) - (abbd_b(4,6)^2/abbd_b(4,4));

astarbstardstarf2_t = [astarf2_t , bstarf2_t ; bstarf2_t ,
dstarf2_t ];

ABBDstarf2_t = inv(astarbstardstarf2_t);
D66f2_t = ABBDstarf2_t(2,2);

astarf2_t = abbd_b(3,3) - (abbd_b(3,4)^2/abbd_b(4,4));
bstarf2_t = abbd_b(3,6) - (abbd_b(3,4)*abbd_b(4,6)/abbd_b(4,4));
dstarf2_t = abbd_b(6,6) - (abbd_b(4,6)^2/abbd_b(4,4));
astarbstardstarf2_t = [astarf2_t , bstarf2_t ; bstarf2_t ,
dstarf2_t ];

rho_sc_f2 = -(bstarf2_t/dstarf2_t)
ABBDstarf2_t = inv(astarbstardstarf2_t);

Astar_t_f2sc = ABBDstarf2_t(1,1);
Bstar_t_f2sc = ABBDstarf2_t(1,2) - rho_sc_f2 * ABBDstarf2_t(1,1);
Dstar_t_f2sc = ABBDstarf2_t(2,2) - 2 * rho_sc_f2 *
ABBDstarf2_t(1,2) + (rho_sc_f2^2) * ABBDstarf2_t(1,1);

D66f2_t = Dstar_t_f2sc
%%
% WEB PLY angle INPUT %

% WEB PLY INPUT %

prompt = {'Enter no of plies for the WEB:'};
dlg_title = 'No of ply';
num_lines = 1;
def = {'1'};
b  = inputdlg(prompt,dlg_title,num_lines,def);
b = str2num(b{1});
thickness_web = b * str2num(a{5});
ply_w= b;
for i=1:b,
prompt = {'Enter thetha in degrees (start with first ply)for WEB
:'};
dlg_title = 'thetha';
num_lines = 1;
def = {'0'};
d(i) = inputdlg(prompt,dlg_title,num_lines,def);
end
```

```
d;
d_w = d
h = [0:b];
for i=0:b
    if i < b/2
        k = 0+i;
        j = 1+i;
        h(1,j) = (-b/2)+k;
   else
     k = i;
     j = 1+i;
     h(1,j) = h(1,j-1)+1;
    end
end
h = str2num(a{5})*h;
h_w = h

% CALCULATION OF ABBD MATRIX OF web

A0 = zeros(3);
B0 = zeros(3);
D0 = zeros(3);
e = 0;
for j=1:b

     angle = str2num(d{b-e});
      e = e+1;
     theta = angle * pi / 180;
     n = sin(-theta);
     m = cos(-theta);
     Tsigma = [m^2 , n^2 , 2*m*n ; n^2 , m^2 , -2*m*n ; -m*n ,
m*n , m^2 - n^2];
     n = sin(theta);
     m = cos(theta);
     Tepsilon = [m^2 , n^2 , m*n ; n^2 , m^2 , -m*n ; -2*m*n ,
2*m*n , m^2 - n^2];
     Qbar = Tsigma * Q * Tepsilon;
     n = sin(-theta);
     m = cos(-theta);
     TepsilonN = [m^2 , n^2 , m*n ; n^2 , m^2 , -m*n ; -2*m*n ,
2*m*n , m^2 - n^2];
     A = A0 + Qbar*(h(1,j+1) - h(1,j));
     f = ((h(1,j+1)*h(1,j+1)) - ((h(1,j)*h(1,j))));
format short
     B = B0 + (Qbar*f)/2;
format short
     D = D0 + (Qbar*(h(1,j+1)^3 - h(1,j)^3))/3;
     A0 = A;
     B0 = B;
     D0 = D;
```

```
end
A;
B;
D;

ABBD=[A,B;B,D];

%CALCULATION OF A*B*B*D* matric

abbd_w = inv(ABBD);
astar = abbd_w(1,1) - (abbd_w(1,6)^2/abbd_w(6,6));
bstar = abbd_w(1,4) - (abbd_w(1,6)*abbd_w(4,6)/abbd_w(6,6));
dstar = abbd_w(4,4) - (abbd_w(4,6)^2/abbd_w(6,6));

astarbstardstar_w = [astar , bstar ; bstar , dstar ];
centroid_web1 = (-bstar / dstar );
thickness_web

ABBDstar_w = inv(astarbstardstar_w);
Dw = ABBDstar_w(2,2);
Aw = ABBDstar_w(1,1);

%%-----------------------------------------------------------------
---
%calculation for torsional stiffness elements by method 1
(smeared)
d66w_1 = abbd_w(6,6);

%%-----------------------------------------------------------------
---
%%calculation for torsional stiffness elements by method 2
abdbarw_2 = [abbd_w(1,1), abbd_w(1,4), abbd_w(1,6);
             abbd_w(1,4), abbd_w(4,4), abbd_w(4,6);
             abbd_w(1,6), abbd_w(4,6), abbd_w(6,6)];
ABDbarw_2 = inv(abdbarw_2);

GJw_2 = ((ABDbarw_2(3,3))/(1-(ABDbarw_2(1,3)*abbd_w(1,6))-
(ABDbarw_2(2,3)*abbd_w(4,6))));

%%-----------------------------------------------------------------
---
%%calculation for torsional stiffness elements by method 3

D66w_t= 1 / ( abbd_w(6,6) - ((abbd_w(4,6)^2)/abbd_w(4,4)));

%%
%width of flanges
```

```
prompt = {'Enter width of top flange in inches:'};
dlg_title = 'top flange width';
num_lines = 1;
def = {'0.25'};
bf1  = inputdlg(prompt,dlg_title,num_lines,def);
bf1 = str2num(bf1{1});

prompt = {'Enter width of bottom flange in inches:'};
dlg_title = 'bottom flange width';
num_lines = 1;
def = {'1'};
bf2  = inputdlg(prompt,dlg_title,num_lines,def);
bf2 = str2num(bf2{1});

prompt = {'Enter the height of web in inches:'};
dlg_title = 'web height';
num_lines = 1;
def = {'0.5'};
hw  = inputdlg(prompt,dlg_title,num_lines,def);
hw = str2num(hw{1});
centroid_web = hw/2

z1 = thickness_bottom + hw + (thickness_top/2)+ centroid_top
z2 = (thickness_bottom/2)+centroid_bottom
z3 = thickness_bottom + hw/2

Af1
Af2
Dw
Aw

bf1
bf2
hw

zc = ((Af1 * bf1 * z1) + (Af2 * bf2 * z2) +  (hw * z3 * Aw)) /
((Af1 * bf1 ) + (Af2 * bf2 ) +  (hw *  Aw))

EA = (Af1 * bf1 ) + (Af2 * bf2 ) +  (hw *  Aw)

z1c = z1 - zc
z2c = z2 - zc
hwc = z3-zc

EIyy = bf1*(ABBDstar_t(2,2)+2*ABBDstar_t(2,1)*z1c +
z1c*z1c*ABBDstar_t(1,1)) +
bf2*(ABBDstar_b(2,2)+2*ABBDstar_b(2,1)*z2c +
```

```
z2c*z2c*ABBDstar_b(1,1)) + (1/12 * hw *hw * hw + hw * hwc * hwc
)* ABBDstar_w(1,1)

EIzz = ((ABBDstar_t(1,1) * bf1^3) /12) + ((ABBDstar_b(1,1) *
bf2^3)/12) + Dw*(hw)

%%-----------------------------------------------------------------
----------
%% Shear center calculation

%% width reduction factor"

prompt = {'Enter width reduction factor for top flange:'};
dlg_title = 'width reduction factor ';
num_lines = 1;
def = {'0.897'};
mu1_f1  = inputdlg(prompt,dlg_title,num_lines,def);
mu1_f1 = str2num(mu1_f1{1});

prompt = {'Enter width reduction factor for bottom flange:'};
dlg_title = 'width reduction factor ';
num_lines = 1;
def = {'0.96'};
mu2_f2  = inputdlg(prompt,dlg_title,num_lines,def);
mu2_f2 = str2num(mu2_f2{1});

prompt = {'Enter width reduction factor for web laminate:'};
dlg_title = 'width reduction factor ';
num_lines = 1;
def = {'0.96'};
mu_w  = inputdlg(prompt,dlg_title,num_lines,def);
mu_w = str2num(mu_w{1});

%%Mathod 1 - from centroid - suggested my Vishal Sanghavi
e_sc_1 = (((z1c*Af1*bf1^3)/12)+((z2c*Af2*bf2^3)/12))* (1/EIzz);
e_bottom_1 =  zc+ e_sc_1

%% Method 2 -  smeared property
heightweb = (hw + (thickness_top/2)+(thickness_bottom/2));
e_sc_2 = (heightweb * Etf1_smeared *(bf1^3))/( Etf1_smeared
*(bf1^3)+ Etf2_smeared *(bf2^3)) + (thickness_bottom/2)

%%Method 3 - Suggested by Syed - total ABD property
% CALCULATION OF ABBD MATRIX OF web
A0 = zeros(3);
B0 = zeros(3);
D0 = zeros(3);
e = 0;
for j=1:b
```

```
     angle = str2num(d{b-e});
      e = e+1;
     theta = angle * pi / 180;
     n = sin(-theta);
     m = cos(-theta);
     Tsigma = [m^2 , n^2 , 2*m*n ; n^2 , m^2 , -2*m*n ; -m*n ,
m*n , m^2 - n^2];
     n = sin(theta);
     m = cos(theta);
     Tepsilon = [m^2 , n^2 , m*n ; n^2 , m^2 , -m*n ; -2*m*n ,
2*m*n , m^2 - n^2];
    %%Qbar = Tsigma * [1,0,0;0,0,0;0,0,0]* Q
*[1,0,0;0,0,0;0,0,0]* Tepsilon;
    Qbar = Tsigma * Q * Tepsilon;
     A = A0 + Qbar*(h(1,j+1) - h(1,j));
     f = ((h(1,j+1)*h(1,j+1)) - ((h(1,j)*h(1,j))));
format short
     B = B0 + (Qbar*f)/2;
format short
     D = D0 + (Qbar*(h(1,j+1)^3 - h(1,j)^3))/3;
     A0 = A;
     B0 = B;
     D0 = D;

end
A;
B;
D;

ABBD=[A,B;B,D];
Abarw = [1,0,0;0,0,0;0,0,0]*A*[1,0,0;0,0,0;0,0,0];
Bbarw = [1,0,0;0,0,0;0,0,0]*B*[1,0,0;0,0,0;0,0,0];
Dbarw = [1,0,0;0,0,0;0,0,0]*D*[1,0,0;0,0,0;0,0,0];
htf1 = (hw/2) + (thickness_top/2);
htf2 = (hw/2) + (thickness_bottom/2);
Abarcomplete = hw*Abarw + bf1*Abarf1 + bf2*Abarf2;
Bbarcomplete = hw*Bbarw + bf1*(Bbarf1+((htf1)*Abarf1)) +
bf2*(Bbarf2-((htf2 )*Abarf2));
Dbarcomplete = (hw*Dbarw + ((hw^3)*Abarw / 12 ))+ bf1*(Dbarf1
+(2*(htf1)*Bbarf1)+((htf1)^2*Abarf1)) + bf2*(Dbarf2 -
(2*(htf2)*Bbarf2)+((htf2)^2*Abarf2));

ABDcomplete =
[Abarcomplete,Bbarcomplete;Bbarcomplete,Dbarcomplete];
abdcomplete = inv(ABDcomplete);
centroid_3_bottom = -(abdcomplete(1,4)/abdcomplete(4,4)) + (hw/2)
+ (thickness_bottom);
sc_3 = -(abdcomplete(3,6)/abdcomplete(6,6)) + (hw/2)  +
(thickness_bottom)
```

```
EA_ABD = (abdcomplete(4,4)/((abdcomplete(1,1)*abdcomplete(4,4))-
(abdcomplete(1,4)^2)))
EI_ABD = (abdcomplete(1,1)/((abdcomplete(1,1)*abdcomplete(4,4))-
(abdcomplete(1,4)^2)))
%%-----------------------------------------------------------------
----------

prompt = {'Enter Torsional Moment applied in lbs/inch'};
dlg_title = 'Torsion';
num_lines = 1;
def = {'1'};
Torsion  = inputdlg(prompt,dlg_title,num_lines,def);
Torsion = str2num(Torsion{1});

prompt = {'Enter the effective length of beam in inches'};
dlg_title = 'Lenght';
num_lines = 1;
def = {'10'};
Lenght = inputdlg(prompt,dlg_title,num_lines,def);
Lenght = str2num(Lenght{1});


%%-----------------------------------------------------------------
----------
%%Torsional Stiffness - Smeared properties - Method 1:

GJ_1 = ((4*bf1)/d66f1_1) + ((4*bf2)/d66f2_1) + ((4*hw)/d66w_1)
theta_1 = (Torsion * Lenght)/GJ_1
%%-----------------------------------------------------------------
----------
%%Torsional Stiffness -Skudra - Method 2:

GJ_2 = ((4*bf1)*(GJf1_2)) + ((4*bf2)*(GJf2_2)) + ((4*hw)*(GJw_2))
theta_2 = (Torsion * Lenght)/GJ_2
%%-----------------------------------------------------------------
----------
%%Torsional Stiffness - present method  - Method 3- suggested my
Vishal
%%Sanghavi

GJ_3 = ((4*mu1_f1*bf1)*D66f1_t) + ((4*mu2_f2*bf2)*D66f2_t) +
((4*mu_w*hw)*D66w_t)
theta_3 = (Torsion * Lenght)/GJ_3
%%-----------------------------------------------------------------
----------
%%-----------------------------------------------------------------
----------
%%Warping Stiffness suggested my Vishal Sanghavi
```

```
ef2 = e_bottom_1 - (thickness_bottom/2);
eff1 = heightweb - ef2 ;

warpingstiffness_1 = ( (((ABBDstar_t(1,1) * bf1^3) /12)* eff1^2)
+ (((ABBDstar_b(1,1) * bf2^3)/12)*ef2^2) )
%%warpingstiffness_1 = ( (((Etf1_smeared * bf1^3) /12)* eff1^2) +
(((Etf2_smeared * bf2^3)/12)*ef2^2) )
%%-----------------------------------------------------------------
----------
%%Warping Stiffness by smeared properties

e_sc_2_warping = e_sc_2 - (thickness_bottom/2);
warpingstiffness_2 = ((heightweb * Etf2_smeared *(bf2^3))/12) *
e_sc_2_warping

%%-----------------------------------------------------------------
----------
%% Calculation of total angle of twist - (warping effect included
) -
% present formulation used
L = 10; % total lenght of beam
z = 10; % point at which the thetha needs to be evaluated
mu_1 = sqrt( GJ_3  / warpingstiffness_1);
theta_warp_1 = ((Torsion /(GJ_3 )))* (z + (sinh( mu_1*(L-z)) /
(mu_1 * cosh( mu_1 * L))) - (((sinh( mu_1 * L)) /( mu_1 *cosh(
mu_1 * L)))))
theta_warp_1_deg = theta_warp_1  * 180 / pi

%%-----------------------------------------------------------------
----------
%% Calculation of total angle of twist - smeared properties
mu_2 = sqrt( GJ_1  / warpingstiffness_2);

theta_warp_2 = ((Torsion /(GJ_1 )))* (z + (sinh( mu_2*(L-z)) /
(mu_2 * cosh( mu_2* L))) - (((sinh( mu_2 * L)) /( mu_2 *cosh(
mu_2* L)))))
theta_warp_2_deg = theta_warp_2  * 180 / pi
```

Appendix B

APDL code for Modeling 2D composite I-Beam

```
/PREP7
!*
ET,1,SHELL181
!*
KEYOPT,1,1,0
KEYOPT,1,3,0
KEYOPT,1,8,2
KEYOPT,1,9,0
!*
!*
MPTEMP,,,,,,,,
MPTEMP,1,0
MPDATA,EX,1,,21.75e6
MPDATA,EY,1,,1.595e6
MPDATA,EZ,1,,1.595e6
MPDATA,PRXY,1,,0.25
MPDATA,PRYZ,1,,0.45
MPDATA,PRXZ,1,,0.25
MPDATA,GXY,1,,0.8702e6
MPDATA,GYZ,1,,0.5366e6
MPDATA,GXZ,1,,0.8702e6
sect,1,shell,,Top Flange
secdata, 0.005,1,45,3
secdata, 0.005,1,-45,3
secdata, 0.005,1,0,3
secdata, 0.005,1,90,3
secdata, 0.005,1,90,3
secdata, 0.005,1,0,3
secdata, 0.005,1,-45,3
secdata, 0.005,1,45,3
secoffset,MID
seccontrol,,,, , , ,
sect,2,shell,,Bottom Flange
secdata, 0.005,1,45,3
secdata, 0.005,1,-45,3
secdata, 0.005,1,0,3
secdata, 0.005,1,0,3
secdata, 0.005,1,90,3
```

```
secdata, 0.005,1,90,3
secdata, 0.005,1,0,3
secdata, 0.005,1,0,3
secdata, 0.005,1,-45,3
secdata, 0.005,1,45,3
secoffset,MID
seccontrol,,,, , , ,
sect,3,shell,,Web
secdata, 0.005,1,45,3
secdata, 0.005,1,-45,3
secdata, 0.005,1,-45,3
secdata, 0.005,1,45,3
secoffset,MID
seccontrol,,,, , , ,
sect,3,shell,,Web
secdata, 0.005,1,45,3
secdata, 0.005,1,-45,3
secdata, 0.005,1,-45,3
secdata, 0.005,1,45,3
secoffset,MID
seccontrol,,,, , , ,
K,1,0,0,0,
K,2,10,0,0,
K,3,0,0.375,0,
K,4,10,0.375,0,
K,5,0,0.75,0,
K,6,10,0.75,0,
K,7,0,0.375,0.545,
K,8,10,0.375,0.545,
K,9,0,0.125,0.545,
K,10,10,0.125,0.545,
K,11,0,0.625,0.545,
K,12,10,0.625,0.545,
FINISH
/SOL
FINISH
/PREP7
!*
```

```
LOCAL,11,0,0,0.375,0, ,90, ,1,1,
!*
LOCAL,12,0,0,0,0,0,0,0,1,1,
FLST,2,4,3
FITEM,2,3
FITEM,2,1
FITEM,2,2
FITEM,2,4
A,P51X
FLST,2,4,3
FITEM,2,5
FITEM,2,3
FITEM,2,4
FITEM,2,6
A,P51X
!*
APLOT
LPLOT
FLST,5,2,5,ORDE,2
FITEM,5,1
FITEM,5,-2
CM,_Y,AREA
ASEL, , , ,P51X
CM,_Y1,AREA
CMSEL,S,_Y
!*
CMSEL,S,_Y1
AATT,      1, ,   1,     12,   2
CMSEL,S,_Y
CMDELE,_Y
CMDELE,_Y1
!*
FLST,5,4,4,ORDE,4
FITEM,5,1
FITEM,5,3
FITEM,5,5
FITEM,5,-6
CM,_Y,LINE
```

```
LSEL, , , ,P51X
CM,_Y1,LINE
CMSEL,,_Y
!*
LESIZE,_Y1, , ,75, , , , ,1
!*
FLST,5,3,4,ORDE,3
FITEM,5,2
FITEM,5,4
FITEM,5,7
CM,_Y,LINE
LSEL, , , ,P51X
CM,_Y1,LINE
CMSEL,,_Y
!*
LESIZE,_Y1, , ,200, , , , ,1
!*
MSHKEY,0
FLST,5,2,5,ORDE,2
FITEM,5,1
FITEM,5,-2
CM,_Y,AREA
ASEL, , , ,P51X
CM,_Y1,AREA
CHKMSH,'AREA'
CMSEL,S,_Y
!*
AMESH,_Y1
!*
CMDELE,_Y
CMDELE,_Y1
CMDELE,_Y2
!*
KPLOT
!*
!*
FLST,2,4,3
FITEM,2,7
```

```
FITEM,2,9
FITEM,2,10
FITEM,2,8
A,P51X
FLST,2,4,3
FITEM,2,11
FITEM,2,7
FITEM,2,8
FITEM,2,12
A,P51X
!*
LPLOT
FLST,5,2,5,ORDE,2
FITEM,5,3
FITEM,5,-4
CM,_Y,AREA
ASEL, , , ,P51X
CM,_Y1,AREA
CMSEL,S,_Y
!*
CMSEL,S,_Y1
AATT,      1, ,   1,     12,   1
CMSEL,S,_Y
CMDELE,_Y
CMDELE,_Y1
!*
FLST,5,4,4,ORDE,4
FITEM,5,8
FITEM,5,10
FITEM,5,12
FITEM,5,-13
CM,_Y,LINE
LSEL, , , ,P51X
CM,_Y1,LINE
CMSEL,,_Y
!*
LESIZE,_Y1, , ,50, , , , ,1
!*
```

```
FLST,5,3,4,ORDE,3
FITEM,5,9
FITEM,5,11
FITEM,5,14
CM,_Y,LINE
LSEL, , , ,P51X
CM,_Y1,LINE
CMSEL,,_Y
!*
LESIZE,_Y1, , ,200, , , , ,1
!*
MSHKEY,0
FLST,5,2,5,ORDE,2
FITEM,5,3
FITEM,5,-4
CM,_Y,AREA
ASEL, , , ,P51X
CM,_Y1,AREA
CHKMSH,'AREA'
CMSEL,S,_Y
!*
AMESH,_Y1
!*
CMDELE,_Y
CMDELE,_Y1
CMDELE,_Y2
!*
KPLOT
FLST,2,4,3
FITEM,2,3
FITEM,2,7
FITEM,2,8
FITEM,2,4
A,P51X
CM,_Y,AREA
ASEL, , , ,       5
CM,_Y1,AREA
CMSEL,S,_Y
```

```
!*
CMSEL,S,_Y1
AATT,      1, ,   1,     11,   3
CMSEL,S,_Y
CMDELE,_Y
CMDELE,_Y1
!*
LPLOT
FLST,5,2,4,ORDE,2
FITEM,5,15
FITEM,5,-16
CM,_Y,LINE
LSEL, , , ,P51X
CM,_Y1,LINE
CMSEL,,_Y
!*
LESIZE,_Y1, , ,110, , , , ,1
!*
FLST,5,2,4,ORDE,2
FITEM,5,4
FITEM,5,11
CM,_Y,LINE
LSEL, , , ,P51X
CM,_Y1,LINE
CMSEL,,_Y
!*
LESIZE,_Y1, , ,200, , , , ,1
!*
MSHKEY,0
CM,_Y,AREA
ASEL, , , ,      5
CM,_Y1,AREA
CHKMSH,'AREA'
CMSEL,S,_Y
!*
AMESH,_Y1
!*
CMDELE,_Y
```

```
CMDELE,_Y1
CMDELE,_Y2
!*
NPLOT
```

References

[1] L. P. Kollar and G. S. Springer, Mechanics of Composite Structures, Cambridge University Press, 2003.

[2] L. P. Kollar and A. Pluzsik, “Analysis of Thin walled Composite Beams with Arbitrary Layup”, Journal of Reinforced Plastics and Composites, Vol. 21, 1423-1465, 2002.

[3] M. Ata, “Torsional Analysis of thin-walled fibrous composite beams” PhD thesis, Cranfield Institute of Technology, 1992-93

[4] J. Loughlan and M.Ata, “The behavior of open and closed section carbon fiber composite beams subjects to constrained torsion”, Composite Structures Vol. 38, No 1-4, pp. 631-647, 1997.

[5] J. C .Massa and Ever J. Barbero,“ A strength of Material Formulation for thin walled composite beams with Torsion”, Journal of Composite Materials, Vol. 32, No 17/1998 pp 1560-1594.

[6] Hani A. Salim and Julio F. Davalos,“ Torsion of Open and Closed Thin- Walled Laminated Composite Sections”, Journal of Composite Materials, Vol. 39, No 6/2005 pp 497-524.

[7] T. M. Roberts and H. Al-Ubaidi, “Influence of shear deformation on restrained torsional warping of pultruded FRP bars of open cross-section” , Journal of Thin-walled Structures, Vol. 39, pp 395-414.

[8] Ramesh Chandra and Inderjit Chopra, “Experimental and Theoretical Analysis of Composite I-Beams with Elastic Couplings”, AIAA Journal, Vol. 29, NO. 12, December 1991, pp 2197-2206

[9] Jaehong Lee, “Canter of gravity and shear center of thin walled open section composite beams”, Composite Structures, Vol. 52, pp 255-260.

[10] A. M. Skudra, F. Ya. Bulavs, M. R. Gurvich and A. A. Kruklinsh, Structural Analysis of Composite Beam Systems, Technomic Publishing Company, Inc. 1991.

[11] Daniel Gay, Suong V. Hoa, Stephen W. Tsai, Composite materials – Design and Applications, CRC press LLC, 2003.

.

[12] T.H.G. Megson, Aircraft Structures for engineering students, Third edition, Butterworth Heinemann publications, 1999.

[13] Robert L. Ketter, George C. Lee and Sherwood P. Prawel, Jr., Structural Analysis and design, McGraw-Hill Inc, 1979

[14] Institute for Steel Development and Growth, India. Teaching Material – Chapter 17, http://www.steel-insdag.org/NewWebsite/TeachingMaterial/Chapter17.pdf

[15] Raymond J. Roark and Warren C. Young, Formulas for Stress and Strain, Fifth edition, McGraw-Hill Inc.

[16] Stephen P. Timoshenko and James M. Gere, Theory of Elastic stability, Second edition, McGraw-Hill Inc, 1985

[17] Walter D.Pilkey, Analysis and Design of Elastic Beams: Computational Methods, John Wiley & Sons, 2002.

[18] Huie-Huang Lee, Finite element Simulations with ANSYS™ Workbench 13, SDC publications, 2011.

[19] Ever J. Barbero, Finite Element Analysis of Composite Materials, CRC Press, 2008.

[20] Doe Jhon Chen, "Efficient Finite Element Analysis of Composite Laminate", Department of Mechanical and Aerospace Engineering, University of Texas at Arlington, December, 1995.

[21] Farhan Alamgir, "Issues on Finite element modeling of Laminated Composite Structures", Department of Mechanical and Aerospace Engineering, University of Texas at Arlington, May, 2011

[22] ANSYS™ help files, http://www.kxcad.net/ansys/ANSYS/ansyshelp/index.htm

[23] I. M. Daniel and Ori Ishai, Engineering Mechanics of Composite Materials, Oxford University Press, 1994

[24] W. S. Chan, Notes of graduate course ME 5315, Introduction to Composites, Fall 2011

[25] Rios, G., "A Unified Analysis of Stiffener Reinforced Composite Beams with Arbitrary Cross-Section", PhD thesis, The University of Texas at Arlington, 2009

[26] J. C. Parambil, "Stress Analysis of Laminated Composite Beam with I-Section", Master's thesis, The University of Texas at Arlington, May 2010

[27] J. C. Parambil, W. S. Chan, K. L. Lawrence and V. M. Sanghavi, "Stress Analysis for Composite I-Beam by a Non- Conventional Method" In Proceedings of the 26th ASC Annual Technical Conference, Canada, Sep 2011

[28] Syed, K. A. and Chan, W. S., "Analysis of Hat-Sectioned Reinforced Composite Beams",
Proceedings of American Society of Composites, Sept. 2006.

[29] Drummond, J. A., and Chan, W. S., "Fabrication, Analysis, and Experimentation of a Practically Constructed Laminated Composite I-Beam under Pure Bending", Journal of Thermoplastic Composite Materials, May 1999, pp. 177-187.

[30] Ugural, A. C., and Fenster, S. K., Advanced Strength and Applied Elasticity, 4th edition, Prentice Hall, PTR

Biographical Information

Vishal Sanghavi received his Bachelor's in Mechanical Engineering from Mumbai University, India. He served in Larsen and Toubro as Executive – Design and Engineering before coming to USA to pursue Master's in Mechanical Engineering. His academic interest lies in structural analysis, design and modeling. He further plans to work in the related field of interest and "BE HAPPY".